43

Self Assembly in Linear-Dendritic Diblock Copolymer Films

By

Jyotsna Iyer

Bachelor of Technology, Chemical Engineering
Indian Institute of Technology, Madras, India, 1992

Master of Science in Chemical Engineering Practice
Massachusetts Institute of Technology, Cambridge, Massachusetts, 1994

SUBMITTED TO THE DEPARTMENT OF CHEMICAL ENGINEERING IN PARTIAL FULFILLMENT OF THE REQUIREMENTS FOR THE DEGREE OF

DOCTOR OF PHILOSOPHY IN CHEMICAL ENGINEERING

AT THE

MASSACHUSETTS INSTITUTE OF TECHNOLOGY

FEBRUARY, 1999

Signature of Author: _____

Department of Chemical Engineering
January 28, 1999

Certified by: _____

Paula T. Hammond
Thesis Supervisor

Certified by: _____

Robert E. Cohen
St. Laurent Professor of Chemical Engineering
Chairman, Committee for Graduate Students

SELF ASSEMBLY IN LINEAR-DENDRITIC DIBLOCK COPOLYMER FILMS

by

JYOTSNA IYER

Submitted to the Department of Chemical Engineering on January 28, 1999 in partial fulfillment of the requirements for the degree of Doctor of Philosophy in Chemical Engineering

ABSTRACT

Dendrimers are an exciting class of symmetrically branched polymeric materials with interesting properties which include a nanoporous interior and a large number of end groups. Their potential use as catalysts, hosts for smaller molecules, and selective membranes is being actively investigated. While retaining the dendritic properties, a hybrid linear-dendritic diblock structure allows the formation of cohesive films because the linear block introduces entanglements. This thesis describes the synthesis, characterization, and ultrathin films of two series of novel linear-dendritic diblock copolymers. The hybrid diblock copolymers were designed to be amphiphilic with a linear hydrophilic polyethyleneoxide(PEO) block and a dendritic hydrophobic polyamidoamine(PAMAM) block. ^{1}H NMR, FTIR, and MALDI-TOF MS results establishing the structure of the PEO-PAMAM diblocks are reported.

The aqueous solution behavior of the hybrid copolymers at 30°C studied using intrinsic viscosity and GPC techniques was found to be influenced by the length of the PEO block and the end group functionality of the dendrimer. The intrinsic viscosity trends exhibited by the diblocks with the shorter PEO chain length did not deviate greatly from that of linear polymers, and those exhibited by the diblocks with the longer PEO chain length indicates the formation of unimolecular micelles.

The synthesis scheme used to modify the amine functionalities on the dendrimer block of PEO(2000)-dendrimer diblocks to various chemical functionalities is described. The amphiphilic behavior of the modified diblocks was studied by spreading monolayers of the material at the air-water interface of a Langmuir trough and recording the pressure-area isotherm. Stearate terminated diblocks were found to give stable monolayers which formed condensed phases on compression. The limiting area per molecule in the condensed phase measured from the pressure-area isotherm suggests interesting effects of dendrimer morphology, curvature, and size on the organization of the diblock monolayer at the air-water interface. Langmuir-Blodgett films of linear-dendritic diblock copolymers were made and are reported here for the first time. Z type multilayer films were formed for all the diblocks studied. A method, which involved the use of a linear water soluble polymer capable of hydrogen bonding with the PEO block in the subphase of the

Langmuir trough, was developed for improving the stability of the transferred multilayer film.

Bulk morphology of the PEO-PAMAM diblock copolymers was studied using DSC, SAXS, WAXD, and optical microscopy. Thermal characterization suggests that these diblock copolymers exhibit some degree of micro-phase segregation irrespective of the composition of the diblocks. Glass transition temperatures were observed for some of the diblocks. Dependence of glass transition temperatures on end group functionality of the dendrimer block was observed for the first time in such linear-dendritic diblock copolymers. The stearate terminated PEO(2000)-PAMAM diblocks had some unusual transitions in the DSC trace suggesting the formation of ordered structures in the bulk. The end modified diblocks also showed clear SAXS patterns with d spacings around 150Å. WAXD results indicate that the PEO block is crystalline in the bulk state of the copolymers. Birefringence was observed in the optical microscope for films of the end modified diblocks. The morphology results suggest that the PEO block exists as a fully extended molecule in the bulk for the PEO-dendrimer diblocks.

Spin coated films of the first and third generation end modified PEO(2000)-dendrimer diblocks imaged using atomic force microscopy showed the presence of uniform sized features at the surface. The sizes of these features were comparable to those measured in bulk films using SAXS.

The study of PEO-PAMAM linear-dendritic diblock copolymers reported in this thesis gives a fundamental understanding of the properties of these new materials. The thin film studies have illustrated the parameters that govern the making of defect free membranes of the diblocks. The results reported here will be helpful in directing the future work needed to test these material systems for potential applications.

Thesis Supervisor: Paula T. Hammond
Title: Herman P. Meissner Assistant Professor of Chemical Engineering

Acknowledgments

I would like to thank my advisor, Paula Hammond, for her valuable comments, suggestions, and ideas. I admire her optimistic attitude to almost everything. It was very motivating, especially through all the frustrating failures in the first year of synthesis.

I would like to thank my committee members - Prof. Alan Hatton, Prof. Michael Rubner, and Prof. Ed Merrill - for all their help. I have learned a lot from them. I would like to thank Prof. Phil Gschwend for his time and help during the early part of my stay at MIT. He taught me how to do scientific research in a few meetings and I believe that I owe a lot of my understanding of doing 'research' to him.

I would like to thank all my group members for the good time I had in Paula's group. Bindu, Sarah, Cathy, Aaron, and Wen - I will have fond memories of the first year when we worked together to set up the lab.

I want to thank Janet and Elaine for all their help during the course of my rather long stay at MIT. Jane, Colleen, Fred, and Mike have made the department a friendly place for me. Jane, practice school would have been a lot worse without you. Aparna and Anu have been the best of friends and great moral support over these years. Lalitha, Rohini, Samita, Sujatha, Chitra, Banana, Ganta, and Mottai - that you all were just a phone call away to take my side on anything has been a wonderful source of comfort. I want to thank Srikanth(alias Freaky), Sriku, Ram, Satyan, and Jayesh for scintillating conversations, badminton, and memorable times.

I would like to thank my parents, Annapoorna, and Ramu for supporting me through all my decisions, stupid or otherwise. Their confidence, love, and understanding has helped me achieve whatever I have. My brother has always paved the way for me and encouraged me to follow him. Ramu, I value that very much.

I would like to thank the Environmental Protection Agency for providing the financial support for this project and Bruker Analytical Systems for doing the MALDI-TOF MS experiments reported here.

TABLE OF CONTENTS

Abstract		2
Acknowledgements		4
Table of Contents		5
List of Figures		8
List of Tables		12
Chapter 1.	Introduction and Background	13
1.1	Motivation	13
1.2	Research Objectives	15
1.3	Background	16
1.3.1	Dendrimers	16
1.3.2	Langmuir-Blodgett Technique	21
1.4	Gas permeation through LB films	24
1.5	References	26
Chapter 2.	Synthesis of PEO-PAMAM Linear-Dendritic Diblock Copolymers	29
2.1	Introduction	29
2.2	Experimental Section	30
2.2.1	Materials	30
2.2.2	Instrumentation	30
2.2.3	Synthesis of PEO(5000) series	31
2.2.4	Synthesis of PEO(2000) series	31
2.2.5	End group modification of PEO(2000)-PAMAM diblocks	32
2.3	Results and Discussion	32
2.4	Chapter Summary	41
2.5	References	41

Chapter 3. Solution Behavior of PEO-PAMAM Linear-Dendritic Diblock Copolymers 43
3.1 Introduction 43
3.2 Experimental Section 44
3.3 Intrinsic Viscosity Results 44
3.3.1 PEO(2000)-dendrimer series 44
3.3.2 PEO(5000)-dendrimer series 47
3.4 GPC Results 51
3.5 Chapter Summary 53
3.6 References 53

Chapter 4. Amphiphilic behavior of linear-dendritic diblock copolymers at the air-water interface 55
4.1 Introduction 55
4.2 Experimental Section 56
4.3 Results and Discussion 57
4.3.1 Pressure-area isotherms for PEO-PAMAM diblocks 57
4.3.2 Effect of end group functionality on the π-a isotherm 59
4.3.3 Effect of dendrimer generation on the π-a isotherm of stearate terminated PEO-PAMAM diblock copolymers 61
4.3.4 Effect of subphase conditions on the π-a isotherms for stearate terminated PEO-PAMAM diblock copolymers 66
4.4 Chapter Summary 69
4.5 References 69

Chapter 5. Ultrathin films of PEO-PAMAM diblock copolymers 71

5.1 Introduction 71
5.2 Experimental Section 72
5.3 Results and Discussion 74
5.3.1 Ultrathin transferred films of PEO-PAMAM diblock copolymers 74
5.3.2 Engineering multilayer build-up 80
5.4 Chapter Summary 86
5.5 References 86

Chapter 6. Bulk morphology of linear-dendritic diblock copolymers 88
6.1 Introduction 88
6.2 Experimental Section 91
6.3 Results and Discussion 91
6.3.1 DSC Results 90
6.3.2 Bulk morphology of stearate terminated PEO(2000)-dendrimer diblocks 96
6.3.3 Spin-coated films of linear-dendritic diblocks 107
6.4 Chapter Summary 110
6.5 References 111

Chapter 7. Summary and Conclusions 114
Appendix A. Synthesis of PEO-PAMAM Linear-Dendritic diblock copolymers 118
A.1 PEO(5000) series 118
A.2 PEO(2000) series 121

List of Figures

Figure 1.1	Schematic of the linear-dendritic diblock architecture and its monolayer at the air-water interface of a Langmuir trough	16
Figure 1.2	Two dimensional representation of an initiator core, core cell, and tridendron dendrimers of different generations	17
Figure 1.3	A trough for deposition of monolayers on solid substrates	22
Figure 1.4	A monolayer in the spread form, in the compressed form, and being deposited onto a substrate	22
Figure 1.5	Schematic of surface pressure(π) vs. area per molecule(Å) for stearic acid on 0.01M HCl	23
Figure 2.1	Synthesis of PEO-PAMAM linear-dendritic diblock copolymer	34
Figure 2.2	^{1}H NMR spectra of PEO(2000)-1.5G. d_6-DMSO was used as the solvent	36
Figure 2.3	MALDI-TOF mass spectra of PEO(5000)-1.5G	37
Figure 2.4	End group modification of PEO(2000)-3.0G with stearic acid	38
Figure 3.1a	Variation of intrinsic viscosity with dendrimer generation for PEO(2000)-dendrimer diblocks at 30°C in water	45
Figure 3.1b	Relation between intrinsic viscosity and molecular weight for PEO(2000)-dendrimer diblocks	46
Figure 3.1c	Plot of hydrodynamic radius vs dendrimer generation for PEO(2000)-dendirmer diblocks	46
Figure 3.2a	Variation of intrinsic viscosity with dendrimer half generation for PEO(5000)-dendrimer diblocks at 30°C in water	48
Figure 3.2b	Variation of intrinsic viscosity with dendrimer full generation for PEO(5000)-dendrimer diblocks at 30°C in water	48
Figure 3.2c	Variation of hydrodynamic radius with generation number for PEO(5000)-dendrimer diblocks	51

Figure 4.1	Pressure-area isotherms at 20°C for ester terminated PEO(5000)-dendrimer diblock copolymers	58
Figure 4.2	Pressure-area isotherms at 20°C for ester(2.5G) and amine(3.0G) terminated PEO(2000)-dendrimer diblocks having eight end groups	58
Figure 4.3	Pressure-Area isotherms measured at 20°C for one unfunctionalized [PEO(2k)-2.5G] and two functionalized diblock copolymers [PEO(2k)-3.0G-M, PEO(2k)-3.0G-S)]. All three have the same PEO chain length and number of dendrimer end groups	60
Figure 4.4a	Pressure-Area isotherms measured at 20°C for four diblock copolymers with stearate end groups and the same PEO chain but different dendrimer generations	62
Figure 4.4b	Schematic of the organization of linear-dendritic diblock copolymers at the air-water interface for different dendrimer generations at high area's per molecule	62
Figure 4.4c	A close up of the condensed phase regime in the Pressure-Area isotherms measured at 20°C for four diblock copolymers with stearate end groups and the same PEO chain but different dendrimer generations	63
Figure 4.4d	Schematic of the organization of linear-dendritic diblock copolymers at the air-water interface for different dendrimer generations in the condensed phase	63
Figure 4.5	Effect on salt in the subphase on the pressure-area isotherm of PEO(2000)-2.0G-S	67
Figure 4.6	Effect of complexing polymer in the subphase on the pressure-area isotherm of PEO(2000)-2.0G-S	68
Figure 5.1	Atomic Force Micrograph of a film of PEO(2k)-3.0G-S transferred at 30mN/m and 20°C onto hydrophobically functionalized gold substrate	77

Figure 5.2 AFM of a bilayer film of PEO(2k)-3.0G-S transferred at 54mN/m and 20°C onto hydrophobically functionalized gold substrate 77

Figure 5.3 Histogram of the area transferred from the air-water interface onto a hydrophobically functionalized gold substrate for PEO(2k)-3.0G-S at a surface pressure of 54mN/m and 20°C 78

Figure 5.4a,b AFM of bilayer and multilayer films of PEO(2k)-4.0G-S transferred at 20mN/m and 40mN/m respectively and 20°C 79

Figure 5.4c Details of the multilayer films of PEO(2k)-4.0G-S transferred at 40mN/m 80

Figure 5.5 Schematic of the organization at the water air-water interface of the PEO-PAMAM diblock/polmer complex. The cartoon shows the adsorption of the monolayer complex onto the substrate 82

Figure 5.6 Histogram showing the area transferred from the air-water interface on to a carboxylic acid functionalized gold substrate for PEO(2000)-2.0G-S at a surface pressure of 20mN/m and 20°C. The aqueous subphase had 0.2g/l of PMAA dissolved at a pH~2 84

Figure 5.7 Histogram of the area transferred from the air-water interface onto a carboxylic acid functionalized gold substrate for PEO(2000)-2.0G-S at a surface pressure of 20mN/m and 20oC. The subphase was deionised water at pH~2 85

Figure 5.8 Atomic force micrograph of the PEO(2000)-2.0G-S multilayer deposited at 20mN/m from a water/PMAA(pH~2) subphase 85

Figure 6.1a Depression of PEO melting point with increasing dendrimer generations in PEO(5000)-dendrimer diblocks 92

Figure 6.1b Enthalpy change for PEO(5000) melting as a function of dendrimer generation (■) ΔH J/g from DSC, (X) normalized ΔH J/g 92

Figure 6.2 Plot of observed glass transition temperature vs. dendrimer generation for PEO(5000)-dendrimer diblocks. ( ) amine terminal

groups, (■) ester terminal groups 93

Figure 6.3a Depression of PEO melting point with increasing dendrimer generations in PEO(2000)-dendrimer diblocks 94

Figure 6.3b Enthalpy change for PEO melting as a function of dendrimer generation (■) ΔH J/g from DSC, (X) normalized ΔH J/g 95

Figure 6.4 Plot of observed glass transition temperature vs. dendrimer generation for PEO(2000)-dendrimer diblocks 96

Figure 6.5 SAXS pattern and DSC trace(second heating) for PEO(2000)-1.0G-S. The arrow indicates the annealing temperature for the melt cast film. 100

Figure 6.6 SAXS pattern and DSC trace for PEO(2000)-2.0G-S. The arrow shows the annealing temperature of the melt cast film. 101

Figure 6.7 SAXS patterns and DSC trace for PEO(2000)-3.0G-S. The arrows indicate the annealing temperatures of the melt cast sample. 102

Figure 6.8 Optical micrographs showing the birefringence of a PEO(2000)-3.0G-S film as function of temperature. 109

Figure 6.9 Optical micrographs showing the birefringence of a PEO(2000)-2.0G-S film as a function of temperature. 109

Figure 6.10 Atomic force micrograph(a) of a PEO(2000)-1.0G-S film and the corresponding 2-D FFT(b). 110

Figure 6.11 Atomic force micrograph of a PEO(2000)-3.0G-S film coated on a freshly cleaved mica substrate. 110

List of Tables

Table 2.1 Table of theoretically expected and experimentally obtained ratios between the unreactive PEO methoxy terminal group and the methyl terminal groups of the half generation PEO-PAMAM diblock copolymers 35

Table 2.2 Percentage of amine groups on the dendrimer block substituted determined using ^{1}H NMR. Tabulated as a ratio of the methyl groups on the stearate ends of the dendrimer block to the PEO backbone protons. 40

Table 3.1 GPC results for PEO-PAMAM diblock copolymers 52

Table 4.1 Limiting area per molecule from extrapolation of the condensed phase region of the isotherm for the modified linear-dendritic diblock copolymers 65

Table 6.1 Thermal characterization of stearate terminated PEO(2000)-dendrimer diblock copolymers 98

Chapter 1. Introduction and Background

1.1 Motivation

Dendrimers are a new class of polymers and have a well-defined, symmetrically branched architecture. This uniquely branched architecture of the dendrimer macromolecule leads to a number of interesting properties, which have generated much excitement in the use of dendrimers as building blocks for new functional materials. In particular, the presence of nano-voids in the interior of the molecule at high molecular weights has led to extensive speculation but little research on their potential as separations materials. Apart from separations applications, nanoporous dendrimers are promising candidates for the enhancement of a host of other applications including the encapsulation and controlled release of guest molecules, catalysis sites, ion channels etc.

Most of these potential applications would benefit from an ability to form cohesive films of dendrimers. However, the highly branched nature of dendrimers also results in very few entanglements and poor film forming capabilities. The combination of dendrimeric molecules and linear polymers to give novel hybrid linear-dendritic diblock copolymers is one approach to engineering a material that offers the ability to exploit the nanoporous nature of the dendrimer while introducing entanglements to obtain better films. The diblock copolymer also presents the possibility of obtaining self assembled structures, especially if bulk morphology is induced by phase segregation of the two component blocks. Despite this recognized potential for hybrid linear-dendritic diblocks, very few studies on the properties and film forming capabilities of these copolymers have been published so far. The thesis research reported here was aimed at investigating some of the fundamental issues involved in making ordered films of novel linear-dendritic diblock copolymers. Although, a study of the films of linear-dendritic diblock copolymers is relevant to all potential applications, gas separation applications were targeted to focus the scope of this research.

The concept of separating gases with polymeric membranes is more than a hundred years old. Today, most of the organic polymers used for gas separation fall into

the category of solution-diffusion membranes[1]. These membranes are so named because transport occurs when gas molecules dissolve into the membrane and diffuse across it; separation is based on the inherent differences in solubility and diffusivity. Examples of polymers used for gas separation include cellulose derivatives, polysulfones, polyamides, and polyimides. Most commercial solution-diffusion membranes have an asymmetric morphology consisting of a dense, thin top layer, referred to as the skin, supported by a porous sublayer. Separation is achieved in the homogenous top layer of the membrane, and flux through the membrane is inversely proportional to the thickness of this layer. To achieve higher throughput, it is important to make the skin layer as thin as possible while maintaining integrity. Film thickness of 1500Å or less are desirable for the selective skin in these composite membranes.

Synthesis of polymeric materials capable of achieving gas separation based on the principle of molecular sieving has been very difficult because of the small sizes of gases. Although microporous polymeric membranes have been made, the control of pore sizes in the range needed for size-based separation of gases has not been possible. In this regard, hybrid linear-dendritic diblock copolymers are promising candidates for the construction of ultrathin nanoporous films for gas separation applications. For these materials, the size and shape of the nanopores in the dendrimer block are defined by the chemical structure and branched nature of the dendrimer repeat unit. These two structural parameters can be engineered to make the hybrid copolymeric materials suitable for size-based separations in general. The diblock structure allows the use of self-assembly techniques such as Langmuir-Blodgett method, block copolymer selective adsorption, or ionic multilayer adsorption to make ultrathin films. As the diblock structure introduces the possibility of forming microphase segregated block copolymer morphologies, bulk diffusion properties of thicker films should also prove to be interesting.

1.2 Research Objectives

The objective of this project was to design, synthesize, and characterize a series of new linear-dendritic diblock copolymers as part of a program directed towards the investigation of their use as separations materials. As a first step towards making membranes, Langmuir-Blodgett(LB), spin-cast, and melt cast films were investigated. The hybrid copolymer was designed to be amphiphilic with a hydrophilic polyethyleneoxide(PEO) linear block and a hydrophobic polyamidoamine(PAMAM) dendritic block. In addition to the potential for self-assembly afforded by the amphiphilic nature of the diblock copolymer, the presence of the hydrophilic and hydrophobic components was essential to the use of LB techniques to make ordered thin films.

PEO was chosen as the linear block because it is soluble both in water and organic solvents, and is available in a number of different molecular weights. PAMAM was chosen as the dendron block for its ease of synthesis and functionalizable terminal amino groups. A schematic of the molecular architecture of the diblock copolymer and its orientation at the air-water interface of a Langmuir trough is shown in Figure 1.1. The functionalized hydrophobic dendron is expected to lie at the air side of the interface(Figure 1.1). Such monolayers can be transferred onto a solid substrate to build multilayer ultrathin films of the hybrid copolymers.

This chapter has a discussion on dendrimer macromolecules and the Langmuir-Blodgett(LB) technique. A literature review of the studies on gas permeation through LB films is included.

Chapter 2 provides the details relating to the synthesis and chemical modifications of PEO-PAMAM diblock copolymers. Chapter 3 discusses the solution properties of the synthesized diblocks. Chapter 4 presents the behavior of these diblock copolymers at the air-water interface. Chapter 5 describes the films made using the LB technique. Chapter 6 discusses the bulk morphology results and how they may be used to make ordered spin coated films. Chapter 7 summarizes this investigation and suggests future directions.

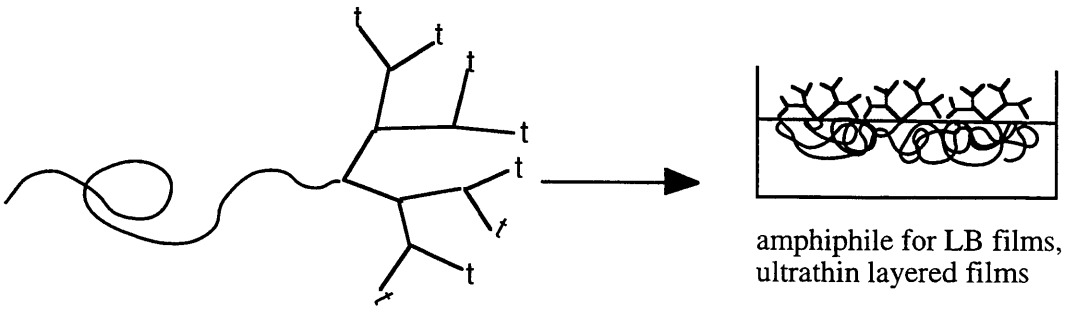

Figure 1.1 Schematic of the linear-dendritic diblock architecture and its monolayer at the air-water interface of a Langmuir trough.

1.3 Background

1.3.1 Dendrimers

Dendrimer macromolecules are regularly branched polymers with a treelike structure that possess three distinguishing structural features: (a) initiator core, (b) interior layers (number of generations = G) of repeating units radially attached to the core, and (c) exterior surface of terminal functionality. Two dimensional projections of dendrimers, with core multiplicity, N_c=3, and branch multiplicity, N_b=2, illustrating the concentric construction of tiers (generations) around the initiator core, I, are shown in Figure 1.2.

The synthesis of dendritic polymers with many different chemical compositions and architectures have been reported in the literature[2,3]. Some examples of dendrimers include polyamido alcohols (arborols), polyamides (denkewalter), polyarylester, polyamidoamines (PAMAM), and polyimines. The most well characterized of these are the polyamidoamines (PAMAM) synthesized by Tomalia and coworkers[2c] and the polyarylethers synthesized by Frechet et al.[4]

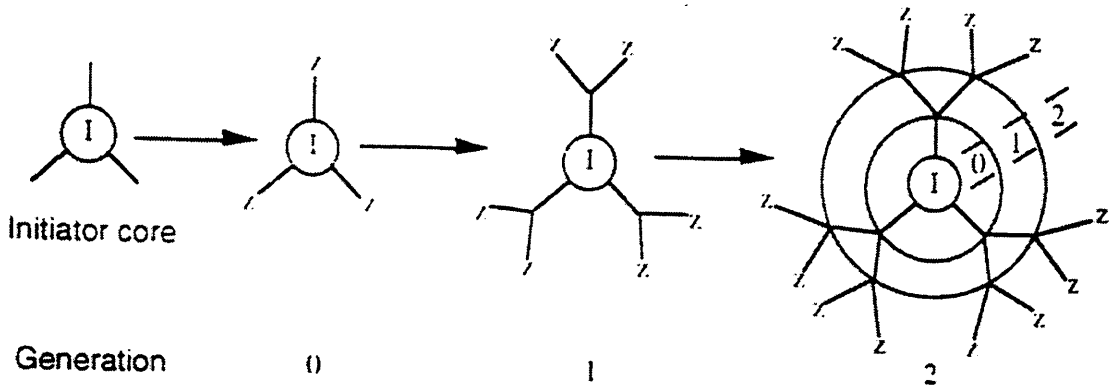

Figure 1.2[5] Two dimensional representation of an initiator core, core cell, and tridendron dendrimers of different generations.

Dendrimer synthesis is typically a stepwise process. The two basic strategies employed include the divergent growth or the core-first method and convergent growth or the arm-first method[6]. In the divergent route to dendrimer synthesis, generations of repeat units are built around a multifunctional core and molecule grows radially outward. This technique was developed by Tomalia and coworkers[2c] and used to synthesize the first PAMAM dendrimers. Frechet and associates[5] and Miller et al.[7] pioneered the convergent synthetic approach for dendrimer synthesis. In this case, wedge shaped dendrons are synthesized starting from the periphery and then attached to a multifunctional core. Among the dendrimers synthesized with this technique are phenyl ether and aryl ester based compounds.

As concentric tiers are added to the central core, the diameter of these dendrimers grows about 10 Å/generation in an approximately linear fashion. The molecular mass on the other hand increases exponentially, and is proportional to $2^{(G\# - 1)}$ where G# is the number of the generation. The surface groups also accumulate exponentially, and so the surface becomes saturated at a given generation number beyond which it is impossible to grow the molecule to completion, i.e. steric constraints prevent all the end groups from reacting. This is referred to as the 'starburst limited' generation[8].

A consequence of the exponential growth in the number of surface groups is expressed in the solvation characteristics of the dendrimer. The solubility of these macromolecules tends to be strongly dependent on the functionality of the surface groups[3]. For example, polybenzylethers with very hydrophobic interiors can be made water-soluble if functionalised with ionic groups at the surface[8]. Another physical property that is affected by the number and the chemical functionality of end groups is the glass transition temperature(T_g). The individual contributions from the chain end groups and the repeat units in the transition temperature is currently not well understood. However, the glass transition temperature of a dendrimer is found to increase with an increase in the polarity of the end groups[9].

Dendrimeric macromolecules have some unique and interesting properties which can be correlated to their architecture. For linear polymers and most macromolecules including branched polymers, the intrinsic viscosity increases with molecular weight according to the Mark-Houwink-Sakurada equation. Unlike all these other macromolecules, dendrimers do not obey this relationship once a threshold molecular weight is reached[10]. The volume of the dendrimer molecule increases cubically while the molecular weight increases exponentially with generation number G, a relation which does not hold true for other polymers. This relationship in dendrimers can be utilized to estimate the variation of intrinsic viscosity, which is proportional to the ratio of volume and molecular weight, with generation number. For example, the ratio of volume and molecular weight for dendrimers with a branch multiplicity of two is $G^3/2^{(G-1)}$. The value of this ratio is 4 for generation 2, 6.75 for generation 3, 8 for generation 4, 7.8125 for generation 5, and 6.75 again for generation 6.

The unusual relationship between the intrinsic viscosity and molecular weight can also be correlated to the shape of the molecule. The dendrimer has an extended structure at low molecular weights that becomes more spherical at higher generations. The aspect ratio which quantifies this transition (for PAMAM's) decreases from 4.5 for generation 0

to 1.3 for generations 5 and 6[11]. It is noteworthy that this transition takes place at approximately the same molecular weight as implied by the intrinsic viscosity results.

A few theoretical and numerical studies aimed at calculating the intramolecular density profiles have been attempted. The theoretical studies predict the presence of void volume in the interior, i.e. a nonhomogenous density profile capable of hosting smaller molecules[12]. Numerical studies, in contrast, predict that the density will be uniform throughout the molecule[13]. Experiments done by Jansen et al. on polypropyleneimine dendrimers show that they can act as hosts for small dye molecules and confirm the presence of internal voids in these dendrimers[14]. PAMAM and polybenzylether dendrimers have shown a similar capability to act as hosts for smaller molecules. The unsymmetrically branched denkewalter dendrimers on the other hand have a less dense surface compared to their core[15]. The ability of the exterior repeat units of the dendrimer to fold back into the interior of the molecule greatly affects the density distribution. Chemical differences between the exterior and the interior of a dendrimer, flexibility of repeat units and end groups, and choice of solvent will also modify the density profile.

Dendrimeric homopolymers have been combined with linear polymers giving a variety of fascinating copolymeric architectures. Linear-dendritic diblock copolymers are one example of this class of novel copolymers.

Linear-Dendritic Block Copolymers

Hybrid linear-dendritic block copolymers have been synthesized by several groups. Frechet et al.[16] synthesized diblocks and triblocks with a polyethylene oxide (PEO) block and a polyether dendrimer block. Depending on the solvent and the molecular weights of the two blocks, the copolymer forms unimolecular micelles or multimolecular micelles[16]. Meijer and co-workers synthesized diblocks where the linear block was polystyrene and the dendritic one was poly(propylene imine). They have shown that the aggregation behavior of these amphiphiles in solution is a function of the

molecular weights of the two blocks[17]. Similar work has been done by Chapman et al.[18] with linear PEO and dendritic poly(α-ε-L-lysine) and Aoi and co-workers[19] with linear polyoxazoline and dendritic polyamidoamine(PAMAM).

Although these studies have shown that linear-dendritic diblock copolymers can behave like surfactants, the behavior of these polymers at the air-water interface has not been investigated so far. Studies on the bulk morphology of these hybrid amphiphiles have also not been reported.

Thin films of Dendrimers

To investigate the potential for various applications, thin films of dendrimers have been studied by a number of groups. A variety of techniques have been used to make these films. Watanabe and Regen[20] studied multilayers of dendrimers (PAMAM's) prepared by sequential deposition of these macromolecules on a Pt^{+2} bearing silicon surface. The presence of Pt^{+2} at the surface was found to be necessary for the growth of the multilayers. AFM scans revealed that the dendrimer coverage was extensive and that the surface was smooth at the molecular level. Tsukruk et al. used alternate layers of acid and amine terminated PAMAM dendrimers to make thin films[21]. The film thickness was in the range of 20 to 80nm for these ionic dendrimer multilayers. Spin-coated films of luminescent dendrimers with a thickness of 60-120nm were made by Wang et al.[22] Additionally, there are a few examples of thicker films made by solvent casting[23]. PAMAM dendrimers have been covalently attached to a self-assembled monolayer for chemical sensing applications[24]. These dendrimers embedded within self-assembled monolayers have been shown to act as ion gates of molecular dimension[25]. PAMAM modified surfaces, made by spontaneous chemisorption onto glass, have been used as substrates for the deposition of noble metal colloids[26]. Electrode surfaces have also been modified with redox-active polymetallic dendrimers[27].

White and Frechet[28] used neutron reflectivity and π-A isotherm measurements to study Langmuir monolayers of polyether dendrimers at the air-water interface. They

measured the thickness of the dendrimer monolayer at the air-water interface as a function of the surface pressure. Interestingly, the shape of the molecules at the interface though spherical initially, became distorted and assumed an ellipsoidal shape, twice as high as broad. White and Frechet did not attempt to transfer the monolayer onto a substrate to form films. A couple of attempts at making LB films of dendrimers have been reported. Multilayer LB films of hyperbranched polyphenylenes prepared by transfer of monolayers onto a silicon substrate was reported by Kim[29]. Schenning et al.[30] made multi layer films of palmitoly-functionalized polypropyleneimine dendrimers.

No comparable studies on the Langmuir behavior or LB films of linear-dendritic diblock copolymers have yet been published.

1.3.2 Langmuir-Blodgett Technique

The Langmuir-Blodgett(LB) technique for the preparation of thin films has been around for a long time and a vast amount of literature exists on the subject[31]. A lot of the initial work dealt with characterizing the films and studying the relationship between the chemical structure of the amphiphile and the properties of the corresponding LB film.

Figure 1.3 is a schematic of the basic apparatus, the Langmuir trough, used to deposit monolayers on solid substrates. In this scheme, *a* is a bath, usually made out of teflon; *b*, a moving barrier that allows control of the pressure applied on the monolayer; *c*, a motor that moves the barrier; *d*, a control device that gets information from a pressure sensor on the water surface and controls the pressure; *e*, a balance that measures the surface pressure; *f*, a motor with a gearbox that lowers and raises the substrate; and *g*, a solid substrate.

In a typical experiment, a drop of a dilute solution of an amphiphilic molecule in a volatile solvent (e.g., $CHCl_3$) is spread on the water-air interface of a trough. The solvent evaporates leaving a monolayer of the molecules in what is called a two-dimensional gas because of the relatively large distances between the molecules (Figure 1.4). The barrier

then moves and compresses the molecules on the water-air interface, while the pressure and area per molecule are recorded.

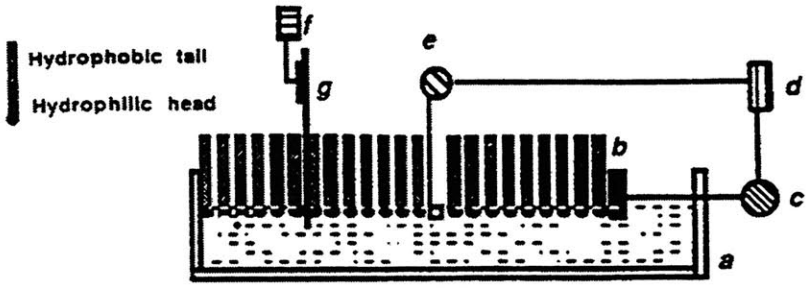

Figure 1.3[31] A trough for deposition of monolayers on solid substrates.

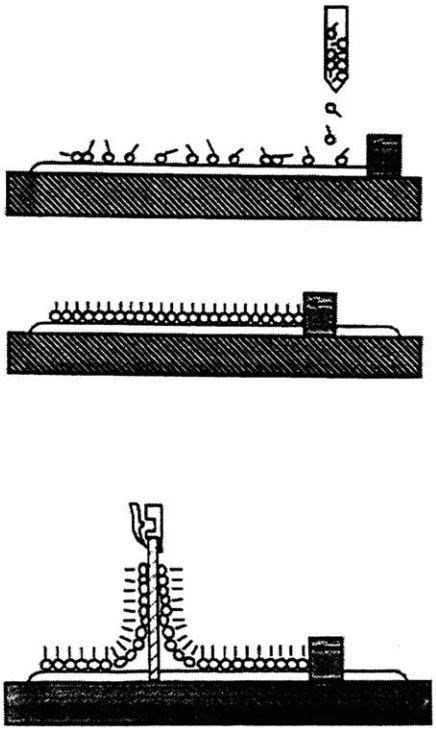

Figure 1.4[31] A monolayer in the spread form, in the compressed form, and being deposited onto a substrate.

The surface pressure, π, is equal to (σ_o- σ) (in newtons/meter, or dyne/cm) where σ_o is the surface tension of water and σ is the surface tension of water covered with a monolayer. The total number of molecules and the total area that the monolayer occupies being known, the area per molecule can be calculated. From these values, a π-A isotherm describing the surface pressure as a function of the area of the molecule can be constructed. Figure 1.5 presents a schematic isotherm of stearic acid on 0.01 HCl[31]. Phase transitions that take place when the molecules are compressed can be observed in the isotherm. The pressure-area isotherm gives valuable information about the stability of the monolayer at the water-air interface, phase transitions, and conformational transformations.

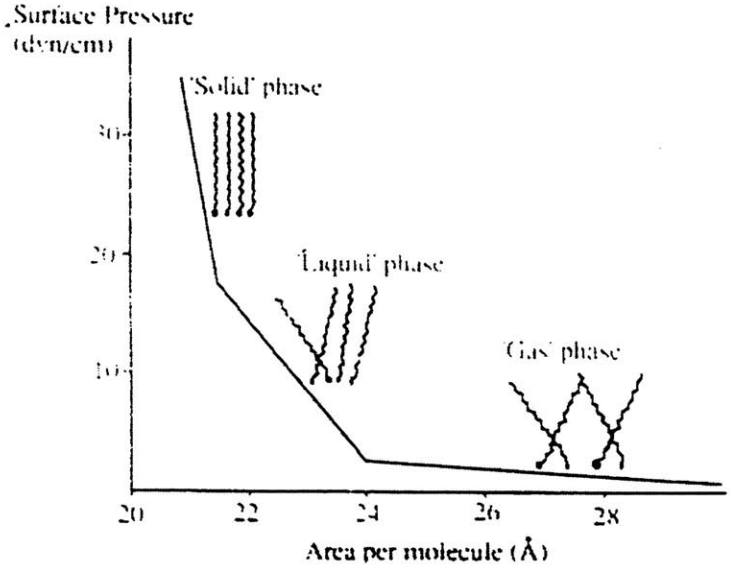

Figure 1.5[31] Schematic of surface pressure(π) vs. area per molecule(Å) for stearic acid on 0.01M HCl.

When a substrate is moved through the monolayer at the water-air interface, the monolayer can be transferred during emersion (retraction or upstroke) or immersion (dipping or downstroke). A monolayer usually will be transferred during retraction when the substrate is hydrophilic, and the hydrophilic head groups interact with the surface. If the substrate is hydrophobic, the monolayer will be transferred in the immersion, and the hydrophobic alkyl chains interact with the surface. If the deposition process starts with a hydrophilic substrate, it becomes hydrophobic after the first monolayer, and thus the second monolayer will be transferred in the immersion. This is the usual mode of multilayer formation and is called Y-type deposition. In some cases, transfer of the monolayer occurs only on one stroke. Multilayers formed by deposition on the downstroke only are called X-type films and those formed by deposition on the upstroke are called Z-type films.

The monolayer behavior at the air-water interface of a Langmuir trough is usually a kinetic phenomenon and the transfer of these monolayers onto substrates gives physisorbed films. Therefore, a number of parameters such as subphase pH, compression time, speed of monolayer transfer, interactions between layers in a film etc. affect the quality of LB films obtained. Typically, for a given amphiphile the conditions needed for the formation of good multilayer films are dependent on all these parameters.

1.4 Gas permeation through LB films

In pioneering studies, Rose and Quinn examined the permeation characteristics of a series of conventional LB films that were transferred to a silicone support[32]. They found that the peameability of the LB component was consistently greater for CO_2 than for either He or N_2, indicating that the mass transfer process was not primarily a result of molecular sieving.

To improve the mechanical and chemical stability of the LB film the replacement of the conventional film forming molecules by polymerizable amphiphiles and amphiphilic polymers has been attempted. Albrecht et al.[33] carried out the UV

polymerization of diacetylene LB films deposited on a polypropylene support and reported that the polymerization did not affect the CH_4 flow rate. Usually, polymerization reactions bring about structural reorganizations which induce defects in the multilayers. The latter result is therefore significant and demonstrates that LB films can be stabilized by polymerization without necessarily inducing defects.

However, the polymerization of the diacetylene results in a LB film with a very rigid, inflexible backbone limiting the application for separation processes. To overcome this problem, preformed polymers in which the hydrocarbon part is separated from the polymer backbone either by a hydrophilic spacer unit or by ionic bonds have been designed. Stroeve and coworkers[34] investigated the permeation properties of multilayers of pre-formed amphiphilic methacrylate polymers transferred onto a stretched polypropylene substrate (Celgard). Gas permeation did markedly decrease with an increasing number of layers, but in two of the three polymers, the gas permeability of N_2, CH_4, and CO_2 was merely a function of molecular weight.

Higashi and co-workers[35] have reported a modest separation of O_2 and N_2 by employing 76 layers of a fluorocarbon amphiphile on a porous alumina membrane. Separation was achieved by exploiting the difference in solubility of the gases in the thin surfactant skin. The ratio of the oxygen and nitrogen permeation rates, α, was found to be 3.2 at 16.5°C. It is noteworthy that this value is slightly higher than the α-value of a plasma-polymerized hexamethyldisiloxane film of 150nm thickness. It is also the highest reported α value for a LB layer.

Permeation of O_2 and N_2 through an LB film of poly(N-dodecylacrylamide) was studied by Miyashita et al.[36] The separation factor, α, was slightly smaller than that reported for the fluorocarbon amphiphile in the preceding paragraph, but the permeation rate of oxygen was about an order of magnitude higher.

In almost all the amphiphiles discussed above, the linear hydrocarbon or flourocarbon chains crystallize in the densely packed LB layers resulting in very low permeation rates. Moreover, the separation of gases by these LB films is mainly

dependent on the differences in solubility and diffusivity of the gases through the LB layer. The use of molecular sieving as the basis of separation in a LB film has been attempted by only one group so far.

Regen et al.[37] synthesized and characterized the permeation properties of LB multilayers of porous surfactant derivatives of calix(n)arenes (I). They utilized three different types of substrate materials: Celgard and Nuclepore, which both have large permanent pore structures and cast films of poly[(1-trimethylsilyl)-1-propyne] (PTMSP), which is a continuous polymeric surface. They concluded that a continuous polymeric surface was preferable as a LB support. The He/SF_6 and He/N_2 selectivities of LB composites with PTMSP were much higher than those predicted by Graham's law[37]. Further studies showed that permeation across these LB films was governed by diffusion through interstitial pores between neighboring molecules and not through molecular pores of the calix(n)arenes for monolayers greater than four[38].

Dendritic structures have certain inherent advantages when compared to those of the amphiphiles discussed in this section. They are non-crystalline and it is unlikely that LB layers of the linear-dendritic diblock amphiphiles will be crystalline. Secondly, at higher molecular weights they have a porous interior that, though not as well controlled as calix(n)arenes, may enable some separation as a result of molecular sieving.

1.5 References

1. Hensema, E.R., *Adv. Mater.*, **1994**, 6, 4, 269.
2. (a) Buhleier, E.; Wehner, W.; Vogtle, F., *Synthesis*, **1978**, 155, (b) Aharoni, S.M.; Crosby III, C.R.; Walsh, E.K., *Macromolecules*, **1982**, 15, 1093, (c) Tomalia, D.A.; Baker, H.; Dewald, J.; Hall, M.; Kallos, G.; Martin, S.; Roeck,J.; Ryder, J.; Smith, P., *Macromolecules*, **1986**, 19, 2466.
3. Newkome, G.R.; Moorefield, C.N.; Vogtle, F., "*Dendritic Molecules: Concepts, Syntheses, Perspectives,*" **1996**, VCH Publishers, Inc., New York, NY.
4. Wooley, K.L.; Hawker, C.J.; Frechet, J.M.J., *J. Am. Chem. Soc.*, **1991**, 113, 4252.

5. Tomalia, D.A.; Hedstrand, D.M.; Ferrito, M.S., *Macromolecules*, **1991**, 24, 6, 1435.
6. Matthews, O.A.; Shipway, A.W.; Stoddart, J.F., *Prog. Polym. Sci.*, **1998**, 23, 1.
7. Miller, T.M.; Kwock, E.W.; Neenan, T.X., *Macromolecules*, **1992**, 25, 3143.
8. Hawker, C.J.; Frechet, J.M.J., *J. Chem. Soc. Perkin Trans.*, **1992**, 1, 2459.
9. (a) Wooley, K.L.; Hawker, C.J.; Pochan, J.M.; Frechet, J.M.J., *Macromolecules*, **1993**, 26, 1514, (b) Kim, Y.H.; Beckenbaeur, R., *Macromolecules*, **1994**, 27, 1968.
10. Mourey, T.H.; Turner, S.R.; Rubenstein, M.; Frechet, J.M.J.; Hawker, C.J.; Wooley, K.L., *Macromolecules*, **1992**, 25, 2401.
11. Tomalia, D.A.; Naylor, A.M.; Goddard III, W.A., *Agnew. Chem. Int. Ed. Engl.*, **1990**, 29, 138.
12. (a) Maciejewski, M., *J. Macromol. Sci.-Chem.*, **1982,** A17(4), 689, (b) de Gennes, P.G.; Hervet, H., *J. Physique-Lettres*, **1983**, 44, L-351.
13. Lescanec, R.L.; Muthukumar, M., *Macromolecules*, **1991**, 24, 4892.
14. Jansen, J.F.G.A.; de Brabander-van den Berg, E.M.M.; Meijer, E.W., *Science*, **1994**, 1226, 266.
15. (a) Aharoni, S.M.; Murthy, N.S., *Polymer Commun.*, **1983**, 24, 132, (b) Aharoni, S.M., Crosby III, C.R.; Walsh, E.K., *Macromolecules*, **1982**, 15, 1093.
16. (a) Gitsov, I; Wooley,K.L.; Hawker, C.J.; Ivanova,P.T.; Frechet, J.M.J., *Macromolecules*, **1993**, 26, 5621, (b) Gitsov,I.; Frechet, J.M.J., *Macromolecules*, **1993**, 26, 6536.
17. (a) van Hest, J.C.M.; Delnoye, D.A.P.; baars, M.W.P.L.; van Genderen, M.H.P.; Meijer, E.W., *Science*, **1995**, 268, 1592, (b) van Hest, J.C.M; baars, M.W.P.L.; Elissen-Roman, C; Meijer, E.W., *Macromolecules*, **1995**, 28, 6689.
18. Chapman, T.M.; Hillyer, G.L.; Mahan, E.J.; Shaffer, K.A., *J. Am. Chem. Soc.*, **1994**, 116, 11195.
19. Aoi, K.; Motoda, A.; Okada, M.; Imae, T., *Macromol. Rapid Commun.*, **1997**, 18, 945.
20. Watanabe, S; Regen, S.L., *J. Am. Chem. Soc.*, **1994**, 116, 8855.
21. Tsukruk, V.V.; Rinderspacher, F.; Bliznyuk, V. N., *Langmuir*, **1997**,13,8, 2172.
22. Wang, P-W.; Liu, Y-J; Devadoss, C.; Bharathi, P.; Moore, J.S., *Adv. Mat.*, **1996**, 8, 3, 237.
23. (a) Evenson, S.A.; Badyal, J.P.S., *Adv. Mat.*, **1997**, 9,14, 1097, (b) Coen,M.C.; Lorenz, K.; Kressler, J.; Frey, H.; Mulhaupt, R., *Macromolecules*, **1996**, 29, 8069.
24. (a) Wells, M; Crooks, R., *J. Am. Chem. Soc.*, **1996**, 118, 3988, (b) Tokuhisa, H.; Crooks, R., *Langmuir*, **1997**, 13, 5608.

25. Zhao, M.; Tokuhisa, H.; Crooks, R.M., *Angew. Chem. Int. Ed. Engl.*, **1997**, 36, 23.
26. Bar, G.; Rubin, S.; Cutts, R.W.; Taylor, T.N.; Zawodzinski Jr., T.A., *Langmuir*, **1996**, 12, 1172.
27. Alonso, B.; Moran, M.; Casado, C.; Lobete, F.; Losada, J.; Cuadrado, I., *Chem. Mater.*, **1995**, 7,1440.
28. Saville, P.M.; Reynolds, P.A.; White, J.M.; Hawker, C.J.; Frechet, J.M.J.; Wooley, K.L.; Penfold, J.; Webster, J.R.P., *J. Phys. Chem.*, **1995**, 99, 8283.
29. Kim, Y.H., *Advances in Dendritic Macromolecules*, Volume 2, **1995**, JAI Press Inc., 123.
30. Schenning, A.P.H.J.; Elissen-Roman, C.; Weener, J-W.; Baars, M.W.P.L.; van der Gaast, S.J.; Meijer, E.W., *J. Am. Chem. Soc.*, **1998**, 120, 8199.
31. Ulman, A., *An Introduction to Ultrathin Organic Films from Langmuir-Blodgett to Self-assembly*, **1991**, Academic Press Inc., New York.
32. Rose. G.D.; Quinn, J.A., *Science*, **1968**, 159, 636.
33. (a) Albrecht,O.; Laschewsky, A.; Ringsdorf, H., *Macromolecules*, **1984**, 17,937, (b) Albrecht, O.; Laschewsky, A.; Ringsdorf, H., *J. Membr. Sci.*, **1985**, 22, 187.
34. Stroeve, P.; Coelho, M.A.N.; Dong, S.; Lam, P.; Coleman, L.B.; Fiske, T.G.; Ringdorf, H.; Schneider, J., *Thin Solid Films*, **1989**, 180, 241.
35. Higashi, N.; Kunitake, T.; Kajiyana, *Polym. J.*, **1987**, 19, 289.
36. Miyashita, T.; Konno, M.; Matsuda, M.; Saito, S., Macromolecules, 1990, 23, 3531.
37. (a) Conner, M; Janout, V.; Regen, S.L., *J. Am. Chem. Soc.*, **1993**, 115, 1178, (b) Conner, M; Janout, V.; Kudelka, I.; Dedek,P.; Zhu, J.; Regen, S.L., *Langmuir*, **1993**, 9,2389.
38. Dedek, P.; Webber, A.S.; Janout, V.; Hendel, R.A.; Regen, S.L., *Langmuir*, **1994**, 10, 3943.

Chapter 2. Synthesis of PEO-PAMAM Linear-Dendritic Diblock Copolymers*

2.1 Introduction

Dendrimers have been of particular interest to the polymer science community in the past twenty years. These materials present a new, well-defined architecture and a large degree of functionality in a single macromolecule. A wide variety of dendrimers with different chemistries have been synthesized[1,2,3]. The large excess of reagents needed to achieve complete conversion makes the synthesis of the dendrimer macromolecules very challenging. Initially, most of the multifunctional cores used for dendrimer synthesis were small molecules, giving rise to globular structures at high molecular weight. With an increasing understanding of the synthetic conditions, different architectures incorporating the dendrimer structure have been synthesized. These include dendritic diblocks with dendrons of different repeat unit structure attached to the same core[4], dumb-bell shaped copolymers with dendrons at both ends of a linear chain[5], and mushroom shaped structures with dendrons attached to one end of a linear chain[6-10]. Dendrimeric diblock copolymers with one linear block and one dendritic block have been synthesized by a number of different groups. Examples include PEO-Poly(L-lysine)[6], PS-Polypropyleneimine[7], PEO/PS-Polybenzylether[8,9], and Polyoxazoline-PAMAM[10]. The dendrimer blocks in PEO-Poly(L-lysine), PS-Polypropyleneimine, and Polyoxazoline-PAMAM diblocks were synthesized divergently from a monofunctional linear block. A couple of techniques have been used to synthesize the hybrid diblock copolymers containing polybenzylether dendrons. Gitsov and Frechet[8] synthesized the benzylether dendrons using a convergent technique and then attached them to a monofunctionalized linear block. Leduc et al.[9b,c] used a dendron possesing a benzylic halide group at its focal point for the metal catalyzed "living" radical polymerization of styrene. Matyjaszewski and co-workers[9a] used TEMPO-based stable radicals attached to the focal point of a

---

* Sections of this chapter have been published as: Iyer, J., Fleming, K., Hammond, P.T., *Macromolecules*, **1998**, 31, 25, 8757-8765.

dendron for the controlled radical polymerization of styrene, vinyl acetate, and methacrylates. In some cases, the aqueous solubility of the two blocks was dissimilar and the resulting diblocks were shown to be amphiphilic. The solubility of the diblocks have been modified by changing the chemical functionality of the dendrimer end group. van Hest et al.[11] showed that the aggregation behavior of PS-Poly(propyleneimine) diblocks could be changed by functionalizing the dendrimer end groups.

Here we report the synthesis of a new series of hybrid linear-dendritic diblock copolymers with polyethyleneoxide(PEO) as the linear block and polyamidoamine (PAMAM) as the dendritic block. Two different molecular weights of the PEO block were used. The chemical modification of the amine end groups of the dendrimer block to give amphiphilic linear-dendritic diblock copolymers is also reported.

2.2 Experimental Section

2.2.1 Materials

Chromatographically pure methoxy-PEO-amine with molecular weights of 2000 and 5000 were purchased from Shearwater Polymers. Methyl acrylate(99+%) purchased from Aldrich was washed two times with equal amounts of 5% NaOH solution followed by MilliQ (18.2 MΩcm) water to remove the hydroquinone monomethyl ether inhibitor. The washed methyl acrylate was dried with anhydrous magnesium sulfate overnight before use. Ethylene diamine(99+%) from Aldrich was distilled before use. 1,3-dicyclohexylcarbodiimide(DCC) and stearic acid were purchased from Aldrich and used without further purification.

2.2.2 Instrumentation

^{1}H NMR spectra were recorded at room temperature on a Bruker 400 (400 MHz) instrument. FTIR spectra of films cast on KBr pellet were recorded on a Nicolet Magna-IR 550 spectrometer. A Bruker BIFLEX III MALDI-TOF MS was used in the reflector

mode with a HABA matrix at 20kv for recording the spectra of PEO(5000)-1.5G and PEO(5000)-2.5G. A Bruker PROFLEX MALDI-TOF MS was used with an αC-I matrix for recording the spectra of PEO(5000)-3.5G and PEO(5000)-4.5G.

2.2.3 Synthesis of PEO(5000) series

Synthesis of the dendrimer block onto the monofunctionalized PEO core involves two reactions, Michael addition and amidation. For Michael addition, the concentration of methyl acrylate reagent and primary amine in the reaction mixture ranged from 5.4-8.5M and 0.01-0.05M respectively. Methanol was used as the solvent and the reaction was conducted at room temperature for 24-48 hours depending on the generation of the dendrimer, after which the methanol and methyl acrylate were removed under vacuum.

The amidation was run with methanol as the solvent and an ethylene diamine concentration of 11-12M at a temperature of 50°C for 48 hours. At the end of the reaction, ethylene diamine and methanol were removed under vacuum.

For all reactions, the poor solubility of the PEO linear block in anhydrous ethyl ether was exploited to effectively separate the diblock products and the reactants. In general, all the synthesis steps produced yields of about 80-95%. Higher yields were obtained when care was taken to ensure complete removal of solvent(methanol) and excess reactants(methyl acrylate and ethylene diamine) using vacuum after completion of the reactions. NaCN was initially used as a mild catalyst in the amidation step[12] but subsequent synthesis of the linear-dendrimer diblock series without the NaCN catalyst showed the catalyst to be unnecessary. The details of the synthesic conditions and characterization results are given in Appendix A.1.

2.2.4 Synthesis of the PEO(2000) series

The synthesis procedure for the PEO(2000)-dendrimer diblock series from PEO(2000) core follows the scheme and molar concentrations outlined above for the

PEO(5000)-dendrimer diblock series. The details of the ^{1}H NMR and FTIR results are given in Appendix A.2.

2.2.5 End group modification of PEO(2000)-PAMAM diblocks

Stearate terminated groups: 0.597g(2.1mM) of stearic acid and 0.216g(1.05mM) of DCC were each dissolved in 5ml of chloroform, the two solutions mixed together and stirred for one hour. A white precipitate of N,N'-dicyclohexylurea(DCU) was formed and was filtered off. The filtrate, a clear solution of stearic anhydride, was added dropwise to a solution of PEO(2k)-2.0G (0.2g) in chloroform(5ml). The molar ratio of amine groups on the diblock to the stearic anhydride was 1:3.5. After 16 hours, the chloroform was removed by rotovaporation. The remaining residue was washed with 400-500ml of ethyl ether to remove excess reagents. The product[PEO(2k)-2.0G-S], a white precipitate, was dried over vacuum.

Other group: 0.53g(3.0mM) of an aryl vinyl acid($COOH-C_6H_4-O-CH_2-CH=CH_2$) and 0.31g(1.5mM) of DCC were dissolved in DMF and stirred at room temperature for half an hour. This solution was added slowly to 5ml of DMF containing 0.2g of PEO(2k)-3.0G. After 16 hours, the DMF was removed by rotovaporation. 10ml of methylene chloride was added to the residue and the undissolved material was removed by filtration. The methylene chloride was removed under vacuum and 75ml of water was added to the remainder. The undissolved material, being the unreacted reagent, was filtered out. The water was removed with rotovaporation followed by drying under vacuum. The residue obtained, a yellowish and viscous liquid, was the desired product.

2.3 Results and Discussion

A new series of dendrimeric amphiphilic block copolymers were synthesized following the scheme shown in Figure 2.1. The synthesis of the PAMAM dendrimer block onto the CH_3O-PEO-NH_2 core consisted of two steps alternately repeated to achieve higher generations and followed the divergent synthesis technique established by

Tomalia[13]. In the first step, exhaustive Michael addition of methyl acrylate to the primary amine terminal groups of the PEO core resulted in a tertiary amine branch point with methyl ester terminal groups (Figure 2.1). The methyl ester terminal group was reacted in the second step with ethylene diamine to regenerate the primary amine terminal groups (Step 2). Using this scheme, two series of diblock copolymers with a linear PEO block and a dendritic polyamidoamine block were synthesized. In the first series, the PEO tail had a molecular weight of 2000 with dendrimer generations going up to 4.0 [PEO2k-0.5G,1.0G,1.5G...4.0G]. In the second series, the PEO tail had a molecular weight of 5000 with dendrimer generations going up to 4.5 [PEO5k-0.5G,1.0G,1.5G....4.5G].

Most of the synthesized materials were white partially crystalline solids at room temperature. The chemical structure of the copolymers synthesized was verified using ^{1}H NMR and MALDI-TOF MS as described in detail in the experimental section. For illustrative purposes, the ^{1}H NMR spectra of PEO2k-1.5G is shown in Figure 2.2. The extent of conversion was measured by comparing the integral areas of the dendrimer ^{1}H peaks to that of the unreactive methoxy end group of the PEO tail. Good correspondence was found between the theoretically expected and experimentally obtained values for all the products synthesized, as shown in Table 2.1.

MALDI-TOF MS results for the PEO(5000) series are also included in Table 2.1. Figure 2.3 is a representative MALDI-TOF spectra for PEO(5k)-1.5G. These results are analogous to those of the Frechet group for benzylether dendrimer based hybrid-diblocks[14,8b]. MALDI-TOF results also agree well with theoretically expected molecular weight for the diblocks as shown in Table 2.1, suggesting the presence of very few defects in the final structure. Polydispersities calculated from the MALDI-TOF spectra are about 1.01. For the PEO(2000)-dendrimer diblock series, the MALDI-TOF results are available only for PEO(2k)-3.0G. Here too, the measured molecular weight is very close to the theoretically expected value (See Appendix A.2).

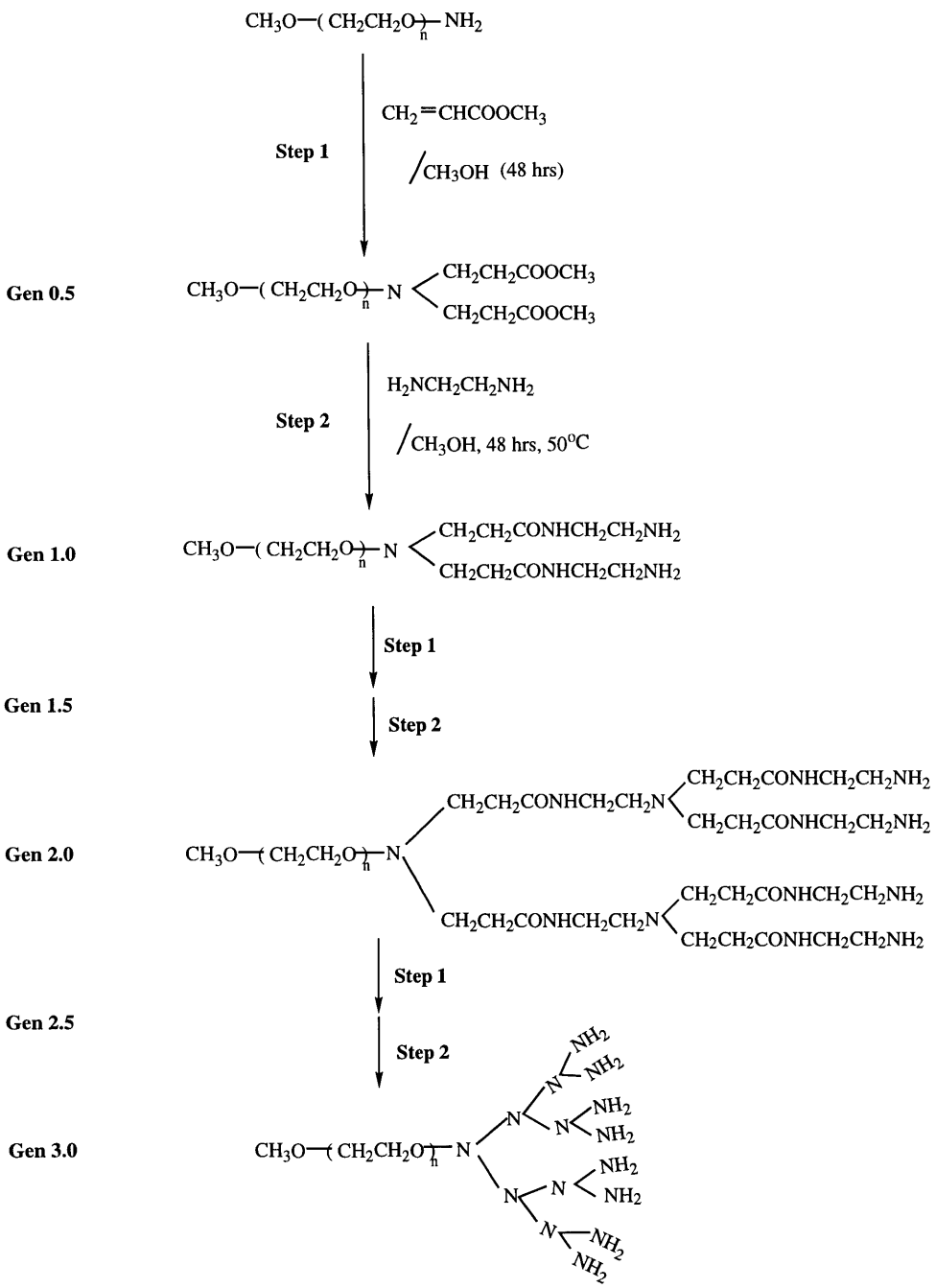

Figure 2.1 Synthesis of PEO-PAMAM linear-dendritic diblock copolymer

Table 2.1 Table of theoretically expected and experimentally obtained ratios between the PEO methoxy terminal group and the methyl ester terminal groups of the half generation PEO-PAMAM diblock copolymers

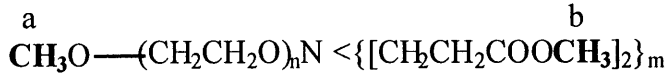

PEO-PAMAM Diblock	No. of dendrimer end groups(theoretical)	Theoretical ratio a:b	Experimental ratio a:b	M_w (theoretical)	M_w(MALDI-TOF)
PEO(5000)-0.5G	2	3:6	3:6	5174	-
PEO(5000)-1.5G	4	3:12	3:13.2	5400	5960
PEO(5000)-2.5G	8	3:24	3:21.4	6374	6056
PEO(5000)-3.5G	16	3:48	3:46.2	7974	7900
PEO(5000)-4.5G	32	3:96	3:92.4	11174	10750
PEO(2000)-0.5G	2	3:6	3:6.3	2174	-
PEO(2000)-1.5G	4	3:12	3:12.8	2400	-
PEO(2000)-2.5G	8	3:24	3:43.5*	3374	-
PEO(2000)-3.5G	16	3:48	3:50	4974	-

* a small amount of the reactant, methyl acrylate {CH_2=CHCOOCH$_3$}, was present and contributed to the signal at 3.65ppm

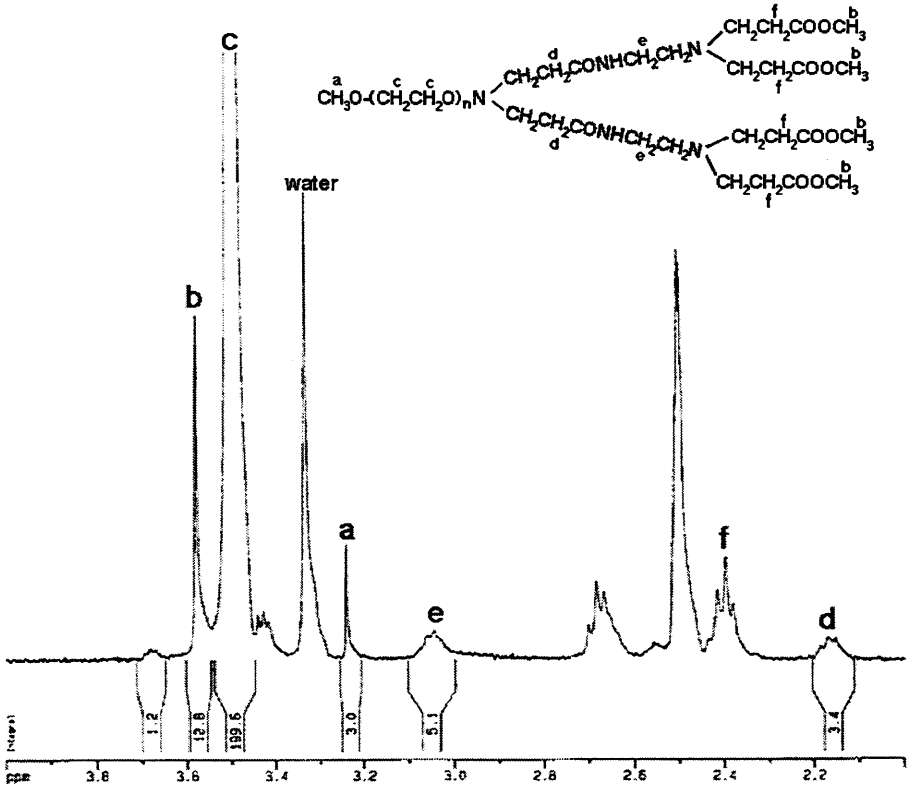

Figure 2.2 1H NMR spectra of PEO(2000)-1.5G. d_6-DMSO was used as the solvent

Though qualitative, FTIR spectra confirm the results obtained from ^{1}H NMR. The peak positions, as reported in Appendix A, are in good agreement with previous values obtained by other researchers for a similar class of materials[15,10].

The synthesis scheme for modification of the amine end groups of the PEO(2k)-PAMAM diblocks is shown in Figure 2.4 using stearic acid as an example[16,17,18]. In the first stage of synthesis, the carboxylic acid end group of stearic acid was reacted with DCC and converted to its anhydride form. The byproduct(DCU) was insoluble in the solvent and was filtered off. The filtrate was then added to a chloroform solution of PEO(2k)-full generation dendrimer diblock. After 16 hours, chloroform was removed by

rotovaporation and the residue was washed with ethyl ether to give PEO(2k)-PAMAM hybrid copolymer with stearate end groups.

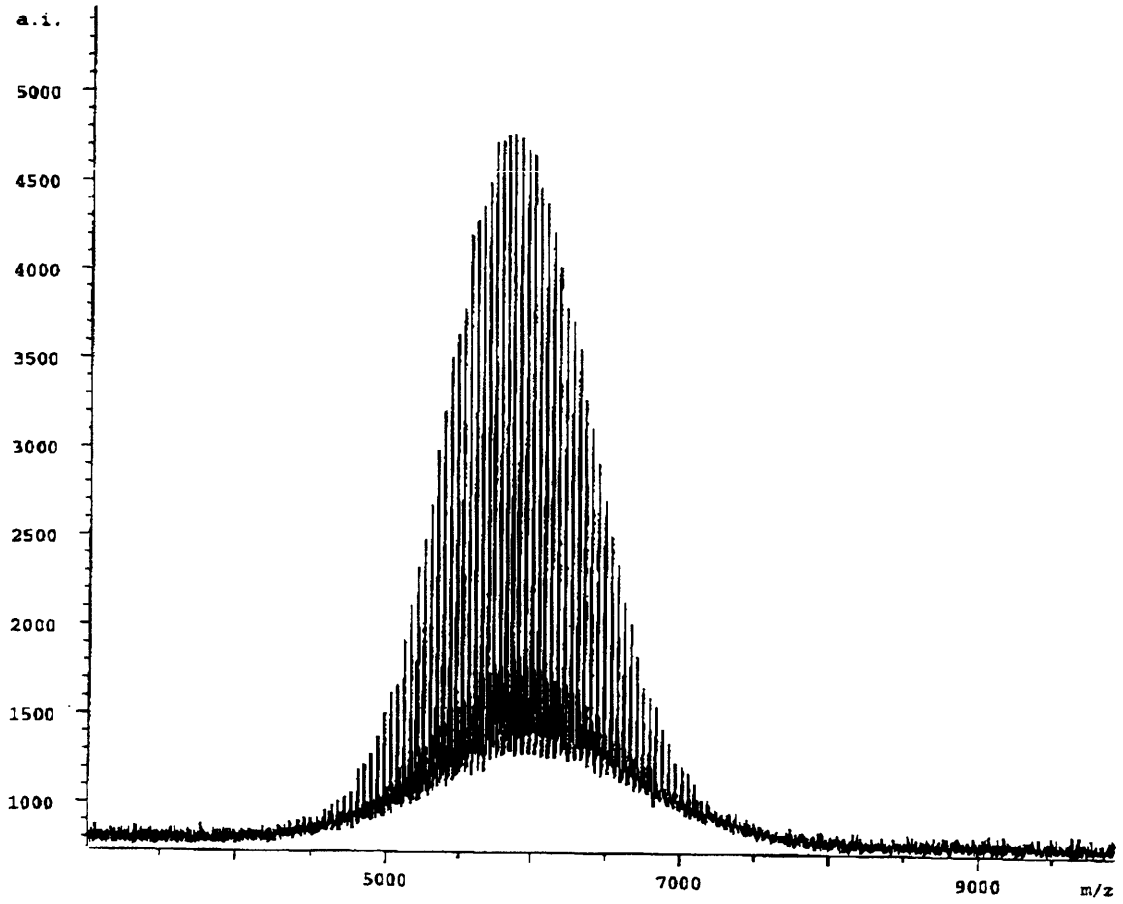

Figure 2.3 MALDI-TOF mass spectra of PEO(5000)-1.5G

The amine end groups of a series of linear-dendritic diblock copolymers, PEO(2k)-0.0G, 1.0G, 2.0G, 3.0G, 4.0G, have been converted to stearate groups using the scheme described above. As the modification step involves the reaction between carboxylic anhydride and amine groups of the dendrimer block, this technique can be used to change the end groups of the dendrimer block to any "R" from an organic molecule of the form "RCOOH". To examine the effects of a different type of nonpolar group, COOH-C_6H_4-O-CH_2-CH=CH_2 was also used to modify the end groups of PEO(2k)-3.0G.

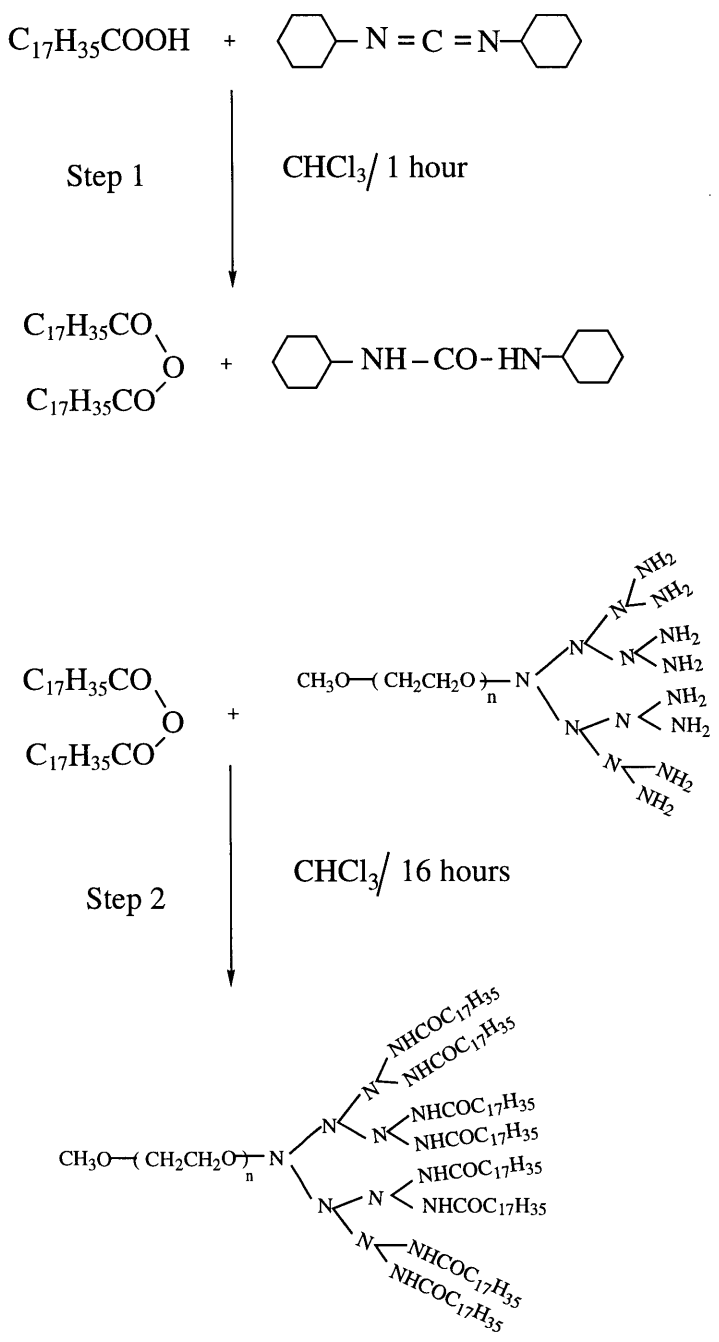

Figure 2.4 End group modification of PEO(2000)-3.0G with stearic acid.

The chemical structure and percent substitution of the stearate terminated diblocks, PEO(2k)-{0.0G-S, 1.0G-S, 2.0G-S, 3.0G-S, 4.0G-S}, and the aryl ether vinyl terminated diblock{PEO(2k)-3.0G-M} was determined using ^{1}H NMR($CDCl_3$ or d_6-DMSO as solvent). ^{1}H NMR results for the modified diblocks, where $CDCl_3$ was used as the solvent, are listed in Table 2.2. Protons for PEO ($C\mathbf{H_2}C\mathbf{H_2}O$) appeared at 3.65ppm. The -$C\mathbf{H_2}$- and -$C\mathbf{H_3}$ protons of the stearate end groups appeared at 1.2ppm and 0.9ppm respectively. Protons corresponding to the PAMAM portion of the dendrimer block are present but difficult to assign individually. The NMR data indicate relative success in functionalization of the dendrimer block copolymers. The lower generations yielded close to 100% conversion; third and fourth generation dendrimers were 80% end-functionalized with stearate groups, and the third generation aryl ether dendrimer was 100% substituted.

The change in solubility of the diblocks by modification of the dendrimer end groups to either stearate or allyloxybenzene is quite dramatic; the unmodified diblocks are very soluble in water but the modified diblocks are only sparingly so. Also, as mentioned earlier, the aqueous solubility decreases as the generation number of the dendrimer increases. The first generation modified diblock, PEO(2k)-1.0G-S, was soluble in both water and chloroform. This solubilization of the modified diblock in very different solvents could be explained by the formation of micelles or reverse micelles. The versatile end group modification reaction could hence be used to synthesize hybrid diblocks with a wide range of amphiphilicities. For example, shortening the length of the alkyl chain may make higher generations of the PEO(2000)-dendrimer diblocks soluble in water.

Table 2.2. Percentage of stearate groups on the substituted dendrimer block determined using ^{1}H NMR. Tabulated as a ratio of the methyl groups on the stearate ends of the dendrimer block to the PEO backbone protons.

a b

CH_3O-($C\mathbf{H_2}C\mathbf{H_2}O)_m$-PAMAM-[$NHCO(CH_2)_{16}C\mathbf{H_3}]_n$

PEO-PAMAM diblock	Theoretical M_w	Number of end groups n	Modified diblock	Theoretical M_w	Theoretical ratio b/a	Experimental ratio b/a
PEO(2k)	2000	1	PEO(2k)-S	2267	-	-
PEO(2k)-1.0G	2230	2	PEO(2k)-1.0G-S	2762	0.033	0.033
PEO(2k)-2.0G	2686	4	PEO(2k)-2.0G-S	3750	0.066	0.070
PEO(2k)-3.0G	3598	8	PEO(2k)-3.0G-S	5726	0.132	0.102
			PEO(2k)-3.0G-M*	4878	0.088	0.087
PEO(2k)-4.0G	5422	16	PEO(2k)-4.0G-S	9678	0.264	0.208

* CH_3O-($C\mathbf{H_2}C\mathbf{H_2}O)_m$-PAMAM-[$NHCOC_6H_4CH_2CH{=}C\mathbf{H_2}]_n$

2.4 Chapter Summary

Two series of new linear-dendrimeric block copolymers have been synthesized in which the linear block is PEO and the dendrimeric block is PAMAM. The molecular weight of the PEO was 5000 in one case and 2000 in the other. The amine end groups of the dendrimer block were functionalized with stearate or allyloxybenzene groups. The functionalization proceeded with 80-100% conversion and led to a drastic change in the solubility of the diblock copolymers in water.

2.5 References

1. Tomalia,D.H.; Naylor,A.M.; Goddard III,W.A., *Angwandte Chemie Int. Ed.*, **1990**, 29, 138-173.
2. Wooley,K.L.; Hawker, C.J.; Fréchet,J.M.J., *J. Am. Chem. Soc.*, **1991**, 113, 4252-4261.
3. Newkome,G.R.; Moorefield,C.N.; Vogtle,F., *Dendritic Molecules: Concepts, Syntheses, Perspectives*, **1996**, VCH Publishers, Inc., New York, NY.
4. (a) Hawker, C.J.; Wooley, K.L.; Frechet, J.M.J., *J. Chem. Soc. Perkin Trans.*, **1993**, 1, 1287, (b) Hawker, C.J.; Frechet, J.M.J., *J. Am. Chem. Soc.*, **1992**, 114, 8405.
5. Gitsov, I.; Frechet, J.M.J., *Macromolecules*, **1994**, 27, 7309.
6. Chapman, T.M.; Hillyer, G.L.; Mahan, E.J.; Shaffer, K.A., *J. Am. Chem. Soc.*, **1994**, 116, 11195.
7. a) van Hest, J.C.M.; Delnoye, D.A.P.; Baars, M.W.P.L.; van Genderen, M.H.P.; Meijer, E.W., *Science*, **1995**, 268, 1592. b) van Hest, J.C.M.; Baars, M.W.P.L.; Elissen-Román, C.; van Genderen, M.H.P.; Meijer, E.W., *Macromolecules*, **1995**, 28, 6689.
8. a) Gitsov,I.; Wooley, K.L.; Hawker, C.J., Ivanova, P.T.; Fréchet, J.M.J., *Macromolecules*, **1993**, 26, 5621-5627, b) Gitsov, I.; Frechet, J.M.J., *Macromolecules*, **1994**, 27, 7309-7315.
9. (a) Matyjaszewski, K.; Shigemoto, T.; Fréchet, J.M.J.; Leduc, M., *Macromolecules*, **1996**, 29, 12, 4167, (b) Leduc, M; Hawker, C.J.; Dao, J.; Fréchet, J.M.J., *J. Am. Chem. Soc.*, **1996**, 118, 11111, (c) Leduc, M.R.; Hayes, W.; Fréchet, J.M.J., *J. Polym. Sci. Polym. Chem.*, **1998**, 36, 1.

10. Aoi, K.; Motoda, A; Okada, M., *Macromol. Rapid. Commun.*, **1997**,18,945-952.
11. van Hest, J.C.M.; Baars, M.W.P.L.; Elissen-Roman, C.; van Genderen, M.H.P.; Meijer, E.W., *Macromolecules*, **1995**, 28, 6689.
12. Hogberg, T; Strom, P; Ebner, M; Ramsby, S., J. Org. Chem., **1987**, 52, 10, 2033.
13. (a) Tomalia, D.A.; Dewald, J.R., U.S.Patent 4 568 737, Feb 4, 1986, (b) Tomalia, D.A.; Baker, H.; Dewald, J.; Hall, M.; Kallos, G.; Roeck, J.; Ryder, J.; Smith, P., *Macromolecules*, **1986**, 19, 9, 2466.
14. Leon, J.W.; Fréchet, J.M.J, *Polymer Bulletin*, **1995**, 35, 449.
15. Tomalia, D.A.; Baker, H.; Dewald, J.; Hall, M.; Kallos, G.; Martin,S.; Roeck, J.; Ryder, J.; Smith, P., *Polymer Journal*, **1985**, 17, No.1, 117-132.
16. Klausner,Y.S.; Bodansky,M.*Synthesis*, **1972**, 453.
17. Newkome,G.R.; Nayak, A.; Behara, R.K.; Moorefield, C.N.; Baker, G.R. *J. Org. Chem.*, **1992**, *57*, 358.
18. Mutter, M.; Bayer, E. *'The Peptides'*, Vol. 2, **1979**, Academic Press, Inc., 285.

Chapter 3. Solution behavior of PEO-PAMAM Linear-Dendritic diblock* Copolymers

3.1 Introduction

Following the synthesis of dendrimeric macromolecules, the question of segment density distribution in the interior of the molecule both in bulk and in solution has generated a lot of research interest[1]. SANS, viscosimetry, NMR, and SAXS have been some of the techniques used to study the solution behavior of dendrimers as a function of molecular weight[2,3]. The scaling relationships obtained from these results have been compared with computer simulations results to get an idea of the shape of the dendrimer macromolecule in solution[4]. One of the most intriguing solution properties of dendrimers is the variation of intrinsic viscosity with molecular weight. For classical linear polymers, intrinsic viscosity increases with molecular weight, and is typically well described by the Mark-Houwink equation{ $[\eta] = KM^a$}. For dendrimers, intrinsic viscosity variation with molecular weight cannot be fitted with a single "a" parameter. A maximum in intrinsic viscosity with increase in molecular weight has been reported for majority of the dendrimeric homopolymers synthesized.

Thus far limited information is available on the dilute solution behavior of dendrimeric diblocks. The exponential increase of molecular weight in dendrimeric homopolymers, when compared to a linear incremental increase of molecular diameter with generation, results in large variations from ideal polymer behavior. In the hybrid linear-dendritic diblocks, the additional effect of the linear block can act to modulate or emphasize these deviations, depending on the interactions between the dendrimeric and linear blocks.

---

* Sections of this chapter have been published as: Iyer, J.; Fleming, K.; Hammond, P.T., *Macromolecules*, **1998**, 31, 25, 8757 - 8765.

To better understand the adsorption behavior and the amphiphilic nature of the synthesized polymers, the effect of PEO chain length and dendrimer end group functionality on the solution behavior of these diblocks was studied. Here, each of these properties is discussed and compared to spherical dendrimers, and where relevant, to linear hybrid systems reported by other groups.

3.2 Experimental Section

Synthesis and characterization of the PEO(5000)-dendrimer series and the PEO(2000)-dendrimer series is described in Chapter 2. Size exclusion chromatography was performed on a Perkin Elmer system with $NaNO_3$(0.05M)/NaN_3(0.02%) aqueous solution as the mobile phase at 30°C. The GPC separation was achieved over three columns (Waters Ultrahydrogel 250,500,2000) varying in pore sizes from 250Å to 2000Å. PEO standards ranging in molecular weight from 145,000 to 2000g/mol were used for calibration. A Cannon-Ubbelohde semi-micro(50) viscometer was used for the intrinsic viscosity measurements.

3.3 Intrinsic Viscosity Results

3.3.1 PEO(2000)-Dendrimer series

Figure 3.1a is a graph of the intrinsic viscosity of the PEO(2000)-dendrimer series in unbuffered MilliQ water plotted against the generation number of the dendrimer block. As expected, the addition of the dendritic block changes the [η] by small but measurable amounts with a trend of increasing [η] with increasing generation number. The Mark-Houwink-Sakurada plot to obtain the **K** and **a** values for this system is shown in figure 3.1b. A reasonably good linear relationship is obtained with the **K** and **a** values being 0.414 (ml/g) and 0.386 respectively. The **K** values obtained from literature for PEO(2000)[5] and PAMAM dendrimer[6] are 0.67(ml/g) and 0.776(ml/g) respectively; the corresponding **a** values are 0.28 and 0.237. These **a** values obtained from literature for PEO(2000) and PAMAM dendrimer are both a little lower than those for classic linear

polymers which are usually in the range of 0.5 to 0.8. The lower value of **a** (0.237) in the case of the PAMAM dendrimer compares favorably with the soft spheroidal structures these polymers are expected to possess and also their symmetrically branched architecture. The value of 0.28 for linear PEO in water at 30°C is applicable only in the low molecular weight range and it is conjectured that the short PEO chains cannot be treated as semipermeable coils. In comparison, the measured value of 0.386 for the PEO(2000)-PAMAM diblock copolymer is a little higher and suggests that the diblock copolymer is slightly more expanded than its component homopolymers.

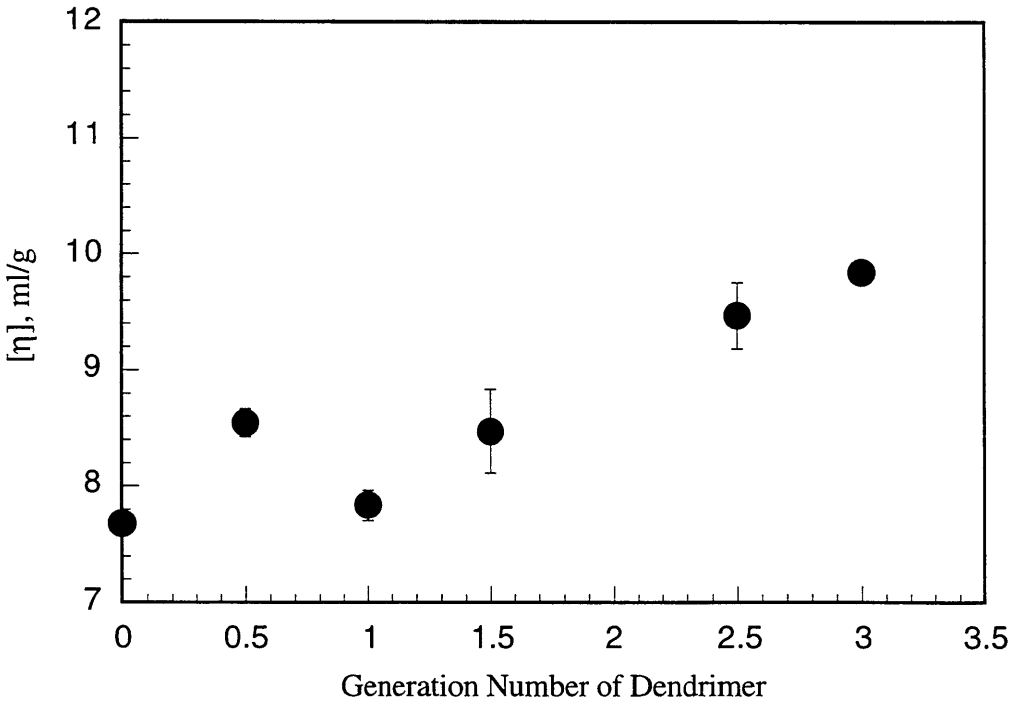

Figure 3.1a Variation of intrinsic viscosity with dendrimer generation for PEO(2000)-dendrimer diblocks at 30°C in water

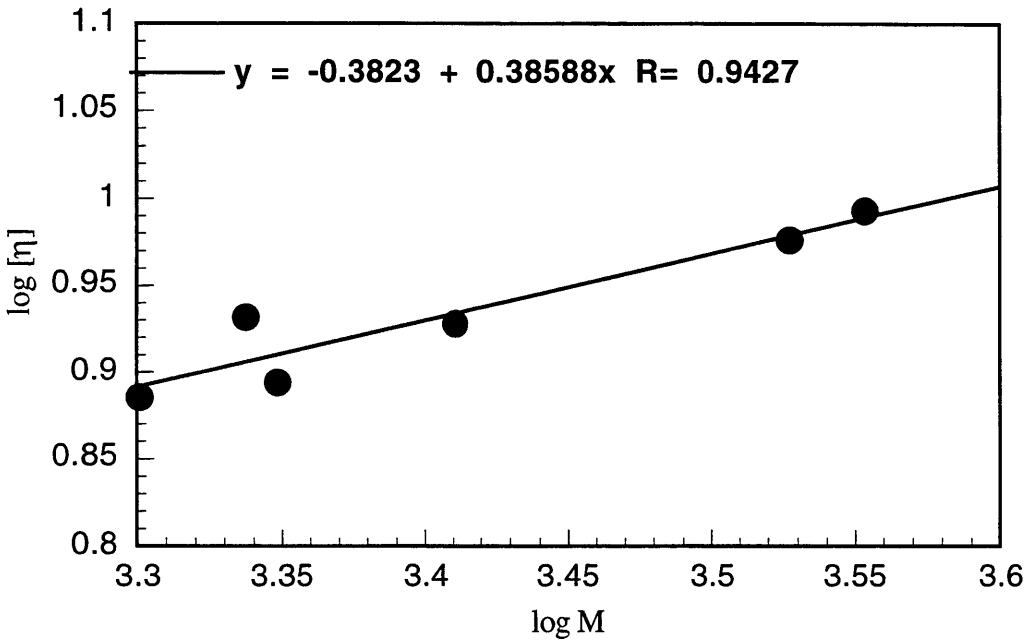

Figure 3.1b Relation between intrinsic viscosity and molecular weight for PEO(2000)-dendrimer diblocks

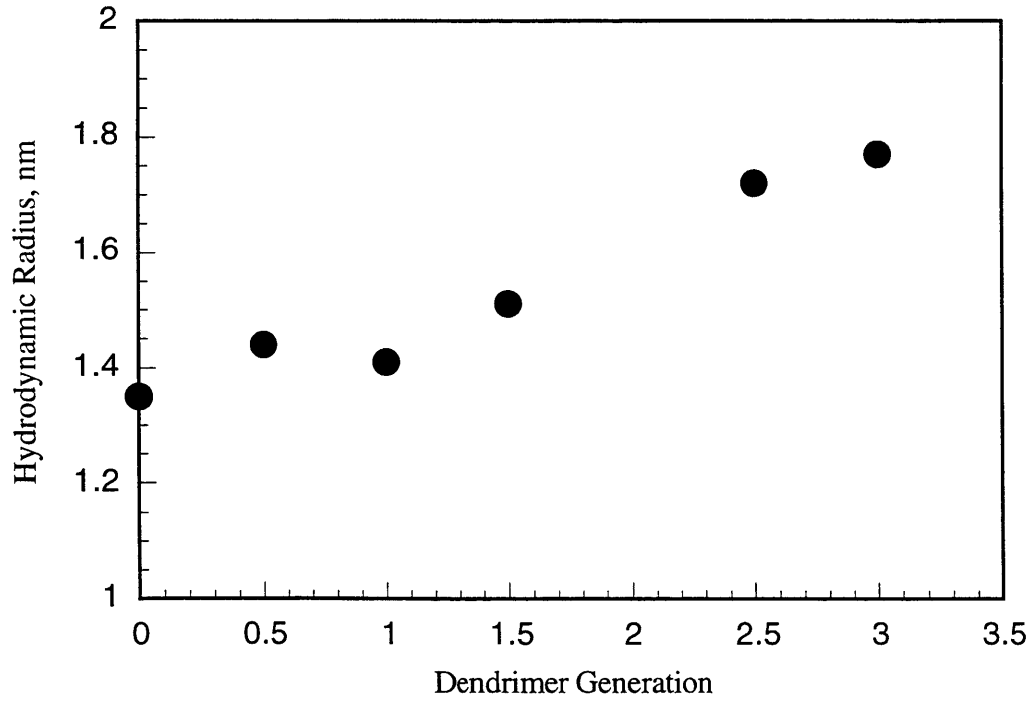

Figure 3.1c Plot of hydrodynamic radius vs dendrimer generation for PEO(2000)-dendirmer diblocks

Using the Einstein equivalent sphere model equation relating the [η] to the hydrodynamic volume and molecular weight, and assuming a spherical shape for the diblock, a hydrodynamic radius, r_h, can be calculated. A plot of the calculated r_h versus the generation number of the dendrimer is shown in figure 3.1c. R_h increases with increasing generation number as well.

3.3.2 PEO(5000)-dendrimer series

The relationship between [η] in water and the generation number of the dendrimer for the PEO(5000)-dendrimer diblock series is very different from that of the PEO(2000) series. Figure 3.2a is a plot of the [η] versus the generation number for the PEO(5000)-half generation diblocks, and Figure 3.2b is a corresponding plot for the PEO(5000)-full generation diblocks. For all of the copolymers with the exception of PEO(5000)-4.0G, the [η] is lower than that for the linear PEO(5000) core. This behavior may be explained by the formation of a PEO corona shielding the hydrophobic dendrimer repeat unit from the solvent, which results in a decrease in [η]. This decrease for early generations of other linear-dendritic diblock series due to the formation of unimolecular micellar structures was observed earlier by Gitsov and Frechet[7]. They found that for PEO(7500)-benzylether dendrimers, the attachment of the first generation to the linear PEO notably decreased the intrinsic viscosity in THF. In contrast, the intrinsic viscosity in methanol/water mixture for the same PEO(7500)-benzylether dendrimer series was lower than the linear precursor from the second generation onwards and not the first generation as seen in THF. Clearly, the interaction between the two blocks and the individual interaction between the blocks and the solvent together contribute to this behavior in linear-dendritic copolymer systems.

In the case of full generation PEO(5000)-dendrimer diblocks (figure 3.2b), favorable interaction of the PEO with the amine end groups probably furthers collapse of the PEO chain initially. The favorable interactions cannot compensate for the increasing size of the dendron with increasing generation number.

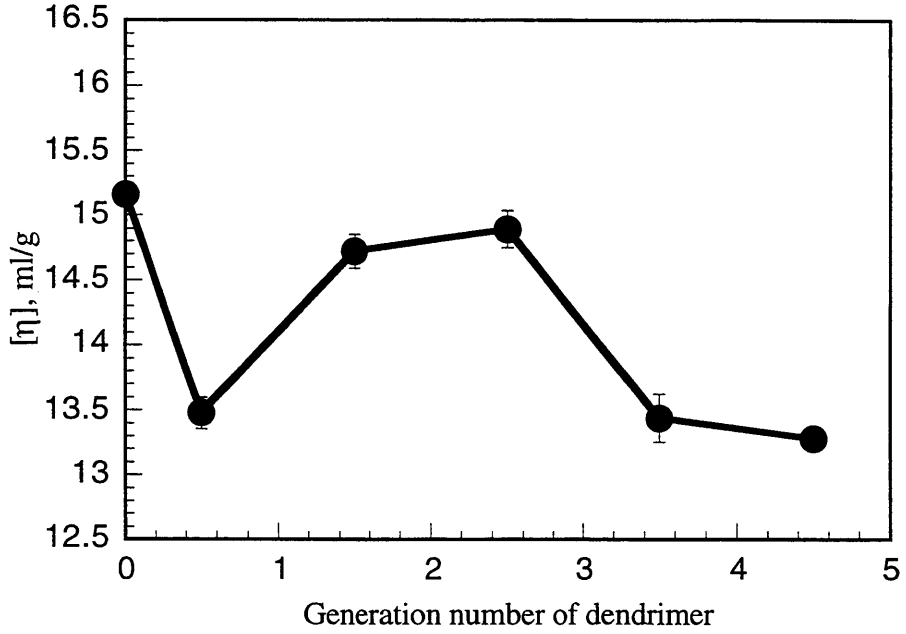

Figure 3.2a Variation of intrinsic viscosity with dendrimer half generation for PEO(5000)-dendrimer diblocks at 30°C in water

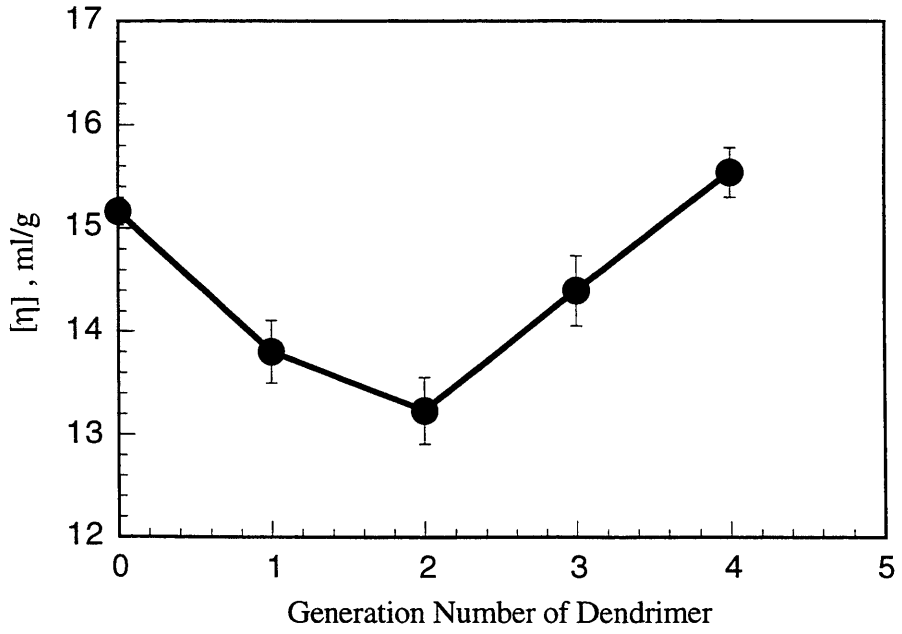

Figure 3.2b Variation of intrinsic viscosity with dendrimer full generation for PEO(5000)-dendrimer diblocks at 30°C in water

Increase in generation number is accompanied by an exponential increase in the number of hydrophilic amine groups. As the number of amine groups increase, the hydrophilicity of the dendrimer block increases and PEO no longer needs to shield the dendrimer and may be too short to do so.

The intrinsic viscosity curve obtained for the PEO(5000)-dendrimer with ester end groups indicates that the ester functionality results in very different solution behavior. The trend includes a maximum in [η] with increasing generation number which mirrors the trends observed for traditional spherical dendrimers[8,6]. For pure PAMAM and benzylether dendrimers, the intrinsic viscosity goes through a maximum at a given generation of the dendrimer. In this case, methyl ester may be water compatible at low generation numbers due to the presence of amide groups and ester polarity. However, PEO/methyl ester interactions may be less favorable than PEO/NH_2 interactions, and less shielding takes place initially. As the dendrimer gets bigger, the relative increase in molecular weight is greater than the increase in molecular size; as a result, the intrinsic viscosity, which is a ratio of size with molecular weight, decreases as observed in dendrimer homopolymers.

The unimolecular micelle or shielding effect is seen in the PEO(5000)-dendrimer series, but not in the PEO(2000)-dendrimer series, due to the increased chain length of the PEO block. For example, although the weight fractions of the two blocks in both PEO(2000)-3.5G and PEO(5000)-4.5G are approximately the same, the size ratio of the PEO block to the dendrimer block is larger for the PEO(5000) diblock. Using hydrodynamic radii from intrinsic viscosity measurements, the size ratio of the PEO(2000) homopolymer to dendrimer homopolymer(3.5G)[6] is 13Å:12.9Å, whereas the size ratio of PEO(5000) to dendrimer homopolymer(4.5G)[6] is 23Å:16.8Å. This dependence of the shielding effect on linear chain length has been observed by other researchers[7]. In PEO-fourth generation benzylether dendrimer diblocks, the intrinsic viscosity in THF was found to be higher than the linear precursor for PEO molecular weights upto 7500; conversely, for a PEO molecular weight of 26000 and higher, the

intrinsic viscosity of the diblocks was observed to be lower than the linear core[7]. ABA triblock copolymers where the A block is dendritic and the B block is linear also show this behavior[9]. In an ABA triblock copolymer with a linear polystyrene B block and a dendritic benzylether A block, the values of [η] for the triblocks in THF were found to be increasingly lower than those of the linear polystyrene B blocks when the molecular weight of the latter exceeded 40000. What is interesting with respect to the polymers described here is the relatively low molecular weight of PEO at which the shielding behavior is observed.

The differing intrinsic viscosity behavior between the PEO(2000) and PEO(5000) diblock series may also be influenced by the behavior of the PEO homopolymer in water. Literature results show a transition in the Mark-Houwink parameters(**K** and **a**) for PEO linear polymers at an approximate molecular weight of 3000[5]. Below this molecular weight, the **a** value is low, suggesting a less expanded polymer conformation; however, above this molecular weight the **a** value is 0.78, suggesting a highly expanded polymer in a good solvent. This is probably another factor that should be accounted for in analyzing the different shielding behavior exhibited by the diblock copolymers.

Converting the [η] to hydrodynamic radii, r_h, using the Einstein equivalent sphere model mentioned earlier, gives a more direct picture of what happens in aqueous solutions of PEO(5000)-dendrimer diblocks. The graph of r_h plotted against dendrimer generation is shown in Figure 3.2c. The hydrodynamic radius exhibits a decrease due to the previously described shielding effects until the second generation, and then increases with increasing generation number.

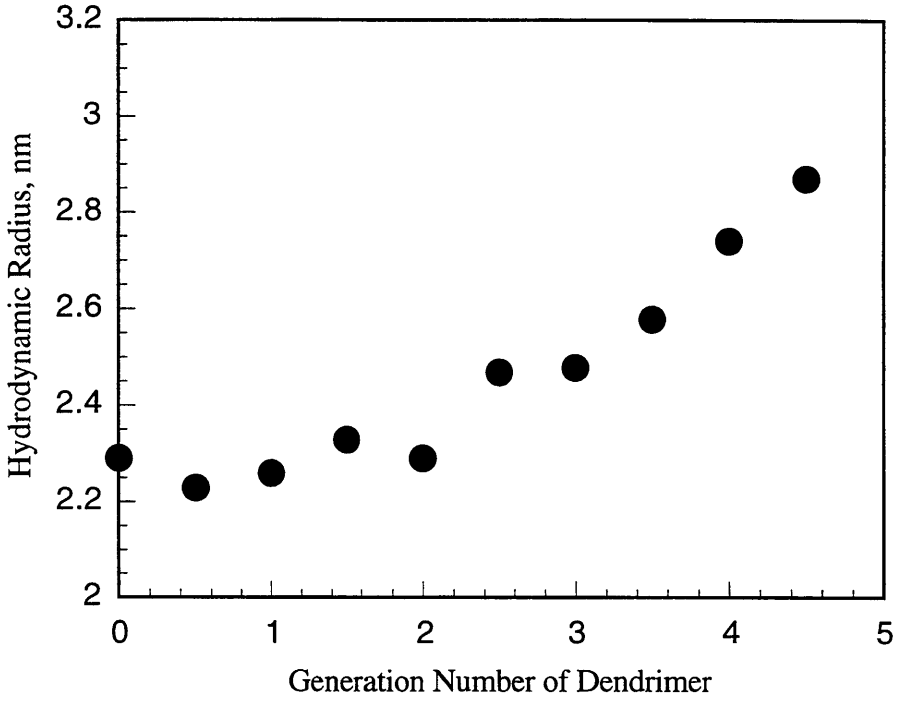

Figure 3.2c Variation of hydrodynamic radius with generation number for PEO(5000)-dendrimer diblocks

3.4 Gel Permeation Chromatography(GPC) Results

Two other techniques, GPC and dynamic light scattering, were used to further probe the solution behavior of the synthesized diblocks and to corroborate the behavior observed in the intrinsic viscosity experiments. Average GPC values for the molecular weight of the PEO(2000)-dendrimer diblocks were ~2200 and those for the PEO(5000)-dendrimer diblocks were ~6000. Use of the calibration curve based on linear polyethylene oxide standards did not give good overall estimates of the molecular weight. This is not surprising because the refractive index increments change with addition of the dendritic blocks. These observations suggest a deviation from the behavior of linear polymers that is consistent with the intrinsic viscosity results. There are two factors in the GPC experiments that could further modulate the effects and hence, prevent the exhibition of trends seen in the intrinsic viscosity experiments: a)the buffered aqueous mobile phase may have reduced the influence of the dendrimer end group functionality on the size and

shape of the diblock for the PEO(5000) series and, b) the existence of secondary interactions of the dendrimer block with the column packing. The PEO(2000)-dendrimer diblocks are probably too close to the size of the lowest molecular weight standard to show specific trends in GPC. The hydrodynamic volume from the GPC results were converted to an equivalent hydrodynamic radius using the Einstein equivalent sphere model equation (see Table 3.1). The hydrodynamic radii fall in the same range as those measured using intrinsic viscoity but it is difficult to interpret anything more from the GPC results.

Table 3.1 GPC results for PEO-PAMAM diblock copolymers

Material	Hydrodynamic Radius, nm
PEO(5000)-0.5G	2.27
PEO(5000)-1.0G	1.61
PEO(5000)-1.5G	2.06
PEO(5000)-2.0G	-
PEO(5000)-2.5G	2.11
PEO(5000)-3.0G	2.16
PEO(5000)-3.5G	2.27
PEO(5000)-4.0G	2.27
PEO(5000)-4.5G	2.16
PEO(2000)-0.5G	1.26
PEO(2000)-1.0G	-
PEO(2000)-1.5G	1.13
PEO(2000)-2.0G	1.34
PEO(2000)-2.5G	-
PEO(2000)-3.0G	1.38

Dynamic light scattering experiments were done in MilliQ water at 30°C for some of the PEO(5000) diblocks. The PEO(2000) diblocks were too small to be studied with the dynamic light scattering setup used. The values for copolymer size obtained from dynamic light scattering techniques also fall in the same range as those calculated from intrinsic viscosity and GPC measurements. However, intrinsic viscosity remains the

most sensitive and reliable technique for determining the hydrodynamic size of these materials.

3.5 Chapter Summary

Intrinsic viscosity studies show that the solution behavior is greatly affected by the length of the PEO linear chain at low molecular weights, and the number and chemical nature of the dendrimer end group. PEO(2000)-dendrimer diblocks exhibit increasing [η] with increasing molecular weight as is observed for traditional linear polymers. For the PEO(5000)-dendrimer diblocks, [η] decreases with the introduction of the dendrimer block, suggesting a unimicellar like structure formed by wrapping of the PEO chain around the dendrimer block. The variation of [η] with dendrimer generation in the PEO(5000) series is reminiscent of the relationship seen for pure dendrimers

3.6 References

1. Matthews, O.A.; Shipway, A.W.; Stoddart, J.F., *Prog. Polym. Sci.*, **1998**, 23, 1.
2. (a) Ramzi, A.; Scherrenberg, R.; Brackman, J.; Joosten, J.; Mortensen, K., *Macromolecules*, **1998**, 31, 1621, (b) Prosa, T. J.; Baeur, B. J.; Amis, E.J.; Tomalia, D.A.; Scherrenberg, R., *J. Polym. Sci. Polym. Phys.*, **1997**, 35, 2913.
3. (a) Meltzer, A.D.; Tirrell, D.A.; Jones, A.A.; Inglefield, P.T.; Hedstrand, D.M.; Tomalia, D.A., *Macromolecules*, **1992**, 25,4541, (b) Meltzer, A.D.; Tirrell, D.A.; Jones, A.A.; Inglefield, P.T., *Macromolecules*, **1992**, 25, 4549.
4. Scherrenberg, R.; Coussens, B.; van Vliet, P.; Edouard, G.; Brackman, J.; de Brabander, E., *Macromolecules*, **1998**, 31, 456.
5. Bailey Jr.,F.E.; Koleske,J.V., *"Poly(ethylene oxide),"* Academic Press, Inc., New York, **1976.**
6. Tomalia, D.A.; Baker, H.; Dewald, J.; Kallos, G.; Martin, S.; Roeck, J.; Ryder, J.; Smith, P., *Polymer Journal*, **1985**, 17, 1, 117.

7. Gitsov,I.; Fréchet,J.M.J., *Macromolecules*,**1993**,26,6536-6546.
8. Mourey, T.H.; Turner, S.R.; Rubinstein, M.; Fréchet, J.M.J.; Hawker, C.J.; Wooley, K.L., *Macromolecules*, **1992**,25,2401-2406.
9. Gitsov,I.; Fréchet,J.M.J., *Macromolecules*, **1994**, 27, 7309-7315

Chapter 4. Amphiphilic behavior of Linear-Dendritic Diblock Copolymers at the air-water interface

4.1 Introduction

Amphiphilic molecules, which have a hydrophobic and a hydrophilic part, exhibit interesting behavior in solution and at interfaces. The effect of the shape of an amphiphile on its aggregation behavior in solution has been described theoretically by Israelachvili et al.[1]. The unique shape of the dendrimer and the controlled way in which different sizes of the dendrimer can be built make the synthesis and study of dendritic amphiphiles an interesting one. Van Hest et al.[2] found that PS-polypropyleneimine linear-dendritic diblock amphiphiles form micelles and reverse micelles in solution depending on the solvent, and that the aggregation behavior could be well described by the theory of Israelachvili. Gitsov and Frechet[3] reported the formation of micelles in solution for similar linear-dendritic diblock amphiphiles having a hydrophilic PEO linear block and a hydrophobic polybenzylether dendritic block. The formation of aggregate structures in solution has been observed for other linear-dendritic diblocks and monodendrons as well[4].

A number of groups have worked on studying the behavior of dendritic amphiphiles at the air-water interface. Some groups have measured the surface activity of dendritic surfactants by the change in surface tension of water[5,6]. Others have used a Langmuir trough to study the behavior of monolayers of dendrimers at the air-water interface. Along with observations on the amphiphilic behavior, the Langmuir trough can be used to probe the change in shape of the dendritic macromolecule on going from lower to higher generations. This change in shape is accepted as an explanation for the unusual intrinsic viscosity behavior of dendrimers, although no direct measurements have been made. Saville et al. were the first to use the Langmuir trough coupled with nuetron reflectivity to study the structure adopted by benzyl ether dendrons and dendrimers at the air-water interface[7]. The comparison of surface activity of benzyl ether dendrons with hydroxyl terminated polystyrene was studied earlier using a Langmuir trough by the

same group[8]. Bo et al. studied the behavior at the air-water interface of benzylether dendrons modified with alkyl chains[9]. The behavior of alkyl functionalized polypropyleneimine dendrimers and hyperbranched polyphenylenes at the air-water interface have also been reported[10,11]. However, the amphiphilic behavior of linear-dendritic diblock copolymers at the air-water interface has not been reported by any other group.

In this chapter, the behavior of PEO-PAMAM linear-dendritic diblock copolymers at the air-water interface will be discussed. The effect of the generation of the dendrimer, the size of the PEO linear block, and the end group functionality of the dendrimer block on the amphiphilic behavior of the diblock copolymer will be reported. The study of the interfacial behavior of these architecturally unique amphiphiles is the first step to making ultrathin film membranes using the LB technique.

4.2 Experimental Section

Synthesis of the diblock copolymers used for the experiments in this chapter is discussed in detail in chapter 2. A Lauda FW-2 trough with a total surface area of 927cm^2 and a subphase volume of 1.3L was used for the monolayer studies. The concentration of the copolymer in chloroform was between 1-10mg/ml. The solutions were filtered with a 0.45μm PTFE filter before use. A monolayer of the diblock was spread drop by drop at the air-water interface with a Hamilton microsyringe. Typically, 50μl was used for making the monolayer. 30-60 minutes was allowed for evaporation of the solvent and spreading of the monolayer before compression was initiated. Pressure-area isotherms were recorded by compressing the monolayers at a speed of 92cm^2 per minute. In all cases, a baseline was established before spreading the polymer monolayer by compressing the water subphase at the same conditions as that subsequently used for the monolayer compression. 2.0mN/m was taken as the maximum acceptable surface pressure in the baseline at any surface area. The air-water interface was cleaned again if this condition was not satisfied before further isotherm measurements were conducted. The

temperature of the subphase was controlled with a Neslab RTE-111 refrigerated circulator. $MgSO_4.7H_2O$ purchased from Mallinckrodt was used without further purification for subphase modification. 189.6g of $MgSO_4.7H_2O$ was dissolved in 2L of deionised Milli-Q water (18.2MΩcm) to give a subphase concentration of 0.385M. Polyacrylic acid, with a molecular weight of 5000, was purchased as a 50% aqueous solution from Polysciences, Inc. To prepare the subphase for isotherm measurements, 0.81g of the PAA solution was added to 2L of deionised Milli-Q water. To this solution, HCl was added drop-wise with constant stirring till the pH was ~2.0. The subphase pH was measured with pH paper.

4.3 Results and Discussion

4.3.1 Pressure-area isotherms for PEO-PAMAM diblocks

Figure 4.1 shows the pressure-area isotherms for three generations of PEO-PAMAM diblock copolymers with a PEO chain length of 5000. The number of ester functionalized end groups varies from 8 for PEO(5000)-2.5G to 32 for PEO(5000)-4.5G. All the diblocks are surface active with PEO(5000)-2.5G being the most surface active. Among the three diblocks shown, the weight fraction of PEO in PEO(5000)-2.5G is the greatest. Since the surface activity seen is because of the PEO block, the higher surface activity of the 2.5G diblock is not surprising. Figure 4.2 shows the pressure-area isotherms for two generations of PEO(2000)-dendrimer diblocks for comparison. These diblocks having a shorter chain length are not as surface active. Here, both the compression and expansion curves for the isotherms are shown. There is considerable hysteresis, especially at low surface concentrations. Such hysteresis in the pressure-area isotherms upon compression to high surface concentrations has been observed for pure PEO monolayers by Shuler and Zisman[12]. Some effect of the end group functionality of the dendrimer on the interfacial behavior is apparent even for these small diblocks. All these diblocks were, however, very water-soluble and the formation of stable condensed monolayers for transfer onto substrates was not possible.

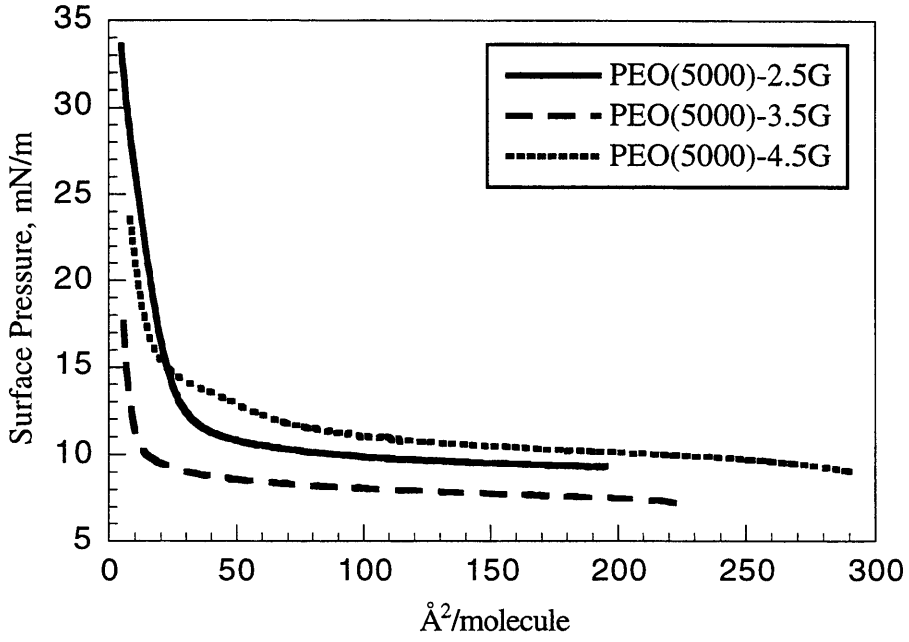

Figure 4.1 Pressure-area isotherms at 20°C for ester terminated PEO(5000)-dendrimer diblock copolymers.

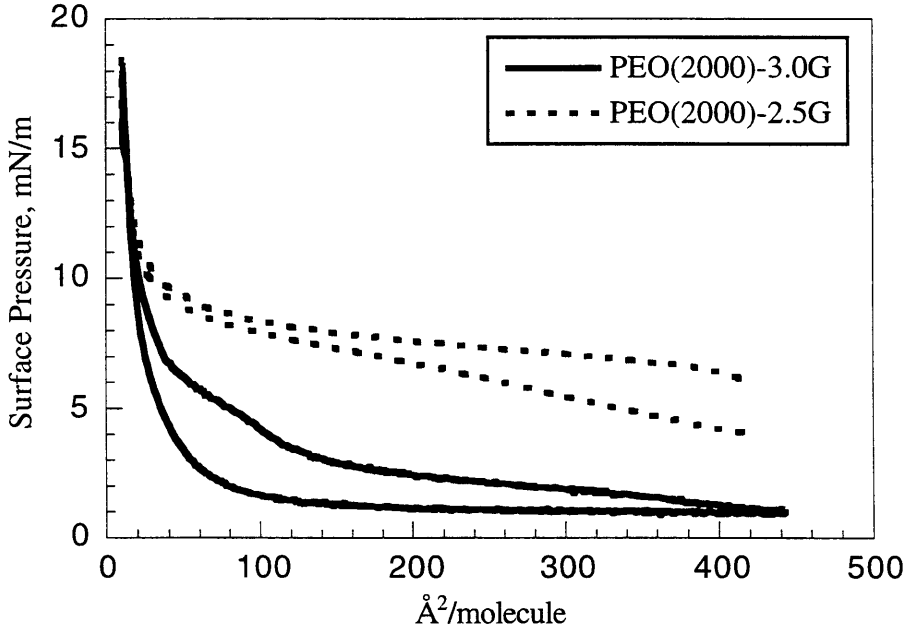

Figure 4.2 Pressure-area isotherms at 20°C for ester(2.5G) and amine(3.0G) terminated PEO(2000)-dendrimer diblocks having eight end groups.

The diblocks were modified to make them more surface active. To obtain a stable condensed monolayer, the diblocks have to be reasonably insoluble in water. Since the considerable solubility of diblocks in water was mainly a result of the PEO tail, the shorter tailed PEO(2000)-dendrimer diblocks were chosen for further chemical modifications and study.

4.3.2 Effect of end group functionality on the π-a isotherm

Figure 4.3 shows the π-a isotherm for one unfunctionalized diblock with terminal ester groups {PEO(2k)-2.5G}and two modified diblock copolymers{PEO(2k)-3.0G-M, PEO(2k)-3.0G-S}with different chemical terminal functionalities. The theoretically expected molecular weight for a fully substituted diblock copolymer was used in calculating the area per molecule shown on the x-axis. The low surface pressure at high compression and the corresponding small area per molecule for the unfunctionalised diblock, PEO(2k)-2.5G, is probably because of loss of molecules into the aqueous subphase due to the considerable solubility of the diblock in water. As seen in figure 4.3, the π-a isotherm for the aryl ether vinyl functionalized diblock, PEO(2k)-3.0G-M, also suggests low pressures due to dissolution into the subphase. The similarity in these two isotherms is surprising as the aqueous solubility of PEO(2k)-3.0G-M is much lower than PEO(2K)-2.5G. Apparently, the presence of the benzoxy group adds to the hydrophilicity of the polymer, despite the relatively nonpolar aromatic group. On the other hand, the stearate terminated PEO(2k)-3.0G-S results indicate a high surface pressure and the presence of a transition at about 50mN/m, suggesting ordering of the monolayer and formation of condensed phases at the interface.

The PEO homopolymer is itself surface active and in the diblocks studied here, is probably the cause of the non-zero surface pressure at low surface concentrations. The high surface pressure at low surface concentration is observed for most PEO based non-ionic surfactants[13]. Studies have shown that at low surface concentration, the surface pressure at a given area per molecule increases as the PEO chain length of the surfactant

increases. However as the length of the PEO chain increases, the monolayer formed by the PEO based non-ionic surfactant becomes more expanded and the tendency of the monolayer to form condensed phases at the interphase on compression is decreased. Monolayers of PEO homopolymer collapse at surface pressures over 6.4mN/m[14].

Therefore, the non-zero surface pressure at low surface concentrations combined with the formation of condensed phases at high surface concentrations in the case of PEO(2k)-3.0G-S, implies that although the low surface concentration behavior is influenced by the PEO block, the behavior at high surface concentration or compression is definitely a result of the functionalized dendrimer block. As the stearate terminated diblock was found to be the most surface active, and to yield the most stable monolayers, we chose to use these materials to further study Langmuir monolayers and transferred L-B films.

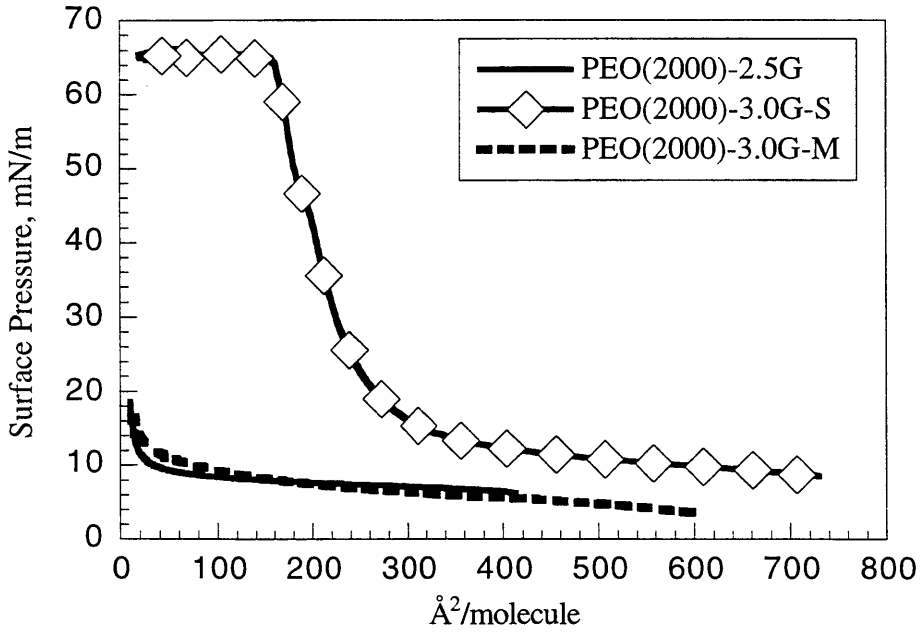

Figure 4.3 Pressure-Area isotherms measured at 20°C for one unfunctionalized [PEO(2k)-2.5G] and two functionalized diblock copolymers[PEO(2k)-3.0G-M, PEO(2k)-3.0G-S)]. All three have the same PEO chain length and number of dendrimer end groups.

4.3.3 Effect of dendrimer generation on the π-a isotherm of stearate terminated PEO-PAMAM diblock copolymers:

Figure 4.4a shows the π-a isotherm for four polymers, all with the same length of the PEO chain but with different generations of stearate terminated dendrimers. Again, the area per molecule is calculated from the theoretically expected molecular weight for the diblocks. Two facts are apparent from the comparison shown in Figure 4.4a. First, the three hybrid linear-dendritic diblocks with stearate end groups form condensed phases at the air-water interface as indicated by the high surface pressures achieved in the isotherm before collapse. Second, the surface pressure for PEO2k-4.0G-S at low surface concentration is practically zero, in contrast to all the other polymers investigated here. As mentioned in the previous section, the non-zero surface pressure at low surface concentrations is a likely consequence of the surface activity of the PEO block. In the case of PEO(2k)-4.0G-S, the PEO block is being excluded from the interface. A schematic of what could be happening at low surface pressures is shown in Figure 4.4b. For the hybrid copolymers up to the third dendrimer generation, the PEO tail is long enough to go around the dendrimer block to access the interface at low surface pressure. The dendrimer block in the fourth generation diblock[PEO(2k)-4.0G-S] is probably larger than the PEO 2000 hydrodynamic radius, and is thus too large for the PEO chain to wrap around and access the interface (Figure 4.4b).

To take a closer look at the area per molecule in the condensed phase of the diblock monolayers, the x-axis of Figure 4.4a is expanded and shown in Figure 4.4c. The extrapolated values of the area per molecule along with the theoretically expected value for the area are listed in Table 4.1. To calculate the theoretically expected area for the hybrid block copolymers in the condensed phase, it is assumed that the stearate end groups are extended into air perpendicular to the interface as shown schematically in figure 4.4d. This assumption is based on the behavior of pure stearic acid, which forms ordered monolayers with the alkyl chains oriented perpendicular to the air-water interface. The area per molecule for stearic acid with this orientation is 20 $Å^2$ [15].

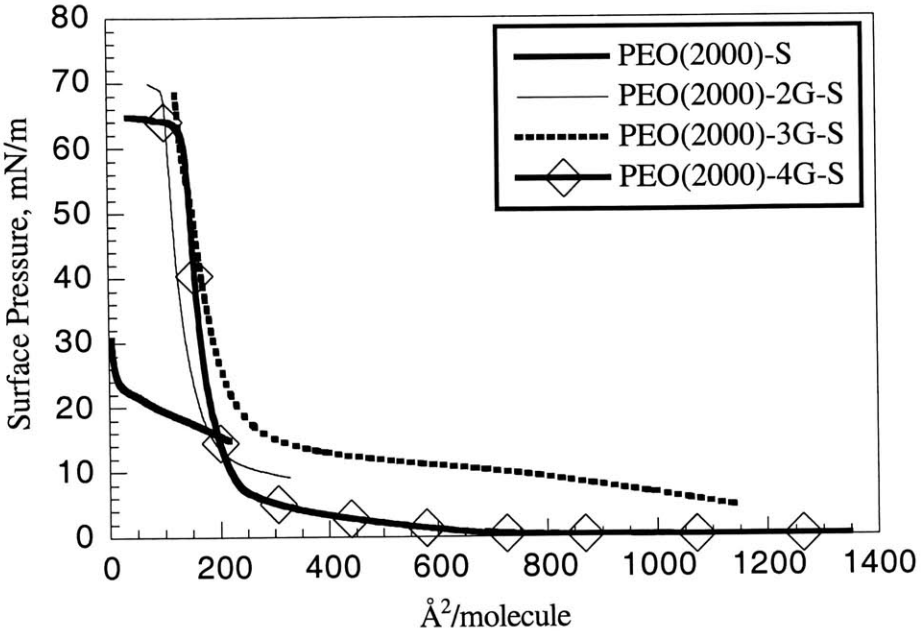

Figure 4.4a Pressure-Area isotherms measured at 20°C for four diblock copolymers with stearate end groups and the same PEO chain but different dendrimer generations.

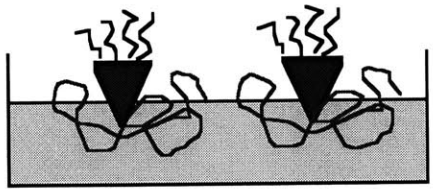

Low dendrimer generation diblocks

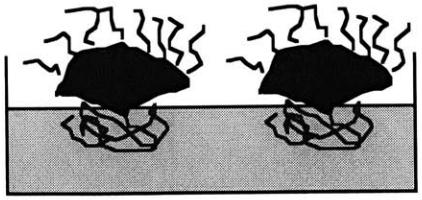

High dendrimer generation diblocks

Figure 4.4b Schematic of the organization of linear-dendritic diblock copolymers at the air-water interface for different dendrimer generations at high area's per molecule.

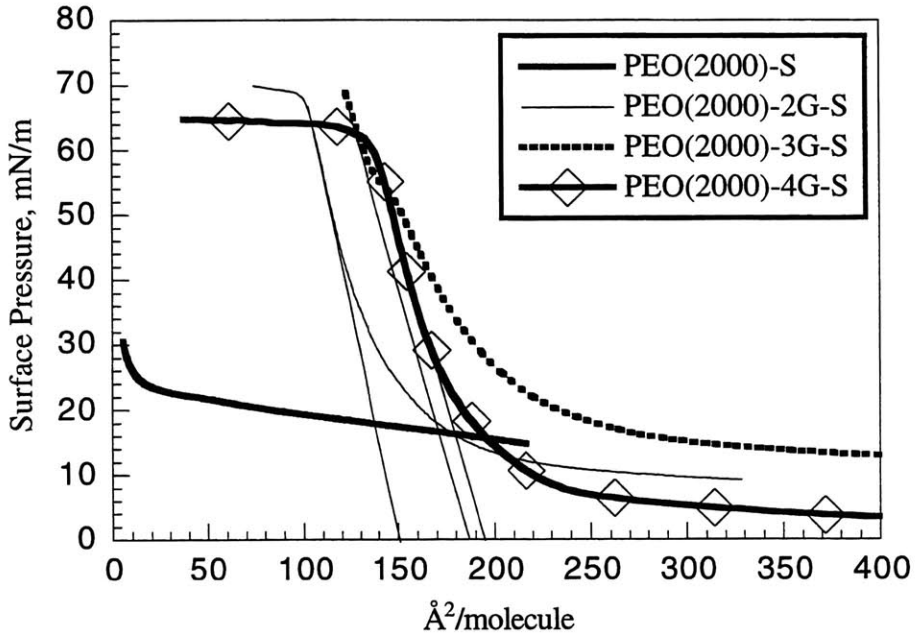

Figure 4.4c A close up of the condensed phase regime in the Pressure-Area isotherms measured at 20°C for four diblock copolymers with stearate end groups and the same PEO chain but different dendrimer generations.

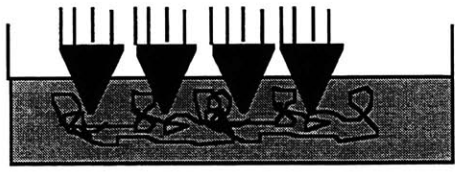

Low generation dendrimer diblocks

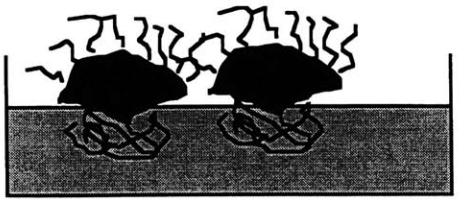

High generation dendrimer diblocks

Figure 4.4d Schematic of the organization of linear-dendritic diblock copolymers at the air-water interface for different dendrimer generations in the condensed phase.

Here, the theoretically expected area is calculated by multiplying the area per stearate molecule (20 $Å^2$) with the number of stearate groups present at the ends of the dendrimer block. PEO(2k)-S having no dendrimer block but a single stearate end group was studied as a standard and the experimental result agrees well with the theoretically predicted value (Table 4.1). For PEO(2k)-2.0G-S and PEO(2k)-3.0G-S, the experimental value for the area is larger than the calculated value, suggesting that the condensed phase in this copolymer may contain some PEO at the interface along with the dendrimer block. This picture is consistent with the non-zero surface pressures found at low pressures in these systems. In the case of PEO(2k)-4.0G-S, the experimental area is less than that calculated from theory. Even accounting for the 80% conversion of dendrimer amine to stearate end groups cannot explain the very low value for the experimentally observed area per molecule in PEO(2k)-4.0G-S; in fact, the third generation polymer, with a similar degree of conversion, has an area that exceeds the theoretical value, as described above. It is probable that the fourth generation dendrimer block has significant curvature, preventing the complete orientation of the stearate alkyl chains at the interface. The lower collapse pressure of PEO(2k)-4.0G-S monolayer also supports the picture of a loss of orientation of the stearate end groups. The condensed phase for this diblock copolymer may be more directly attributable to the dendrons; the dendron block may get distorted at high compressions, leading to the low value for the area. The second part of Figure 4.4d gives a pictorial representation of what could be happening at the interface. Earlier evidence for this sort of deformation of the dendrons at the air-water interface has been seen by Frechet et al.[16], who found from neutron reflectivity studies that the fourth generation polybenzylether monodendron became distorted and assumed an ellipsoidal shape at high compressions. Such compressed structures may apply to these systems as well, as PAMAM dendrimers are a relatively flexible, low T_g polymeric system. What is interesting is that these systems maintain their flexibility despite the outer shell of stearate groups; this fact also suggests that the stearate groups are fairly disordered at the air-water interface.

Diblock	Number of stearate groups, n	Theoretical area ($20Å^2$ x n), $Å^2$	Experimental area $Å^2$
PEO(2k)-S	1	20	25
PEO(2k)-1.0G-S	2	40	245 270
PEO(2k)-2.0G-S	4	80	150
PEO(2k)-3.0G-S	8	160	185
PEO(2k)-4.0G-S	16	320	195

Table 4.1 Limiting area per molecule from extrapolation of the condensed phase region of the isotherm for the modified linear-dendritic diblock copolymers.

The limiting area per molecule for the stearate modified first generation diblock (PEO(2k)-1.0G-S) is very large compared to the theoretically expected area(table 4.1). One possible reason for this behavior is the formation of aggregate micellar structures at the air-water interface. This diblock copolymer is the only one in the modified diblock series that is soluble in water. The solubilization could be taking place by the formation of aggregate structures in solution. Presence of micelles at the air-water interface for other amphiphilic linear diblock copolymers have been reported before[17]. In the reported studies, the monolayers were transferred onto substrates to study the organization at the interface. Although the PEO(2k)-1.0G-S monolayer could be compressed to give high surface pressures, it was not stable enough to permit transfer onto solid substrates.

4.3.4 Effect of subphase conditions on the π-a isotherms for stearate terminated PEO-PAMAM diblock copolymers

The behavior of pure PEO homopolymer at the air-water interface has been studied in some detail because of the commercial importance of PEO surfactants and the unique interaction of PEO with water[18]. These investigations suggest that at low surface concentrations, the PEO homopolymer can be described as a single layer much diluted by water at the interface. At high surface concentrations, the topmost layer concentration remains approximately constant and the polymer penetrates deeper into the subphase. With the presence of the hydrophobic block in the PEO-PAMAM diblocks, exclusion of the PEO tail from the interface with increasing dendrimer generation or at high compressions will probably result in the increased penetration of the PEO into the aqueous subphase. Given this extensive interaction of the PEO tail with the aqueous subphase, there are two extremes in modifying the subphase conditions. One is to make the subphase a poor solvent for the PEO block, considerably altering the extension of the PEO tail into the subphase. Conversely, the subphase can be made a better solvent achieving the opposite effect.

a) Effect of salt

$MgSO_4$ at a concentration of 0.39M in water at 315K is known to be a bulk theta solvent for PEO homopolymers. Henderson et.al.[19] compared the organization of PEO homopolymer monolayers at the air-water interface using nuetron reflectivity at different $MgSO_4$ subphase concentrations. They reported that the bulk theta solvent was not a theta medium for the PEO monolayers. The presence of magnesium sulfate in the subphase, however, severely reduced the thickness of the polymer layer at the interface and markedly increased the concentration of the polymer in the topmost layer. Hence, magnesium sulfate at a concentration of 0.38M and 20°C was used to modify the subphase to be a poor solvent for the PEO block.

Figure 4.5 shows a comparison of the pressure-area isotherms for PEO(2000)-3.0G-S in different subphases at 20^0C. The presence of magnesium sulfate in the subphase did not alter the pressure-area isotherm significantly. The diblock was still able to form condensed phases as seen by the large surface pressures. A phase transition seen for the deionised water subphase at around 50mN/m was seen for the salt subphase too but at a much lower surface pressure of 30mN/m. The collapse pressure for salt subphase was again much lower indicating the decreased stability of the diblock monolayer.

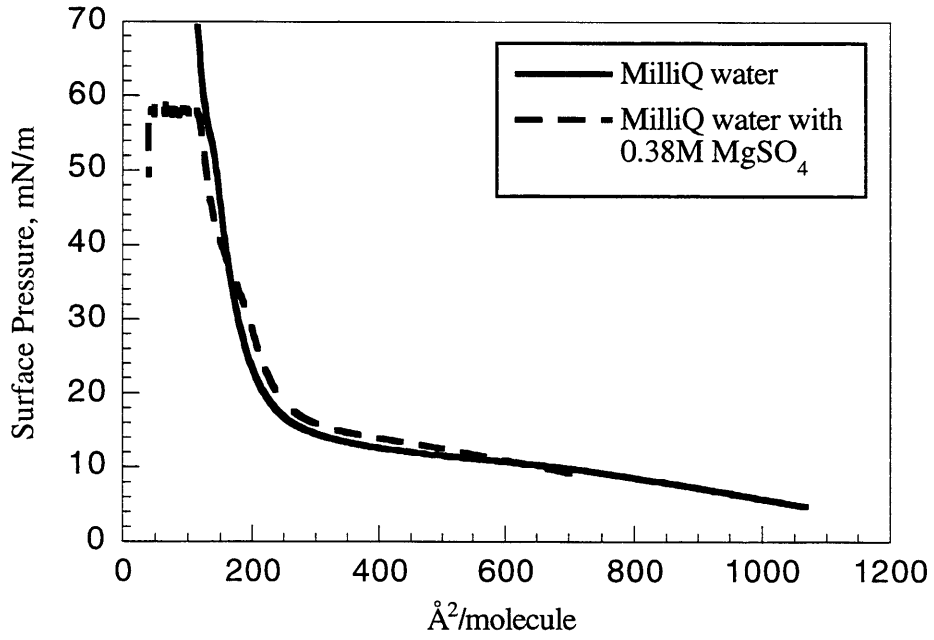

Figure 4.5 Effect on salt in the subphase on the pressure-area isotherm of PEO(2000)-2.0G-S.

b) Effect of polymer in the subphase

The use of water soluble polymers to change the nature and stability of the langmuir monolayer has been used as a technique by a number of researchers. Typically, stability is achieved by the formation of polyion complexes between charged monolayers and water soluble polyions[20]. For amphiphilic diblock copolymers with non-ionic blocks,

formation of hydrogen bonded complexes to increase stability of the langmuir monolayers have been attempted[21]. Niwa and Higashi[22] studied the reversible complexation between PEO-PS amphiphilic block polymers and polyacrylic acid at the air-water interface. They found that complexes between the PEO block and PAA were formed at subphase pH below 5. The effect of PAA in the subphase on the monolayers of PEO-PAMAM was studied at a pH of 2.0. The molecular weight of the PAA chosen was more than twice that of the PEO. In this case, a single PAA molecule will probably hydrogen bond with more than one PEO-PAMAM diblock and act as a physical cross-linking agent.

Figure 4.6 shows the effect of PAA in the subphase on the pressure-area isotherm of PEO(2000)-2.0G-S. The organization of the diblock copolymer at the air-water interface was not affected as seen by the negligible change in the pressure-area curve. However, the lack of a collapse pressure for the monolayer with the PAA subphase compared to the water subphase indicates that the stability of the monolayer is increased.

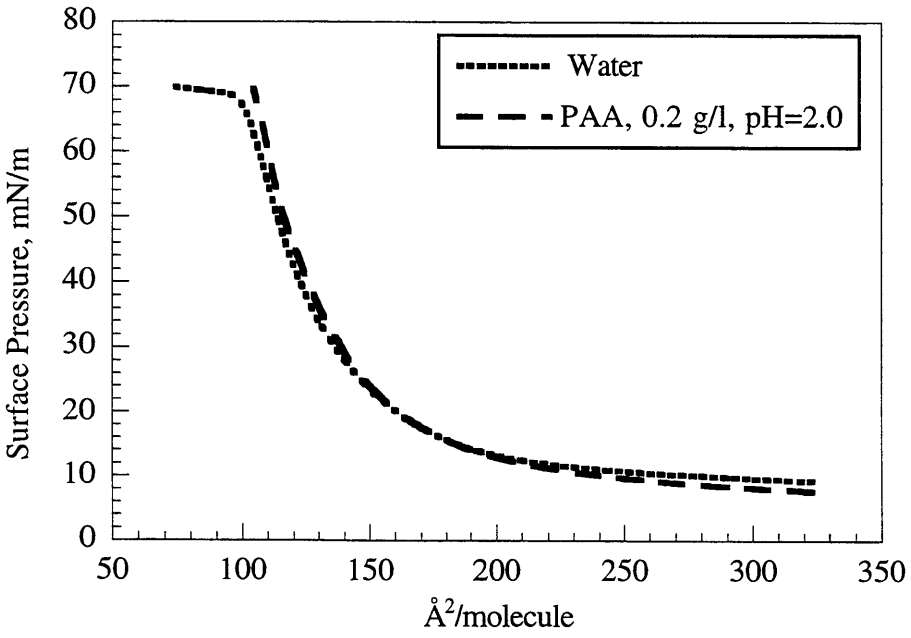

Figure 4.6 Effect of complexing polymer in the subphase on the pressure-area isotherm of PEO(2000)-2.0G-S

4.4 Summary

Stearate terminated linear-dendritic diblocks were found to be highly amphiphilic, and formed the most stable monolayers at the air-water interface of a LB trough. Three interesting effects of increasing dendrimer generation on the amphiphilic behavior of linear-dendritic diblock copolymers, namely the exclusion of the linear PEO block from the interface for large dendron sizes, the effects of curvature of the dendron surface on final surface area per molecule, and deformation of the dendron at high pressure have been reported here. On compression of monolayers of stearate terminated diblocks, a condensed phase was observed for all dendrimer generations. The monolayers of diblocks with third and fourth generation dendrimer blocks were very stable

4.5 References

1. Israelachvili, J.N.; Mitchell, D.J.; Ninham, B.W., *J. Chem. Soc. Faraday Trans.*, **1976**, 2, 72, 1525.
2. van Hest, J.C.M.; Delnoye, D.A.P.; Baars, M.W.P.L.; van Genderen, M.H.P.; Meijer, E.W., *Science*, **1995**, 268, 1592.
3. Gitsov, I; Frechet, J.M.J., *Macromolecules*, **1993**, 26, 6536.
4. (a) Chapman, T.M.; Hillyer, G.L.; Mahan, E.J.; Shaffer, K.A., *J. Am. Chem. Soc.*, **1994**, 116, 11195, (b) Kawa, M.; Frechet, J.M.J., *Chem. Mater.*, **1998**, 10, 286, (c) Zimmerman, S.C.; Zeng, F.; Rei chert, D.E.C.; Kolotuchin, S.V., *Science*, **1996**, 271, 1095, (d) Kraft, A., *Liebigs. Ann./Recueil*, **1997**, 1463, (e) van Hest, J.C.M.; Baars, M.W.P.L.; Elissen-Roman, C.; van Genderen, M.H.P.; Meijer, E.W., *Macromolecules*, **1995**, 28, 6689.
5. Chapman, T.M.; Hillyer, G.L.; Mahan, E.J.; Shaffer, K.A., *J. Am. Chem. Soc.*, **1994**, 116, 11195.
6. Aoi, K.; Motoda, A.; Okada, M.; Imae, T., *Macromol. Rapid Commun.*, **1997**, 18, 945.

7. Saville,P.M.; Reynolds,P.A.; White, J.W.; Hawker, C.J.; Frechet, J.M.J.; Wooley, K.L.; Penfold, J.; Webster, J.R.P., *J. Phys. Chem.,* **1995**, 99, 8283-8289.
8. Saville,P.M.; .; White, J.W.; Hawker, C.J.; .; Wooley, K.L.; Frechet, J.M.J., *J. Phys. Chem.*, **1993**, 97, 293-294.
9. Bo, Z; Zhang, X.; Yi, X; Yang, M; Shen, J.; Rehn, Y.; Xi, S., *Polymer Bulletin*, **1997**, 38, 257-264.
10. Kim, Y., *Advances in Dendritic Macromolecules*, **1995**, Volume 2, 123-156.
11. Schenning, A.P.H.; Elissen-Roman, C.; Weener, J.-W.; Baars, M.W.P.L.; van der Gaast, S.J.; Meijer, E.W., *J. Am. Chem. Soc.*, **1998**, 120, 8199-8208.
12. Shuler, R.L.; Zisman, W.A., *J. Phys. Chem.,* **1970**, 74, 1523.
13. Schick,M.J. *'Nonionic Surfactants'*, **1966**, Marcel Dekker, Inc., 450.
14. Kawaguchi, M; Komatsu, S.; Matsuzumi, M.; Takahashi, A. *J. Col. Int. Sci.*, **1984**, *102:2*, 356-360.
15. Myers,D. *'Surfaces, Interfaces, and Colloids, Principles and Applications'*, **1991**, VCH Publishers, Inc., 165.
16. Saville, P.M.; Reynolds, P.A.; White, J.W.; Hawker, C.J.; Frechet, J.M.J.; Wooley, K.L.; Penfold, J.; Webster, J.R.P. *J. Phys. Chem.*, **1995**, *99*, 8283-8289.
17. Zhu, J.; Eisenberg, A.; Lennox, R.B., *J. Am. Chem. Soc.*, **1991**, 113, 15, 5583.
18. (a) Kuzmenka, D.J.; Granick, S., *Macromolecules*, **1988**, 21, 779, (b) Shuler, R.L.; Zisman, W.A., *J. Phys. Chem.,* **1970**, 74, 1523, (c) Glass, J.E., *J. Phys. Chem.*, **1968**, 72,13, 4459, (d) Sauer, B.B., Yu, H., *Macromolecules*, **1989**, 22, 786, (e) Lu, J.R.,: Su, T.J.; Thomas, R.K.; Penfold, J.; Richards, R.W., *Polymer*, **1996**, 37, 1, 109.
19. Henderson, J.A.; Richards, R.W.; Penfold, J.; Thomas, R.K.; Lu, J.R., *Macromolecules*, **1993**, 26, 4591.
20. Okahata, Y.; Kobayashi, T.; Tanaka, K., *Langmuir,* **1996**, 12, 1326.
21. Niwa, M; Hayashi, T.; Higashi, N., *Langmuir*, **1990**, 6, 263.
22. Niwa, M.; Higashi, N., *Macromolecules*, **1989**, 22, 1002.

Chapter 5. Ultrathin Films of PEO-PAMAM Diblock Copolymers

5.1 Introduction

The use of dendritic macromolecules to modify surfaces or to make thin films has attracted a lot of attention because the dendrimer has a unique architecture containing a large number of functionalizable end groups. PAMAM dendrimers have been covalently attached to a self-assembled monolayer for chemical sensing applications[1]. These dendrimers when embedded within self-assembled monolayers have been shown to act as ion gates of molecular dimension[2]. PAMAM modified surfaces, made by spontaneous chemisorption onto glass, have been used as substrates for the deposition of noble metal colloids[3]. Electrode surfaces have also been modified with redox-active polymetallic dendrimers[4].

So far, thin films of dendritic macromolecules have been made with a layer-by-layer technique utilizing electrostatic interactions between successive layers. Watanabe and Regen built multilayer dendritic arrays by the alternate complexation of amine terminated PAMAM dendrimers and a Pt^{+2} surface[5]. Tsukruk et al. used alternate layers of acid and amine terminated PAMAM dendrimers to make thin films[6]. The film thickness was in the range of 20 to 80nm for these ionic dendrimer multilayers. Spin-coated films of luminescent dendrimers with a thickness of 60-120nm were made by Wang et al.[7] There are a few examples of thicker films made by solvent casting too[8]. As discussed in Chapter 4, the Langmuir monolayers of certain dendritic polymers at the air-water interface have been studied but transfer of these monolayers to solid substrates to make thin films has not been reported. The use of the Langmuir-Blodgett technique to make mono- and multilayers of dendritic macromolecules offers the advantage of being able to control both the thickness of the deposited film and the orientation of the molecules being deposited. This degree of control is not possible with the layer-by-layer or spin-coating technique. All of the studies in making films of dendrimers have been on dendritic homopolymers. Thin films of linear-dendritic diblock copolymers have not been

made by any group so far. The linear-dendritic diblock structure offers some advantages in making films because the linear block yields the entanglements needed to get good physisorbed films.

In this chapter, details of the buildup of mono- and multi- layers of PEO-PAMAM linear-dendritic diblock copolymers using the LB technique will be discussed. The ability to control the degree of ordering in the films will be demonstrated by the transfer of monolayers at different surface pressures. The variation in the film properties and correlation between the surface orientation and the film behavior as the generation number of the dendrimer is increased will be discussed. The techniques used to make ordered multilayer films of these diblocks will be elaborated.

5.2 Experimental Section

Synthesis of stearate terminated PEO-PAMAM linear-dendritic diblocks used to make ultrathin films has been discussed in Chapter 2; the chemical structure was confirmed using NMR and MALDI-TOF MS methods. The molecular weight of the PEO block was 2000 in all cases, and dendrimer generations varied from 1.0 to 4.0. Hexadecanethiol and octadecyltrichlorosilane used to modify surface properties of substrates were purchased from Aldrich and Fluka respectively and used without further purification. PMAA(15000, 30% aqueous solution) used to modify the subphase were purchased from Polysciences. BPEI was purchased from Aldrich Chemical Co. The concentration of the polymers used was 0.2g/L. The pH of the subphase was modified using H_2SO_4 and HCl. $MgSO_4.7H_2O$ was purchased from Mallinckrodt, and used without further purification. Microscope glass slides and n-type test grade silicon wafers(Silicon Sense) were used as substrates for LB monolayer deposition.

A Lauda FW-2 trough was used for the film studies. The total surface area of the trough was 927 cm^2 and the volume of the subphase was 1.3 L. Ellipsometry was used to measure the thickness of the deposited films. Atomic Force Microscopy was used to collect data on the thickness and topography of the deposited films. A Digital

Instruments Division 3000 AFM was used in the tapping mode with a standard etched silicon tip to study areas ranging from 4μm square to 15 μm square.

LB Trough experiments: Monolayers were spread on a Milli-Q water subphase from chloroform solutions of the diblock copolymers. The concentration of the diblocks in chloroform was in the range of 1-3 mg/ml. Typically, 50-100μl of the solution was spread dropwise at the air-water interface using a microsyringe. The temperature of the subphase was controlled at 20°C. 30-60 minutes was allowed for evaporation of the solvent before compression of the monolayer was initiated. The monolayer was compressed at the rate of $92cm^2$/min in most cases. Prior to deposition, stability of the monolayer at the transfer pressure was tested. The monolayer was compressed to the transfer pressure and the change in area over time was recorded. The PEO(2k)-3.0G-S film made at 30mN/m was deposited at 5mm/min. The bilayer film at 54mN/m was deposited at 5mm/min and the multilayer film at the same pressure was deposited at 10mm/min. The films of PEO(2k)-4.0G-S were deposited at 2mm/min.

Substrate Preparation: Gold substrates were prepared by thermally evaporating gold shot(99.99% purity, American Gold and Silver) onto silicon wafers. A 100Å film of evaporated chromium served as the adhesive layer between the 1000Å gold film and the silicon wafer. Typically the surface roughness of the resulting substrate was 1.8nm root mean square(rms) roughness in tapping mode AFM on a $10\mu m^2$ region of the surface. The gold substrate was immersed in 15ml of hexane containing about 0.4ml of hexadecanethiol. After 16 hours, the gold substrate was washed well with ethanol, then with hexane, and dried over a nitrogen stream to give a hydrophobically functionalized surface. In order to produce hydrophobically functionalized glass slides, they were cleaned with a piranha etch. The cleaned glass slides were immersed in about 10ml of toluene containing 1ml of octadecyltrichlorosilane. After half an hour, the slides were washed with toluene, hexane, and ethanol.

5.3 Results and Discussion

.5.3.1 Ultrathin transferred films of PEO-PAMAM diblock copolymers

After establishing the behavior of the polymers at the air-water interface, monolayers of PEO(2k)-3.0G-S and PEO(2k)-4.0G-S were transferred onto substrates to make bilayer and multilayer films; films were transferred at 20°C at 2 to 5 mm/min, as described in the Experimental section. Hydrophobically functionalized gold and glass substrates were used for making films of PEO(2k)-3.0G-S and PEO(2k)-4.0G-S respectively. The stability of the monolayers was studied by compressing the monolayer to the transfer pressure, holding at the specified pressure, and noting the change in surface area over time. The surface area of a PEO(2k)-3.0G-S monolayer changed by $20cm^2$ over seven hours at 30mN/m, indicating a relatively stable Langmuir film. For the PEO(2k)-4.0G-S monolayer, the surface area decreased in the first 10-15 minutes after compression, but stayed stable subsequently over a six hour time period. Since PEO(2k)-4.0G-S is practically insoluble in the aqueous subphase, the initial loss in area suggests that rearrangements in the monolayer are taking place. Monolayers were transferred at surface pressures of 30mN/m and 54mN/m for the PEO(2k)-3.0G-S diblock and at 20mN/m and 40mN/m for the PEO(2k)-4.0G-S diblock. These pressures were chosen at points in the pressure-area isotherm for which the monolayer was in a well-packed, solid state or undergoing a transition from liquid to solid state packing.

Films of PEO(2k)-3.0G-S

At 30mN/m, bilayer thin films of the third generation stearate functionalized block copolymers were successfully transferred to the gold substrate. At this pressure, the monolayer is at the first condensed phase region on the π-a isotherm; in the formation of the bilayer, adsorption took place on both the upstroke and downstroke. The atomic force micrograph of a bilayer film formed using this LB process is shown in figure 5.1. There is good coverage of the substrate, represented by the light regions, indicating the formation of a cohesive film. Portions of the film where no deposition took place (i.e.

holes) are indicated by the dark regions, and island defects are also present. Depth analysis on AFM gave a film thickness of 8.1nm and ellipsometry gave a film thickness value of 8.7nm. These two values are in good agreement with an estimated bilayer thickness of 8.6nm from theoretical calculations. (The hydrodynamic radius of PEO(2k)-3.0G determined from intrinsic viscosity measurements is 1.8nm and the length of a fully extended stearic acid molecule at the interface is 2.5nm[9] giving an estimate of 4.3nm for the thickness of a PEO(2k)-3.0G-S monolayer at the interface.) This number suggests that, as discussed previously, the stearate groups in PEO(2k)-3.0G-S are fully extended at high compressions. It was found that after the first bilayer is deposited, every downstroke resulted in desorption of polymer approximately equal to the adsorption gained on the upstroke. Increasing the speed of the downstroke to decrease desorption did not alter this behavior. Therefore, multilayer films were not successfully formed under these conditions.

Films were also formed with the third generation diblock copolymer at a higher pressure, above the transition regime and closer to the collapse pressure in the p-a isotherm of the samples. Figure 5.2 shows the AFM of a bilayer (1 upstroke/downstroke cycle) film transferred at 54 mN/m and 20°C. A smooth, continuous film with good coverage and no apparent holes is obtained at this surface pressure, although island formation is still present. The film thickness measured using ellipsometry was 11 nm. Depth analysis on AFM showed the presence of two regions: a region of thickness 11.2nm, which corresponds to the continuous film, and a thickness of 22nm corresponding to islands that are twice the thickness of the original monolayer. Similar island defects have been observed in other L-B films of polymeric and low molar mass amphiphiles. These observations suggest that the bilayer is rearranging to some extent, probably before or during deposition. It is notable that the bilayer thickness is larger for the films made at higher pressures, indicating a more highly compressed and extended polymer molecule.

The advancing contact angle of both hexadecane and water on the bilayer film was 40°. The hydrophobically functionalized gold substrate had an advancing contact angle of 40° with hexadecane and 110° with water before monolayer deposition. These results indicate that the bilayer surface is very heterogeneous; a second possibility is that there are surface group rearrangements taking place at the surface during the course of the contact angle measurements.

At a transfer pressure of 54 mN/m, it was possible to build up Z-type multilayers of the third generation material. In this case, after the first bilayer, deposition takes place only on the upstroke. The area deposited from the air-water interface versus the layer number is plotted in figure 5.3; the dotted line shows the area of the substrate immersed. The results imply that a consistent amount of the diblock copolymer is adsorbed on each upstroke. Ellipsometric measurements across the area of the film indicate that the resulting multilayered films vary over a broad range in thickness, and are not highly uniform. The somewhat conflicting information from the trough transfer area results and the ellipsometric measurements of the film suggest that rearrangements and/or surface migration of the molecules are taking place after or during deposition of the film. It is possible that each re-immersion of the substrate during transfer presents an opportunity for the water soluble PEO block in already-deposited layers to rearrange at the surface.

Z-type multilayers were obtained for other dendrimer amphiphiles as well. Schenning et. al.[10] studied the amphiphilic behavior of palmitoyl-functionalized polypropyleneimine dendrimers. For these dendrimeric amphiphilies, transfer of monolayers onto hydrophilic glass slides resulted in Z-type films with transfer ratios between 0.8 and 1.0. Kim[11] studied deposition of the imidazolium salt of hyperbranched polyphenylenes at 20mN/m onto a silicon wafer. He found that the films were of the z-type with a transfer efficiency in the range of 0.5-0.6. The homogeniety of the film deteriorated with increase in the number of deposited layers.

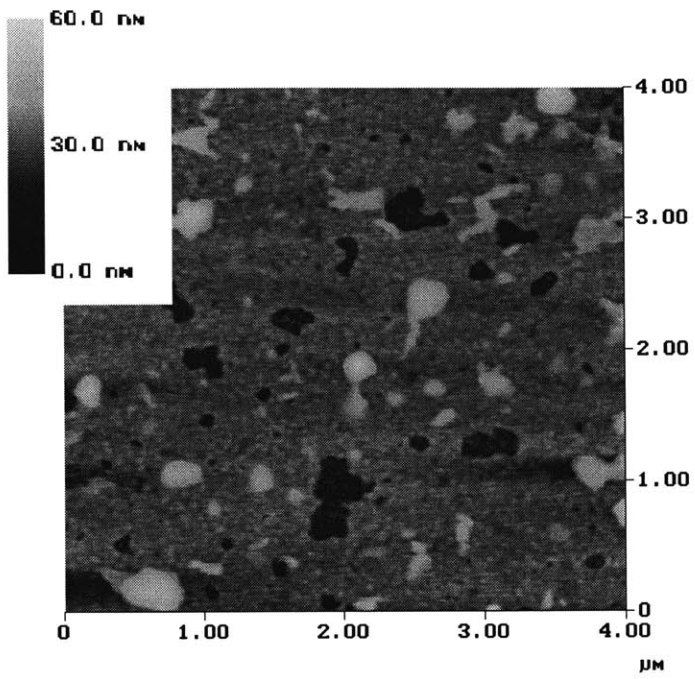

Figure 5.1 Atomic Force Micrograph of a film of PEO(2k)-3.0G-S transferred at 30mN/m and 20°C onto hydrophobically functionalized gold substrate.

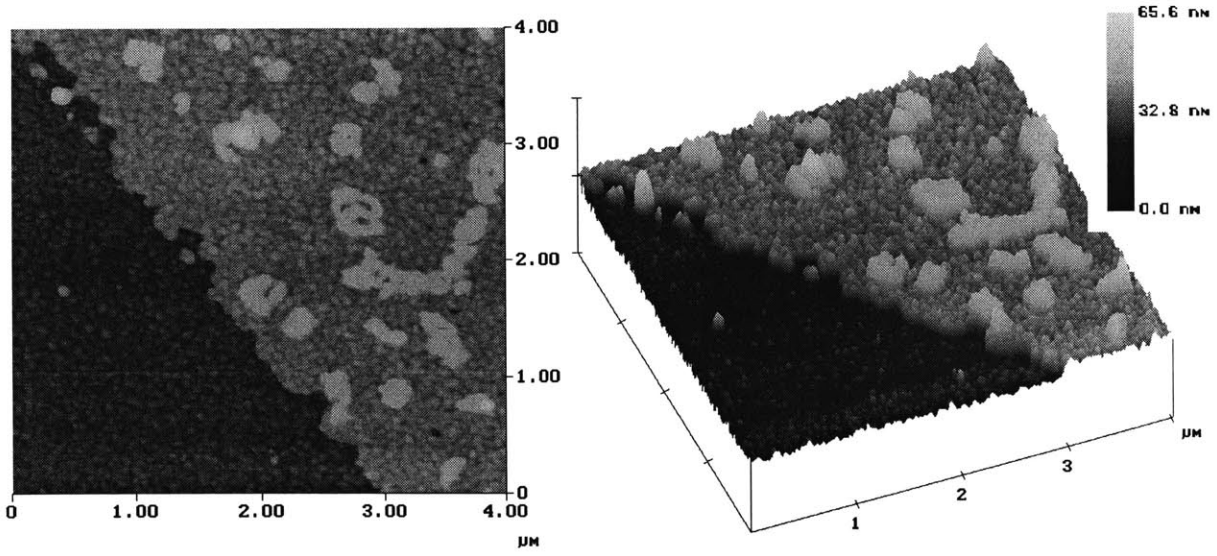

Figure 5.2 AFM of a bilayer film of PEO(2k)-3.0G-S transferred at 54mN/m and 20°C onto hydrophobically functionalized gold substrate.

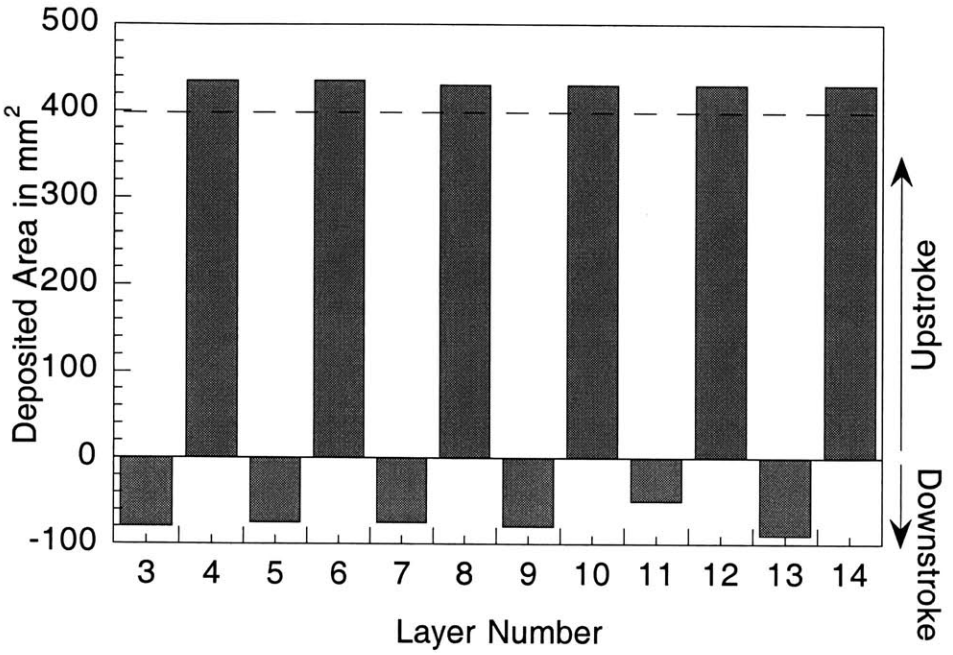

Figure 5.3 Histogram of the area transferred from the air-water interface onto a hydrophobically functionalized gold substrate for PEO(2k)-3.0G-S at a surface pressure of 54mN/m and 20°C.

Films of PEO(2k)-4.0G-S

The gold coated silicon substrates are useful for depositing films because ellipsometry can be used to measure film thickness; however, this type of substrate can only be functionalized on one side. From the area deposited, it appears that deposition is taking place on both sides of the gold substrate. To avoid any ambiguity regarding the amount of film deposited, glass substrates functionalized on both sides were used in the film deposition studies on PEO(2k)-4.0G-S diblocks. The AFM of bilayer films of this fourth generation stearate functionalized polymer transferred at 20mN/m and 20°C is shown in figure 6.4a. This pressure corresponds to the minimum transfer pressure customarily used to make polymer LB films. As was the case for the third generation polymer, at this lower pressure some holes and voids are observed, as well as island defects; despite this, the film appears to be fairly cohesive. Depth analysis on AFM gave a film thickness of 6.0 nm for this bilayer film, which is much smaller than that expected

if the stearate groups and the dendron branches were fully extended. It is also notable that this thickness is also much lower than the bilayer thickness of 8.3 nm found for the third generation block at the lower pressure. These results indicate that the stearate groups are not uniformly oriented perpendicular to the interface, as was the case for the third generation films. This is consistent with the observations of the π-a isotherms and area per molecule for these polymers.

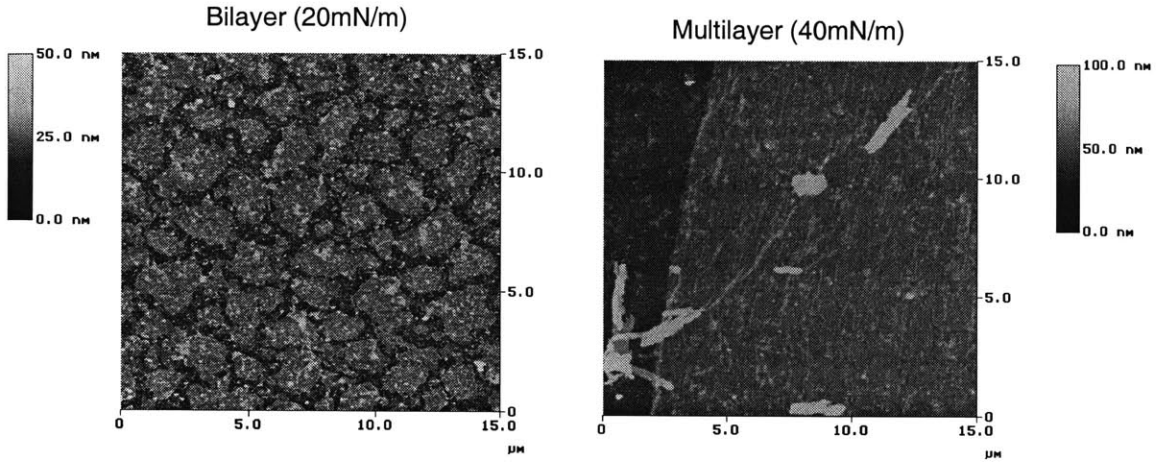

Figure 5.4a and b AFM of bilayer and multilayer films of PEO(2k)-4.0G-S transferred at 20mN/m and 40mN/m respectively and 20°C.

The AFM of a bilayer film transferred at 40mN/m and 20°C is shown in figure 5.4b; the sample was exposed to 3 upstroke/downstroke cycles, but adsorption only occurred on the first cycle; the problem of desorption resulted in little or no multilayer growth. This transfer pressure corresponds to the center of the condensed phase regime on the π-a isotherm. The bilayer film shown indicates that good coverage is obtained. The decrease or elimination of hole defects in the deposited films with increasing transfer pressure seen for PEO(2k)-3.0G-S is observed for the fourth generation materials as well. In fact, most of the phenomena observed for PEO(2k)-3.0G-S films are seen for PEO(2k)-4.0G-S films, but at lower transfer pressures. Depth analysis on AFM gave a film thickness of 6.6nm for the film deposited at 40mN/m. Again, the bilayer film thickness is

lower than that for PEO(2k)-3.0G-S. This suggests that the stearate groups are unable to orient themselves even at high surface pressures. The film looks uniform on the AFM, but no independent measure of film thickness such as ellipsometry was obtained because a nonreflective glass substrate was used. A detail of the bilayer film at 40 mN/m is shown in figure 5.4c.

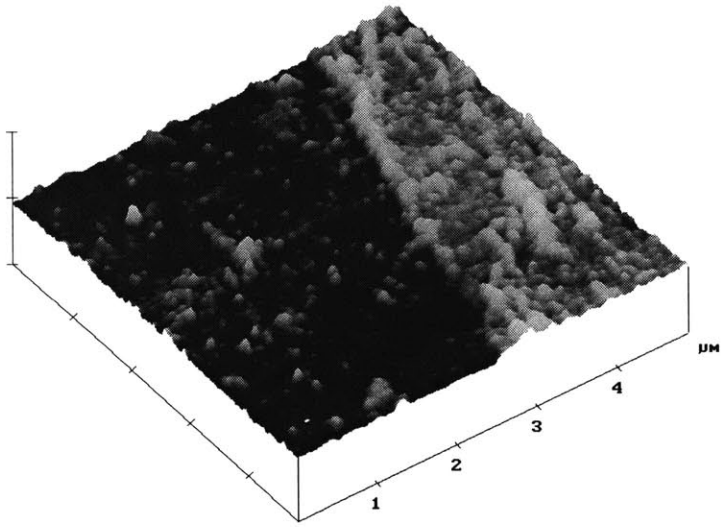

Figure 5.4c Details of the multilayer films of PEO(2k)-4.0G-S transferred at 40mN/m.

5.3.2 Engineering Multilayer Build-up

There are three interactions that play a role in the efficient building of multilayer LB films: a) the interaction between the substrate and the first deposited monolayer, b) the interaction between the monolayer and the air-water interface, and c) the interaction between any two deposited monolayers in a multilayer film. Since it was possible to deposit bilayers on the functionalized substrates, the problem encountered with multilayer deposition at moderate surface pressures cannot be because of the substrate-monolayer interaction. However, the influence of the substrate is lost after depositing the first few monolayers. When an ideal transfer ratio of 1 is achieved during LB deposition, the regeneration of the substrate nature takes place automatically. This is exemplified by the multilayer build-up at 54mN/m for PEO(2000)-3.0G-S, where transfer ratio was

1(figure 5.3). At low transfer ratio's, the second and third interactions are pivotal in deciding if multilayer films are built or not. For the copolymers discussed here, desorption on the downstroke suggests that the interaction between monolayers is too weak and the diblock probably prefers to be at the air-water interface. The weak adhesion could be because of the chemical composition of the diblock. The linear PEO block is very soluble in water and in the presence of water does not like to adhere on or interact with other PEO molecules. Therefore, on the downstroke the air-water interface is energetically more favorable for the PEO linear block than the film. The self-repulsive behavior of the PEO block could be the cause of the rearrangements seen in multilayer films transferred at 54mN/m. To test whether this model of the observed behavior was correct, the effect of subphase modifications on the film forming ability was investigated.

Two types of modifications were made to the subphase. In one study, magnesium sulfate at a concentration of 0.385M was added to the subphase making it a poor solvent for the PEO block. In the second study, water soluble polymers capable of forming hydrogen bonds with the PEO block were dissolved in the subphase. The details of the effect of these subphase modifications on the π-a isotherms of the diblock amphiphiles and the relevant references are discussed in Section 4.3.2. A discussion of the effect of these modifications on the segment density distribution of the PEO block at the interface is also included in the same section. Presumably, a change in PEO orientation in the diblock monolayer at the air-water interface will effect the nature of films formed on transfer to a substrate.

The subphase modifications were designed to improve adhesion between the deposited monolayers. The conditions in the salt subphase were close to the theta conditions for PEO, decreasing considerably its self-repulsive behavior. PAA, PEI, and PMAA are known to hydrogen bond with PEO at low pH in solution[12,13]. When these polymers are present in the subphase, they probably form a hydrogen bonded complex with the PEO-PAMAM amphiphile. Hence, deposition from the polymer modified subphases possibly results in transfer of the hydrogen bonded complex. The presence of

the complexing polymer in the transferred films will probably introduce hydrogen bonds between adjacent monolayers; this will help both in building multilayer films and in preventing rearrangements from taking place once the multilayer is formed (Figure 5.5). The use of water soluble polymers to change the nature of the langmuir monolayer has been used as a technique by a number of other people[12,14].

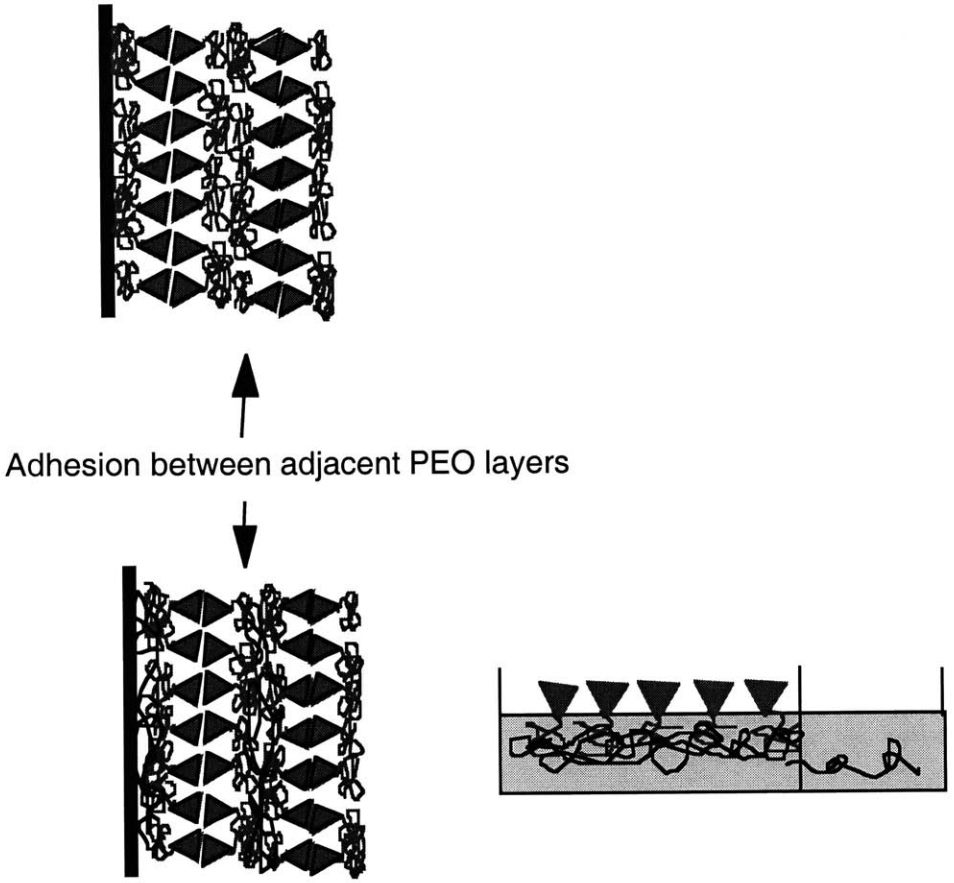

Figure 5.5 Schematic of the organization at the water air-water interface of the PEO-PAMAM diblock/polmer complex. The cartoon shows the adsorption of the monolayer complex onto the substrate.

Deposition of monolayers at 50mN/m from a salt subphase onto hydrophobically functionalized gold substrates was attempted. However, considerable amount of salt was

present in the transferred bilayers because of the high salt concentration in the subphase and it was difficult to analyze. So the use of salt to modify the subphase was discontinued.

The presence of PAA in the subphase did not affect the isotherm of PEO(2000)-2.0G-S (Section 4.3.2). To eliminate the effect of time taken for the polymer in the subphase to migrate to the PEO-PAMAM monolayer, a solution of PEO(2000)-2.0G-S/BPEI solution in chloroform was spread on a deionised water subphase(pH=2). After the first bilayer, deposition took place only on the upstroke at 35mN/m for this system. Considerable desorption was present on the downstroke.

The results for the deposition of films using PMAA in the subphase are shown in Figure 5.6. 19 monolayers of PEO(2000)-2.0G-S were transferred onto a carboxylic acid functionalised gold substrate at a low surface pressure of 20mN/m. The films formed continued to be of the Z-type. The speed of the upstroke and downstroke was 2mm/min with a 20s pause at the end of the downstroke for the first 13 immersions. From the 14th to the 38^{th} immersion, the upsroke speed was 5mm/min and the downstroke speed was 20mm/min with a pause of 120s at the end of the downstroke. Increasing the pause time increases the deposition on the downstroke (figure 5.6). Since the film is immersed in the subphase during this pause time, rearrangements could be taking place promoting the deposition. Surface activity of PMAA dissolved in the subphase was tested by compressing the subphase. The surface pressure was less than 3mN/m at any surface area showing that the PMAA was not surface active. Without PMAA in the subphase, deposition of PEO(2000)-2.0G-S at the same conditions was not possible. The results from this standard test are shown in figure 5.7. The substrate, pH and temperature of the subphase, and the deposition pressure were the same for both the experiments.

Figure 5.8 shows the AFM micrograph of the multilayer film formed. The thickness of the 19 layer film was about 170nm giving an average monolayer thickness of 89Å. Thickness per layer for films transferred from de-ionised water subphase was about 50Å for PEO(2000)-1.0G-S, about 55Å for PEO(2000)-3.0G-S,and about 30Å for

PEO(2000)-4.0G-S. The thickness per layer is greater for films transferred from the PMAA subphase suggesting the inclusion of PMAA in the multilayer film.

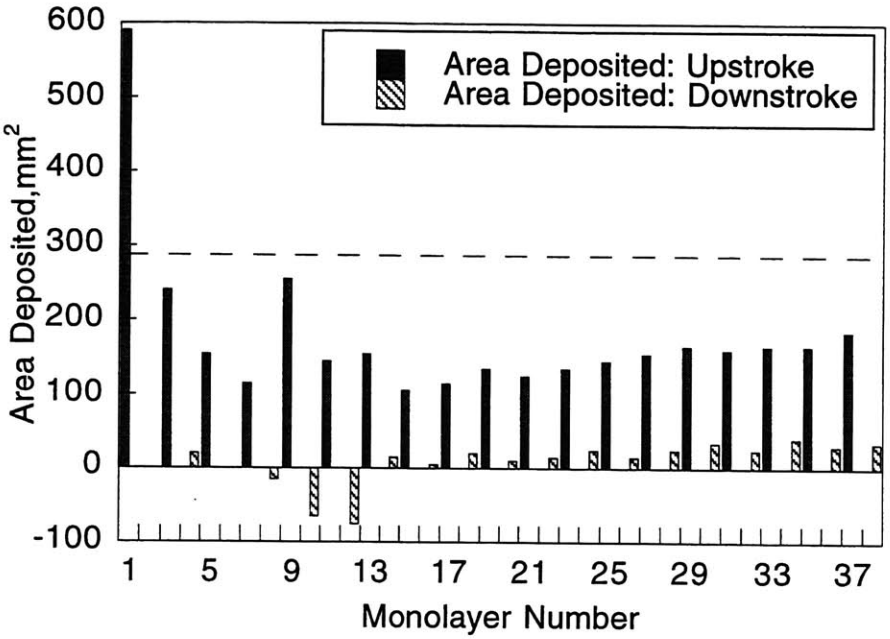

Figure 5.6 Histogram showing the area transferred from the air-water interface on to a carboxylic acid functionalized gold substrate for PEO(2000)-2.0G-S at a surface pressure of 20mN/m and 20°C. The aqeous subphase had 0.2g/l of PMAA dissolved at a pH~2.

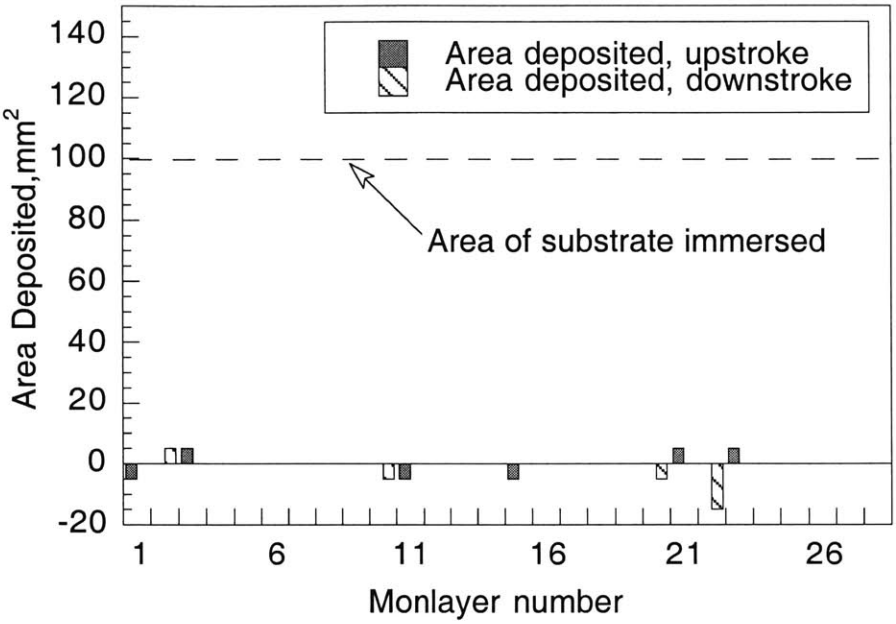

Figure 5.7 Histogram of the area transferred from the air-water interface onto a carboxylic acid functionalized gold substrate for PEO(2000)-2.0G-S at a surface pressure of 20mN/m and 20oC. The subphase was deionised water at pH~2.

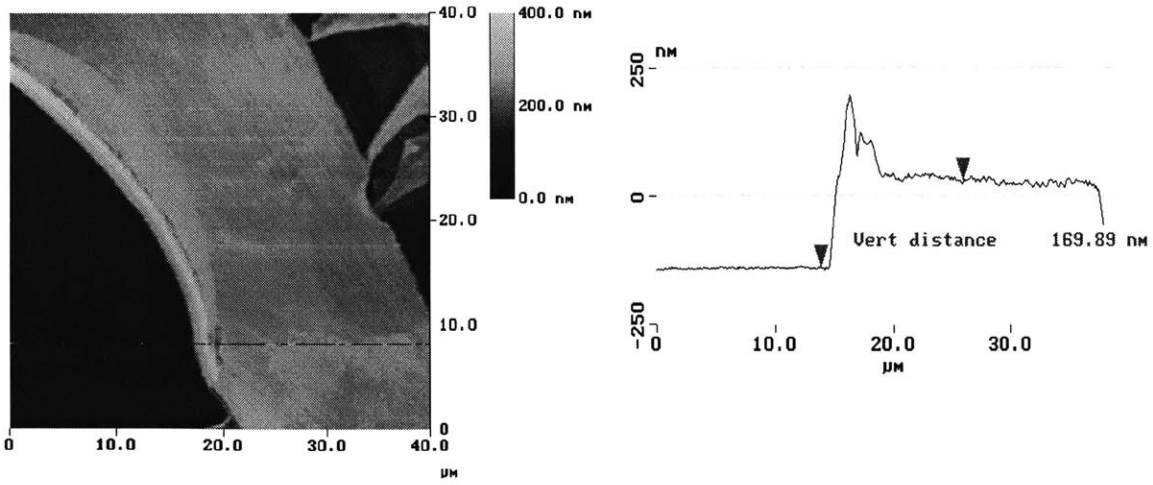

Figure 5.8 Atomic force micrograph of the PEO(2000)-2.0G-S multilayer deposited at 20mN/m from a water/PMAA(pH~2) subphase.

5.4 Chapter Summary

5.4 Chapter Summary

Transfer of diblock copolymer monolayers onto functionalized substrates was found to be possible. Physisorbed uniform films of linear-dendritic diblock copolymers were made and are reported here for the first time. Transfer of films at higher surface pressures gave uniform films with very few defects. Z-type multilayer films were formed for both the diblocks studied. Different subphase conditions were investigated to optimize the formation of multilayer films. Use of PMAA in the water subphase at pH=2 resulted in efficient multilayer build-up for the second generation copolymer. The transfer pressure used to make this multilayer was quite low, about 20mN/m. The combination of a PMAA subphase and high transfer pressures will potentially lead to films which have few defects, similar to the uniform bilayers of the third generation diblock formed by transfer at 54mN/m.

5.5 References

1. (a) Wells, M; Crooks, R., *J. Am. Chem. Soc.*, **1996**, 118, 3988, (b) Tokuhisa, H.; Crooks, R., *Langmuir*, **1997**, 13, 5608.
2. Zhao, M.; Tokuhisa, H.; Crooks, R.M., *Angew. Chem. Int. Ed. Engl.*, **1997**, 36, 23.
3. Bar, G.; Rubin, S.; Cutts, R.W.; Taylor, T.N.; Zawodzinski Jr., T.A., *Langmuir*, **1996**, 12, 1172.
4. Alonso, B.; Moran, M.; Casado, C.; Lobete, F.; Losada, J.; Cuadrado, I., *Chem. Mater.*, **1995**, 7, 1440.
5. Watanabe, S.; Regen, S.L., *J. Am. Chem. Soc.*, **1994**, 116, 8855.
6. Tsukruk, V.V.; Rinderspacher, F.; Bliznyuk, V. N., *Langmuir*, **1997**, 13, 8, 2172.
7. Wang, P-W.; Liu, Y-J; Devadoss, C.; Bharathi, P.; Moore, J.S., *Adv. Mat.*, **1996**, 8, 3, 237.
8. (a) Evenson, S.A.; Badyal, J.P.S., *Adv. Mat.*, **1997**, 9,14, 1097, (b) Coen,M.C.; Lorenz, K.; Kressler, J.; Frey, H.; Mulhaupt, R., *Macromolecules*, **1996**, 29, 8069.

9. Ulman,A. *'An Introduction to Ultrathin Organic Films from Langmuir-Blodgett to Self-Assembly'*, **1991**, Academic Press, Inc., 11
10. Schenning, A.P.H.J.; Elissen-Roman, C.; Weener, J-W.; Baars, M.W.P.L.; van der Gaast, S.J.; Meijer, E..W., *J. Am. Chem. Soc.*, **1998,** *120*, 8199.
11. Kim, Y., *Advances in Dendritic Macromolecules*, **1995**, Volume 2, 123.
12. Niwa, M.; Hayashi, T.; Higashi, N., *Langmuir*, **1990**, 6, 263.
13. Eagland, D.; Crowther, N.J.; Butler, C.J., *Eur. Polym. J.*, **1994**, 30, 7, 767.
14. Niwa, M.; Higashi, N., *Macromolecules*, **1989**, 22, 1002.

Chapter 6. Bulk Morphology of Linear-Dendritic Diblock Copolymers

6.1. Introduction

In the last few years, the focus of research on dendrimer macromolecules has shifted from synthesis to an exploration of their applications. So far, estimates of the size of dendritic molecules have come from measurements done in solution using small angle nuetron scattering(SANS), small angle X-ray scattering(SAXS), gel permeation chromatography(GPC) etc.[1] These studies have revealed that the use of theory pertaining to random coil linear polymers accurately estimate the of size or interaction parameters for dendrimers. The highly branched architecture further complicates the probing of the bulk state of dendrimers.

Only the lower generation dendrimers have been studied using X-ray crystallography[2]. Transmission electron microscopy(TEM) has been used to image different generations of PAMAM dendrimers by a few groups[3]. Jackson et al.[4] were able to resolve PAMAM dendrimers as separate, beam-stable entities using conventional TEM. They obtained an estimate of size and size distribution for these dendrimers from statistical analysis of the TEM images. X-Ray diffraction and TEM have been used to determine the shape, size, and internal structure of self-assembled spherical and cylindrical supramolecular dendrimers. Percec et al.[5] synthesized monodendrons which self assemble in the bulk to give spherical and cylindrical supramolecules. The subsequent organization of the self-assembled supermolecules into regular liquid crystalline phases has enabled the direct visualization of these aggregates using the techniques outlined above.

The only imaging studies performed on linear-dendritic diblock copolymers were done by van Hest et al.[6] In this study, aggregates of amphiphilic polystyrene-polypropyleneimine linear-dendritic diblock copolymers were imaged. It was shown that the formation of spherical micelles, micellar rods, or vesicular structures depended on the generation number of the dendritic block.

For linear-dendritic diblock copolymers, the question of phase segregation and the introduction of morphology in the bulk is an interesting one, given the unique architecture of the two blocks. When diblock copolymers with two linear blocks phase segregate, the morphology of the phases formed changes from spheres to cylinders to alternating lamellae depending on the relative length of the two blocks. The sizes of these morphological features are traditionally determined using a combination of SAXS and TEM. Although a number of different linear-dendritic diblock copolymers have been synthesized, most of the characterization studies have been in solution. The only reported example of the solid state characterization of hybrid dendritic block copolymers is that of AB and ABA hybrid copolymers with polybenzylether dendron as the A block and PEO as the B block[7]. Here, phase segregation was indicated by the presence of a melting point for the crystalline PEO block in the DSC trace. Typically, the thermal characterization of dendrimeric homopolymers gives only a glass transition[8].

When linear diblocks showing phase segregation in the bulk are spread as thin films, the finite film thickness has a strong influence on the block copolymer microstructure[9]. Presence of the two interfaces results in selective segregation of the blocks and can lead to surface induced ordering. This symmetry-breaking surface further leads to the formation of surface defects in ordered copolymeric systems when the film thickness is not an integral multiple of the copolymer domain size. For linear-dendritic diblock copolymers that segregate in bulk, the effect of the surface on the ordering in thin films should make an interesting study. The large number of dendrimer end groups will introduce entropic effects into surface energy considerations that drive selective segregation of two blocks in the presence of a surface. Once these influences are understood, simple techniques such as spin-coating could be used to produce ordered thin films of linear-dendritic diblock copolymers for use as nanoporous membranes.

In this chapter, thermal characterization of linear-dendritic diblock copolymers will be reported. Effect of PEO chain length and generation of the dendrimer on the thermal behavior will be discussed. The effect of end group modifications on the thermal

behavior will be reported. Bulk morphology studied using SAXS and optical microscopy will be elaborated. Finally, the use of information from the bulk morphological studies to make spin coated thin films showing phase segregation will be reported.

6.2. Experimental section

The synthesis, characterization, and properties of the diblocks used for the bulk morphology studies are described in detail in the previous chapters. Differential scanning calorimetry(DSC) scans were recorded on a Perkin Elmer DSC7 calorimeter with heating and cooling rates of 10°C/min. The amount of material used for the DSC runs was between 8 and 14mg. Small angle x-ray scattering(SAXS) was conducted using a Rigaku RU-H3R rotating anode generator producing Cu K_α radiation(λ = 1.54Å) at 40KV and 30mA. Data were collected using a two-dimensional GADDS/HI-STAR area detector manufactured by Siemens, containing an array of 512 X 512 wires. All experiments were conducted in an evacuated flight path at a sample to detector distance of 63.8cm, which enabled the resolution of d-spacings in the range of 20-450Å. Wide angle X-ray diffraction(WAXD) was conducted using a Rigaku RU300 diffractometer. All the SAXS and WAXD samples were prepared by melting the sample above 120°C for a couple of minutes, followed by quenching to the annealing temperature. The samples were annealed for 16 hours. A Leitz optical microscope with a CCD camera attachment and a Mettler FP-90 hot stage (heating rate of 10°C/min) was used to record the optical micrographs having cross polarizers. Sample for the optical studies were thin films cast from a solution of the copolymer in chloroform. The concentration of the modified diblock copolymer in chloroform was between 0.2 and 8.5mg/ml. Freshly cleaved mica and gold functionalized with -COOH terminated alkane thiols were used as the substrates for spin-coating chloroform solutions of the diblocks. Spin-coating was performed at a speed of 6000rpm for two minutes. Ellipsometry was used to measure the thickness of films cast on gold substrates.

6.3. Results and discussion

6.3.1. DSC results

PEO(5000) Copolymer Series

Figure 6.1a shows the melting point of the PEO(5000) block plotted against the generation number of the dendrimer block. The melting point of the PEO block decreases with an increase in the size of the dendrimer block. Pure PEO(5000) has a melting point of 59.5°C; this value decreases to 50°C for the PEO(5000)-4.5G diblock implying less ordered or less stable crystallites within the blocks. In Figure 6.1b, the enthalpy of melting ΔH (J/g) is plotted against the generation number of the dendrimer block. The dark squares are the numbers obtained from DSC. The crosses represent the ΔH values normalized against the weight fraction of PEO in the diblock copolymer. The normalized ΔH values remain nearly constant with increasing generation number (Figure 6.1b), implying a constant percentage of crystallinity in the PEO block, despite the presence of the dendrimer block.

Frechet et al. have studied the thermal behavior of AB and ABA diblock and triblock copolymers with PEO as the A block and benzylether dendrimer as the B block[10]. They found that when the dendrimer block was the majority block, phase mixing took place with no detectable melting point for the PEO block in the DSC trace due to loss of crystallinity in the mixed phase. When the mass of the PEO block was greater than or equal to the benzylether dendrimer block, microphase segregation was found to occur with two thermal transitions being observed - a melting transition associated with the crystalline PEO phase and a glass transition associated with the dendrimer phase.

For the PEO(5000)-PAMAM dendrimer diblocks discussed here, the mass of the PEO block is in excess of the dendrimer for all samples except for PEO(5000)-4.5G, and a melting point for the PEO block is detected in all cases. These results(Figures 6.1a and 6.1b) suggest that the crystalline morphology of the PEO block changes as the dendrimer generation increases, perhaps due to the formation of smaller crystallites induced by

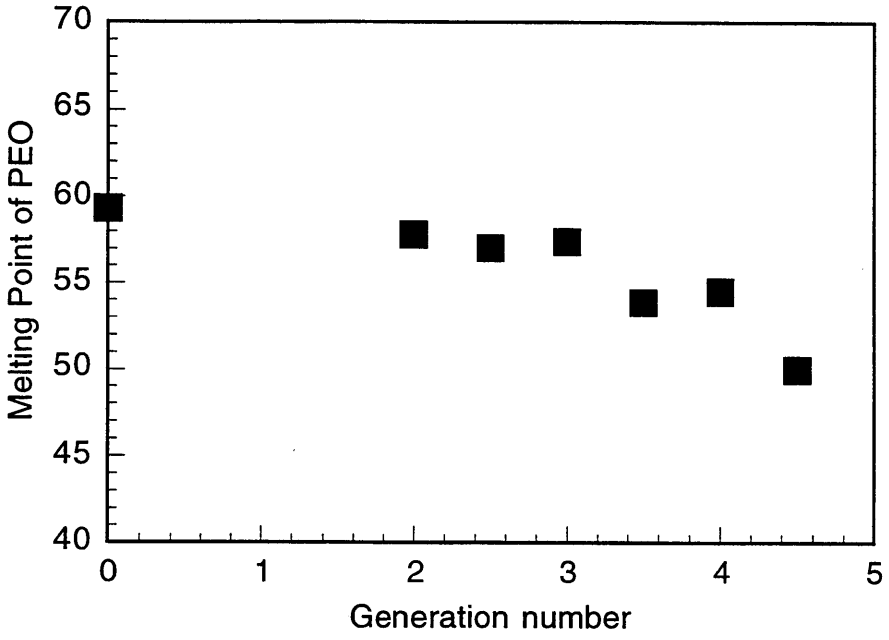

Figure 6.1a Depression of PEO melting point with increasing dendrimer generation in PEO(5000)-dendrimer diblocks.

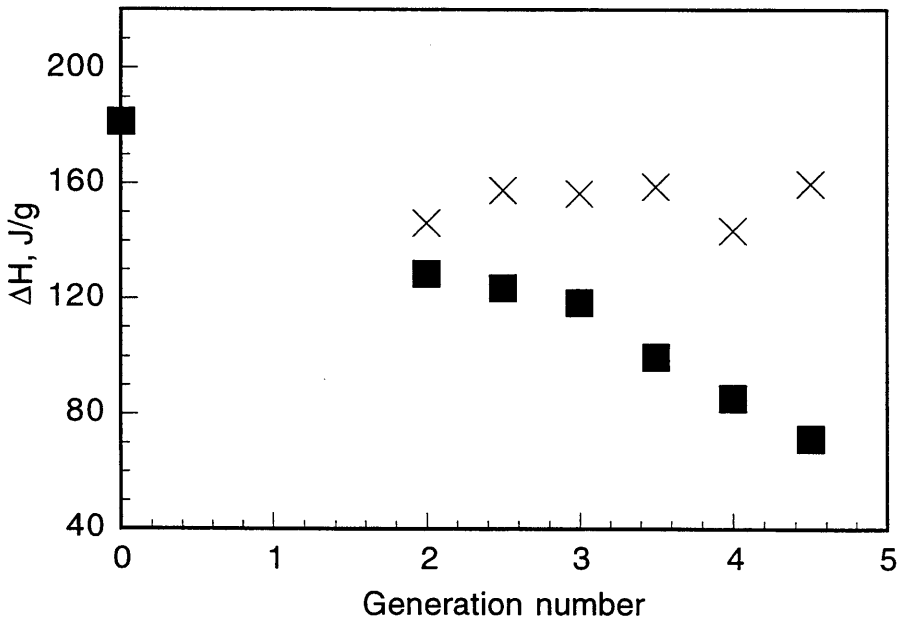

Figure 6.1b Enthalpy change for PEO(5000) melting as a function of dendrimer generation (■) ΔH J/g from DSC, (X) normalized ΔH J/g.

varying block copolymer domain sizes or geometries, or the lowering of T_m due to an increased extent of mixing with larger dendron blocks. However, the constant percent crystallinity indicates that some degree of microphase segregation is present in all cases.

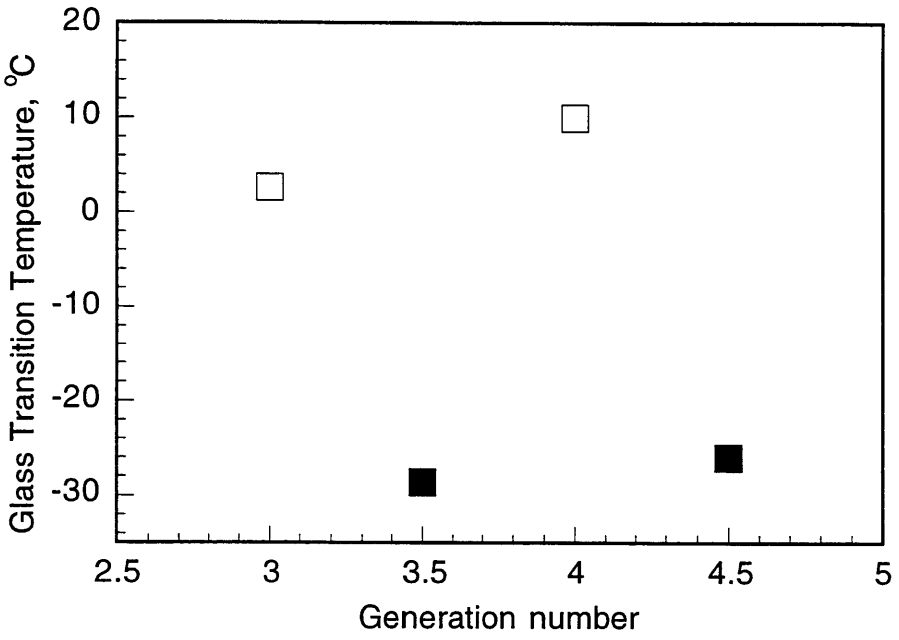

Figure 6.2 Plot of observed glass transition temperature vs. dendrimer generation for PEO(5000)-dendrimer diblocks. ( ) amine terminal groups, (■) ester terminal groups.

Glass transition temperatures(T_g) were observed for PEO(5000)-3.0G,3.5G,4.0G,4.5G diblocks, and the presence of end group influence on T_g in linear-dendritic hybrid diblock copolymers is reported here. Figure 6.2 shows the glass transition temperatures plotted against the generation number of the dendrimer. These glass transition temperatures depend on the chemical nature of the dendrimer end groups with a 30°C difference between the amine terminated (3.0G,4.0G) and the ester terminated (3.5G,4.5G) diblocks. (The T_g of pure PEO(5000) was close to the lower detection limits of the instrument and was not observable.) The strong dependence on end group functionality indicates that the PAMAM dendritic block is the source of the

observed T_g. This end group effect on T_g has been seen before in pure dendrimers[11], although this is the first report of such behavior in linear-dendritic hybrid copolymers. For benzylether dendrimers, increases in T_g's follow increases in chain end polarities.

PEO(2000) Copolymer Series

Figure 6.3a shows the melting point of the PEO(2000) block plotted against the generation number of the dendrimer block. The melting point of the PEO block decreases with increase in size of the dendrimer block, similar to the trend seen for the PEO(5000) series. It goes from 54°C for pure PEO(2000) to 40°C for PEO(2000)-4.0G. The depression in PEO melting point is greater for the PEO(2000) series compared to the PEO(5000) series because the weight fraction of the dendrimer at any given generation is greater in the former case.

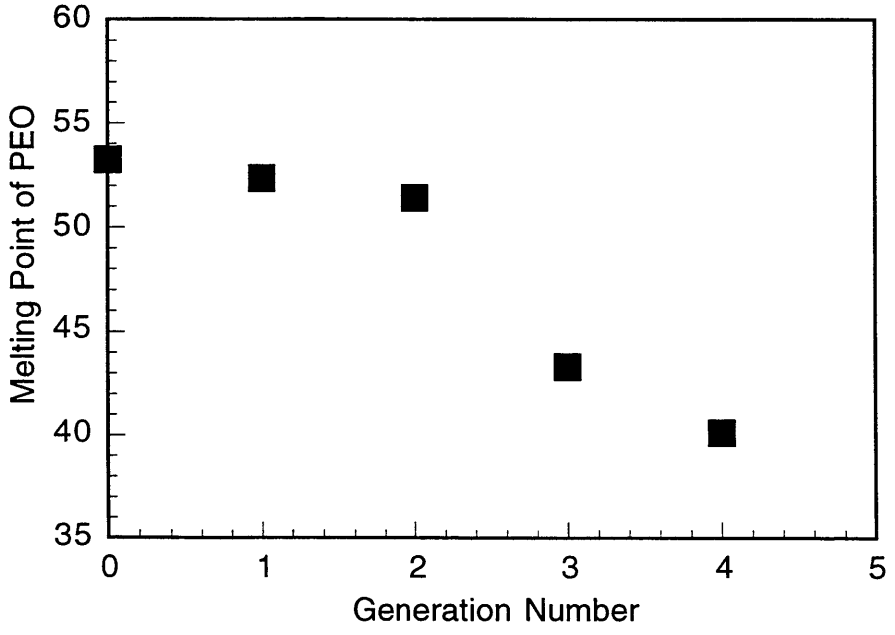

Figure 6.3a Depression of PEO melting point with increasing dendrimer generations in PEO(2000)-dendrimer diblocks.

In figure 6.3b, the enthalpy of melting ΔH (J/g) is plotted against the generation number of the dendrimer block. The dark squares are the numbers as obtained from DSC. The crosses represent the ΔH values normalized against the weight fraction of PEO in the diblock copolymer. Here, the normalized enthalpy of melting decreases significantly with increase in the size of the dendrimer block(figure 6.3b) in contrast to the PEO(5000) series. Although there may be some phase segregation between the two block as suggested by the presence of a PEO melting point, the percentage crystallinity of the PEO block seems to be decreasing indicating some phase mixing. This is again in contrast to the behavior seen for the 5000 series.

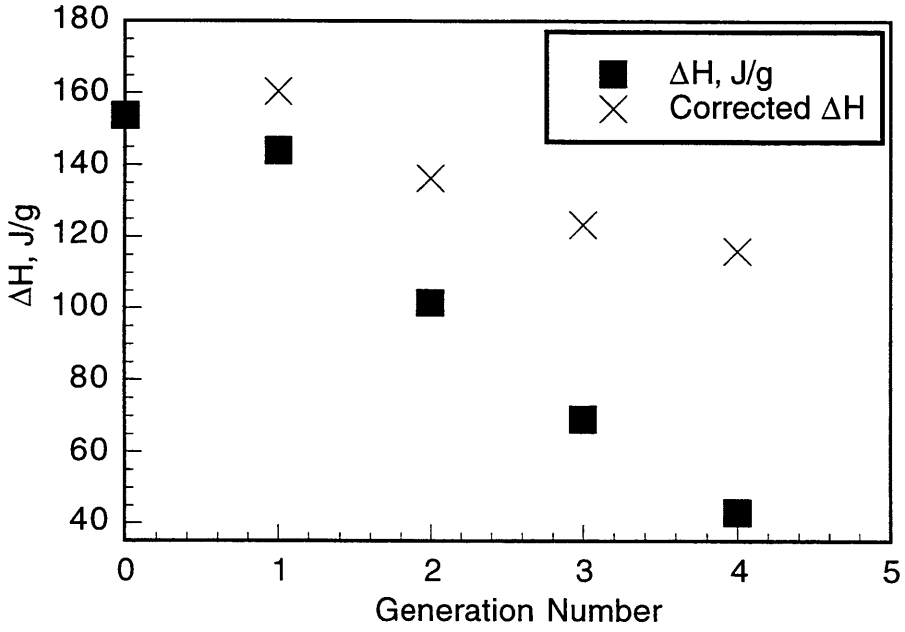

Figure 6.3b Enthalpy change for PEO melting as a function of dendrimer generation (■) ΔH J/g from DSC, (X) normalized ΔH J/g.

Glass transition temperatures(T_g) were observed for PEO(2000)-2.0G,3.0G, 4.0G diblocks. Figure 6.4 shows the glass transition temperatures plotted against the

generation number of the dendrimer for the PEO(2000) diblock series. The glass transition appears to increase exponentially with an increase in dendrimer generation.

Thermal characterization of the unmodified PEO(5000) and PEO(2000) copolymer series provides an understanding of the effect of dendritic block size on the crystallinity of the PEO block. Melting point of the PEO block in the unmodified diblock copolymers is an important reference for the investigation of the end modified PEO-dendrimer series. In these end modified diblocks, because of the large number of dendrimer end groups, interactions between PEO and the end modifying groups are bound to effect significantly the bulk behavior of the copolymer. The next section gives a detailed description of the bulk properties of stearate terminated PEO(2000)-dendrimer diblocks.

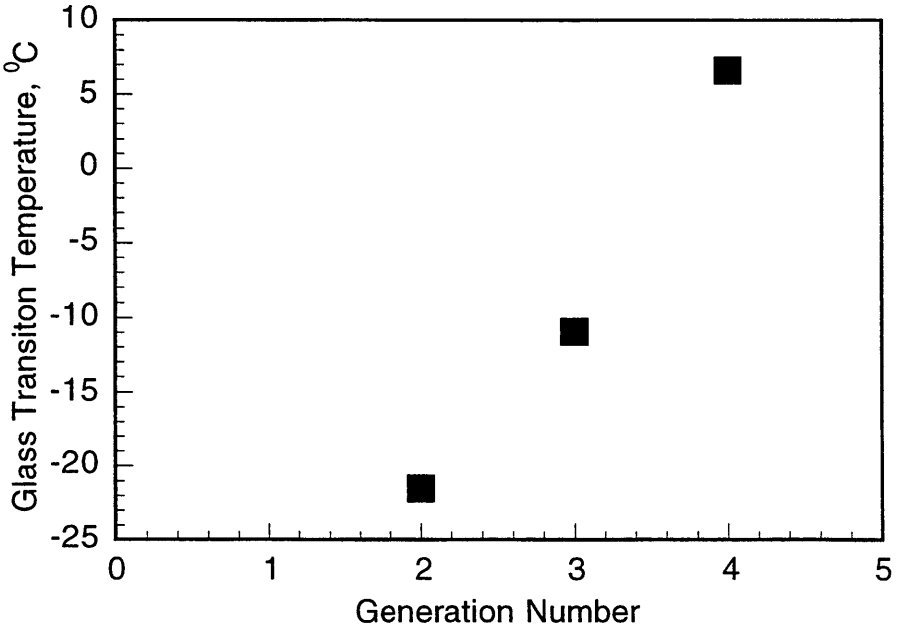

Figure 6.4 Plot of observed glass transition temperature vs. dendrimer generation for PEO(2000)-dendrimer diblocks.

6.3.2 Bulk morphology of stearate terminated PEO(2000)-dendrimer diblocks

Stearate terminated PEO(2000)-dendrimer diblocks are amphiphilic as demonstrated by the behavior of these copolymers at the air-water interface of a

Langmuir trough(Chapters 4 & 5). The amphiphilic nature of the diblocks also suggests that they have the potential to form phase segregated morphologies. Apart from a fundamental interest in the bulk properties of hybrid linear-dendritic diblocks, phase segregation is of interest for the formation of ordered bulk films of these diblock copolymers. In this section, the bulk behavior of the stearate terminated PEO(2000)-dendrimer diblocks investigated using SAXS, DSC, WAXD, and optical microscopy is discussed.

SAXS, WAXD, and DSC Results

The results obtained from DSC for the stearate terminated PEO(2000)-dendrimer diblocks are summarized in Table 6.1. Each copolymer shows more than one melting transition as noted in the second column of the table. Of the transitions observed, the first one was assumed to represent melting of the PEO crystallites. This melting point decreases from 58.4°C for PEO(2000)-S to 32.24°C for PEO(2000)-3.0G-S(table 6.1). In comparison, PEO melting point for the unmodified PEO(2000)-dendrimer diblocks decreased from 54°C for pure PEO(2000) to 43°C for PEO(2000)-3.0G(figure 6.3a). Further, the PEO melting point decreased with increasing dendrimer generation in both cases with the the stearte terminated diblock having a lower melting point than the unmodified copolymer for the same generation. The presence of a melting point that can be attributed to the PEO block suggests that it crystallizes to some extent even after attachment of the long alkyl chain. The ΔH values for the first melting transition were normalized against the weight fraction of PEO in the diblock copolymer and are shown in the fourth column of table 6.1. These ΔH values were also lower for the modified diblocks compared to the corresponding unmodified ones(figure 6.3b). The exception is PEO(2000)-S, where both the melting point(58.4°C) and the ΔH value(177.424J/g) are higher than the corresponding values(54°C, 155 J/g) for pure PEO(2000). The absence of any glass transitions in these modified diblocks is further evidence that the T_g's seen for the unmodified PEO(5000) and PEO(2000) series corresponds to the dendrimer block.

Since no significant impurity can be detected in the ^1H NMR spectra of the stearate terminated PEO(2000)-dendrimer diblocks, the presence of many melting transitions suggests the formation of some kind of self assembled or ordered structures. Presumably, the addition of the long alkyl chains to the ends of the dendrimer part of the diblock enhances the phase segregation between the two blocks. Some indication of this phenomenon is seen in PEO(2000)-S, where the addition of the stearate chain increases both the melting point and the enthalpy of melting; this observation suggests the preference of the PEO block to crystallize by itself. Since both PEO and the long alkyl chains have a tendency to crystallize, the end group modified diblocks probably have a greater affinity for phase segregation. To understand the bulk structures in the modified diblocks that were giving rise to the endothermic transitions seen in the DSC trace, we studied melt cast films of these copolymers using SAXS.

Table 6.1 Thermal characterization of stearate terminated PEO(2000)-dendrimer diblock copolymers

Sample	Melting points, °C	ΔH, J/g	ΔH(corrected), J/g
PEO(2000)-S	58.438 125.6	156.524 -11.528	177.424
PEO(2000)-1.0G-S	49.677 108.474	84.279 34.383	116.47
PEO(2000)-2.0G-S	38.892 118.424 146.521	53.714 23.438 6.236	100.66
PEO(2000)-3.0G-S	32.24 65.498 109.877	24.694 8.720 13.665	70.53

Figures 6.5,6.6, and 6.7 show the SAXS diffractograms for PEO(2000)-1.0G-S, PEO(2000)-2.0G-S, and PEO(2000)-3.0G-S. Shown along with the SAXS profiles are the DSC traces for the second heating recorded for these diblock copolymers. All the SAXS samples were melted above their isotropization temperature and then quenched to the annealing temperature. The arrows shown in figures 6.5, 6.6, and 6.7 refers to the temperatures at which the samples were annealed. The presence of a clear scattering pattern in small angle x-ray when the annealing temperature was above the melting point of the PEO block suggests that there are some organized structures in the diblocks in the temperature range between PEO melting and the next melting transition.

For PEO(2000)-1.0G-S, one other endotherm is observed above the PEO melting point and hence only one phase is probably present giving the scattering seen in the SAXS experiment(figure 6.5). The d-spacing corresponding to the scattering ring for PEO(2000)-1.0G-S was 156Å.

For PEO(2000)-2.0G-S, there are two transitions above $T_{m,PEO}$ as seen in the DSC trace. Since the dendrimer block may not be very stable for extended periods of time above 120°C(the second transition temperature), it was not possible to anneal the sample above this temperature to study the ordering corresponding to the region between 120°C and 140°C (the isotropization temperature). Of the two basic reactions (Michael addition and amidation) used to build the PAMAM dendrimer block, Micheal addition is reversible at higher temperatures(>80°C)[12]. The retro or reversible Michael reaction results in fragmentation and/or crosslinking of the dendrimer block[13]. The PEO(2000)-2.0G-S sample was annealed at 80°C, and the ring of scattering(figure 6.6) represents the size of the structures formed after the melting of the PEO block. The d-spacing measured from this ring was 144Å.

For the PEO(2000)-3.0G-S, there are three transitions, but the transition temperatures are much lower than those for the second generation diblocks. Figure 6.7 shows the SAXS scattering pattern obtained for the same melt cast film but annealed at different temperatures. The film was annnealed at 50°C, remelted at 120°C, then

reannealed at 70°C, in an effort to understand the difference in ordering before and after the transition at 65°C. 2-theta values at which scattering was observed for the sample annealed at two temperatures are very different(figure 6.7). Surprisingly, the size of the features after annealing at 70°C was higher than the one at 50°C; the d-spacing was 150Å for the high temperature phase, and 25Å for the low temperature phase respectively. It is possible that 25Å represents the crystals formed by the alkyl chains. Once these melt at 65°C, the diblock may have more mobility to associate and form larger aggregates.

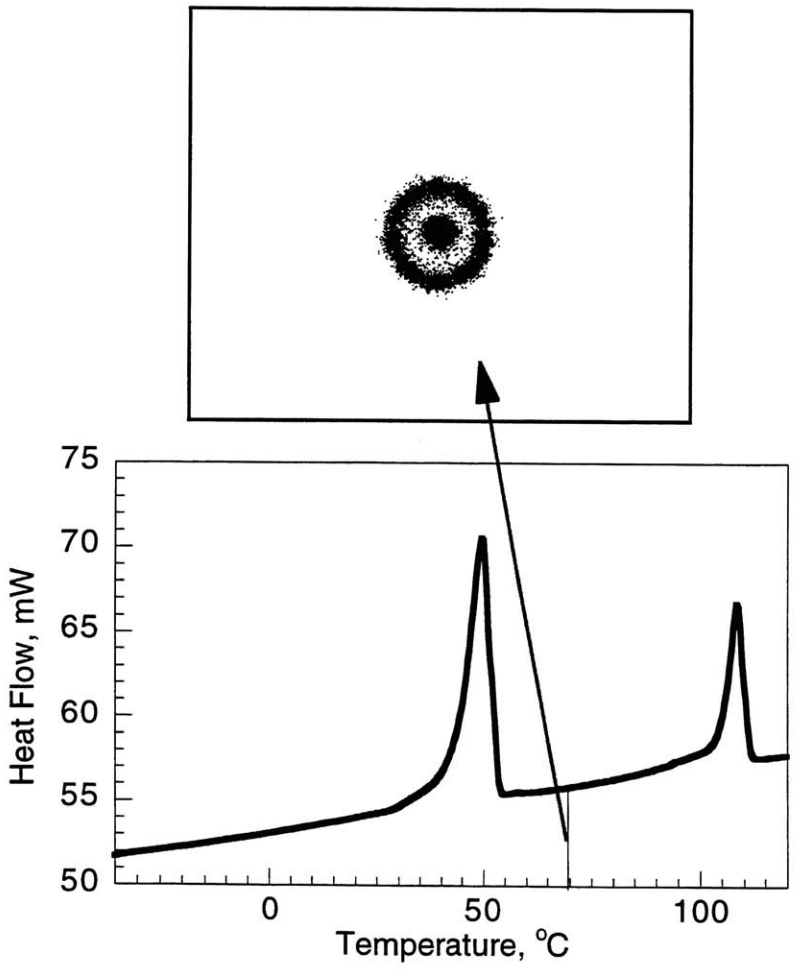

Figure 6.5 SAXS pattern and DSC trace(second heating) for PEO(2000)-1.0G-S. The arrow indicates the annealing temperature for the melt cast film.

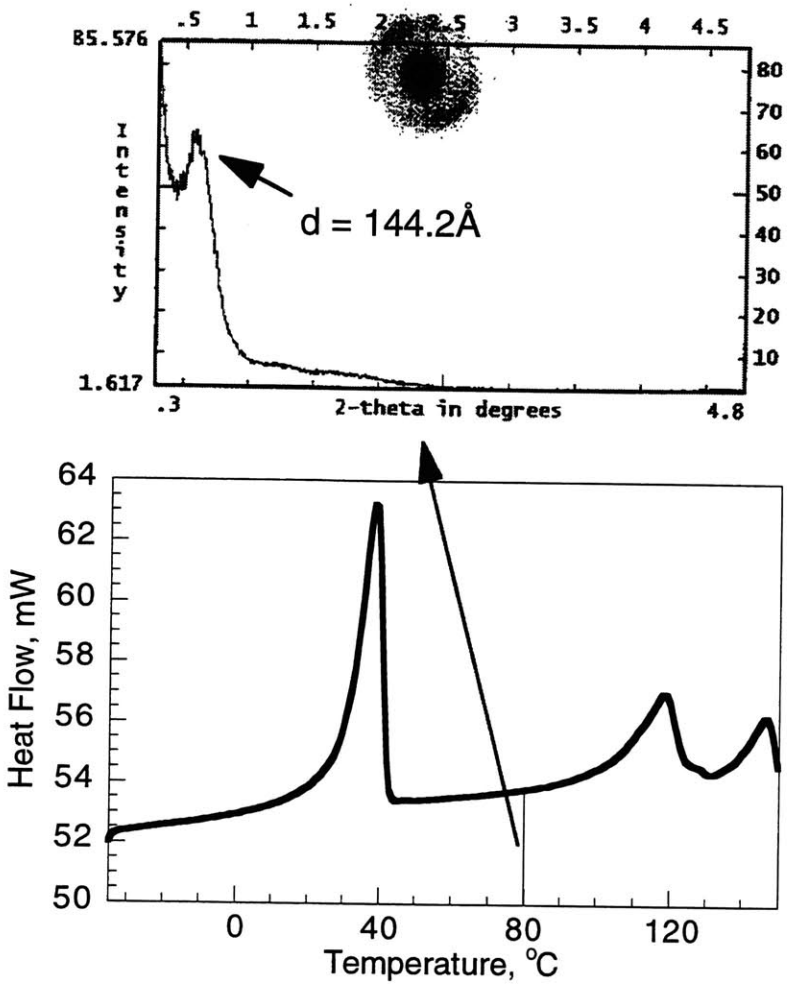

Figure 6.6 SAXS pattern and DSC trace for PEO(2000)-2.0G-S. The arrow shows the annealing temperature of the melt cast film.

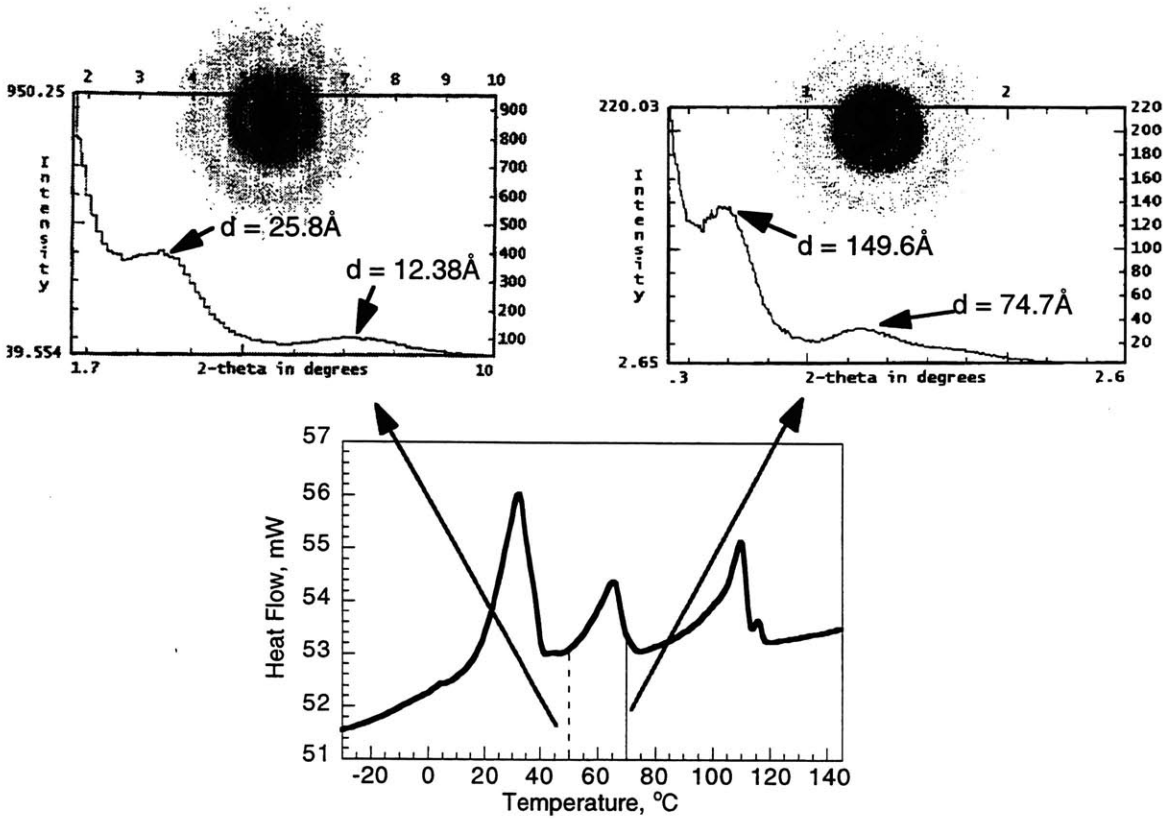

Figure 6.7 SAXS patterns and DSC trace for PEO(2000)-3.0G-S. The arrows indicate the annealing temperatures of the melt cast sample.

For all the three diblocks, the d-spacing of the higher temperature phase is on the order of 150Å suggesting that the superstructure formed by the self-assembly of these diblocks is similar. The hydrodynamic radius of the unmodified diblocks measured in water using intrinsic viscosity is around 14Å(chpater 3). Modification of the end groups with the stearate functionality could increase the length by a maximum of 25Å; this is the length of a fully extended stearate molecule[14]. Hence, size of the aggregates or domains, if present, should be about twice the size of the radius of gyration of the diblock, or ~ 80Å. The size of the features measured on SAXS for the diblocks was much higher than this expected length. This difference could be accounted for if the PEO block is assumed to be fully extended or as having just one fold in the bulk crystalline state. This is not an unlikely scenario as low molecular weight PEO homopolymer is known to crystallize in a

fully extended fashion or with only one or two folds[15]. Presence of large end groups and low supercooling further favors the crystallization of small molecular weight PEO molecules in the fully-extended state[16]. The average length of the fully extended chain crystals in the PEO crystal lattice, as derived from SAXS measurements, is reported to be 130Å[17]. Assuming then that the PEO block in the hybrid copolymer is fully extended in the bulk states studied here, size of the domains should be of the order of 155Å(130 Å + 25 Å). The measured domain sizes(~150Å) are very close to the values predicted by this model of the bulk state of the PEO-dendrimer diblock. Although the model provides a reasonable starting point in picturing the bulk state, details regarding the arrangement of the individual diblocks in the domains cannot be answered with these results.

One other interesting phenomenon is also exhibited by the diblocks. The first and second generation diblocks have only one peak in SAXS. But the profile for the third generation diblock has a second order reflection. The d-spacing corresponding to the second order reflection is half that of the first order one. This may be an indication that the third generation diblock forms a lamella structure with second order reflections(no $\sqrt{3}$ or $\sqrt{7}$ reflections detected). The increase in the order of the self-assembled structure formed with increasing generation number of the dendrimer block is similar to the stabilization effect seen by Percec et. al.[18]

Wide angle X-ray diffraction was used to examine the bulk phase for the presence of PEO crystallites or other ordered structures in the lower domain sizes. Samples of PEO(2000), PEO(2000)-1.0G-S, and PEO(2000)-2.0G-S investigated using WAXD were melted above 120°C for a few minutes and annealed at 70°C overnight. The diffractograms of all three samples looked similar and had a number of peaks with d spacings between 4.77Å and 2.27Å. There were two strong peaks corresponding to d spacings of 4.77Å and 4.04Å. Since peak positions in the first and second generation diblocks were almost identical to the ones in pure PEO, diffraction in all the samples was probably from PEO crystallites. The peaks, however, became broader with increase in

generation number of the dendrimer indicating the loss of crystallinity in the PEO phase suggested by the DSC results discussed earlier.

There are a few examples of the formation of thermotropic phases for end group modified dendritic homopolymers. Frey et. al.[19] synthesized different generations of a carbosilane dendritic homopolymer with perflouroalkyl, cyanobiphenyl, and cholesteryl end groups. The second generation carbosilane dendrimer functionalized with 36 cyanobiphenyl mesogens via a C5-spacer exhibited a broad smectic A phase in the temperature range of 17°C to 130°C. The attachment of cholesteryl groups at the periphery of the carbosilane dendrimer led to the formation of crystalline and liquid crystalline phases. Cholesteryl endcapped G1 and G2 dendrimers with 12 and 36 end groups respectively, were crystalline powders at ambient temperatures and formed smectic phases with transition temperatures between 80 and 90°C. G3 dendrimers of the same family with 106 end groups did not show the formation of mesophases, probably as a result of the increasing spherical geometry of the higher generation dendrimer. In contrast, the unmodified carbosilane dendrimers were liquids at room temperature, and possessed glass transition temperatures below –100°C. Generation dependant thermal behavior was also observed for the perfluoroalkyl terminated carbosilane dendrimers. G0 was obtained as a crystalline material that did not show the formation of mesophases but G1(12 end groups) exhibited the formation of a highly ordered smectic mesophase between –15 and –30°C. In contrast, G2 and G3 did not form mesophases; however, a transition to a hexagonal array of columns was observed in these dendrimers.

Percec et. al.[18] reported the self-organization of tapered and dendritic- molecules in the solid state in a series of papers. They studied the aggregation behavior in the solid phase for different generations of poly(benzylether) monodendrons with C12 terminal alkyl groups. These monodendrons self-assemble into spherical shaped supramolecular dendrimers, which further pack into a cubic liquid crystalline phase. The formation of a cubic LC phase by the aggregated monodendrons was indicated by the presence of many thermal transitions in the DSC trace. For example, the first generation monodendron did

not show any aggregation behavior, and only one thermal transition from a crystal to an isotropic phase was observed at 60°C. The third generation monodendron on the other hand showed one transition from a crystal to a cubic phase at –15°C and another from the cubic to the isotropic phase at 140°C. The stability of the aggregate structures formed by the second, third, and fourth generation monodendrons was found to depend on both the generation number of the monodendron and the functionality of the focal group. The stability of the cubic phase as indicated by the isotropization temperature was greatest for the third generation monodendron. The isotropization temperature was 117°C for the second generation, 140°C for the third generation, and 85°C for the fourth generation. In the second series, Percec and co-workers studied the effect of the length of semiflourinated end groups on the aggregation behavior of first generation tapered monodendrons. All the building blocks studied self-asembled into supramolecular cylindrical or rod-like dendrimers via ion-mediated complexation processes. The rod-like supermolecules formed a thermotropic hexagonal liquid crystalline phase. Again, the formation of different phases was indicated by the presence of more than one melting transition on the DSC curve.

For most of the references cited above, the structure and size of the liquid crystalline phases indicated by the presence of other thermal transitions was further studied using optical microscopy, SAXS, TEM, and X-ray diffraction.

The smectic A phase formed by the mesogen terminated carbosilane dendrimers was studied using WAXD[19]. The resulting diffraction pattern showed two peaks: one corresponding to a layer spacing of 31.5Å for the smectic A and another corresponding to 4.4Å for the mesogen-mesogen spacing[19a]. For the perflouroalkyl terminated carbosilane dendrimers investigated by the same group, only the first generation dendrimer showed mesophases in the DSC trace[19c]. These mesophases investigated using WAXD showed five clearly discernible reflections, three sharp ones located between $0<\theta<5$ and two broad ones at $2\theta = 18.2^{\circ}$ and 38° respectively. The large small angle peak translated to a d value of 26.7Å with the other two small angle peaks being the first two higher order

reflections suggesting a highly layered structure. The higher angle peaks corresponded to the perflouroalkyl units. Although they found no thermal phase transitions for the second and third generation carbosilane dendrimers on the DSC, both these materials showed interesting WAXD patterns in the small angle region indicating the supramolecular ordering of these materials.

Percec et al.[18] studied the self assembled structures in their system using X-ray diffraction. They used the XRD results to assign the morphology of the superstructures formed. Their results are the most thorough study of the effect of the shape of the monodendron on the superstructure of the self assembly in the literature.

All the investigations on the self-assembly of dendritic macromolecules has been for dendrons or dendrimer homopolymers. In these examples, the ordering observed in the bulk was a result of liquid crystalline phases. The small spacings measured were characteristic of most smectic liquid crystalline systems.

For linear-dendritic diblock copolymers, the formation of self-assembled micellar structures has been seen in solution, giving a lyotropic liquid crystalline phase. The amphiphilic nature of the diblocks resulted in its self-assembly into micelles or vesicles in a solvent good for one of the blocks. van Hest et. al.[6] used TEM to visualize the micelles and vesicles formed by polystyrene-polypropyleneimine linear-dendritic diblock copolymer. In the case of PEO-Polybenzylether linear-dendritic diblocks[1e], a melting point for the PEO block and a glass transition associated with the dendrimer block was seen for some of them. The bulk behavior of linear-dendritic diblock copolymers has not been reported by any group so far.

Optical Microscopy

The thermal transitions seen on the DSC and the presence of ordered structures suggested by the SAXS profiles were further investigated using an optical microscope and crossed polarizers connected to a hot stage. The thermal history of the optical microscope sample was the same as that for SAXS. For PEO(2000)-3.0G-S, optical

birefringence was present at all temperatures below 130°C. Some of the crystals melted around 60°C and were probably associated with the PEO block, in good correspondance with the DSC thermogram. Annealing the sample at 80°C overnight, resulted in the formation of very large crystals which grew in size with time. The crystals that formed on remelting the film at 130°C and cooling it to 45°C were much smaller in size, different in habit, and did not grow with time. Apparently, the two d-spacings seen in the SAXS experiments are due to different types of crystals structures. Figure 6.8 shows the optical micrographs recorded at different temperatures for PEO(2000)-3.0G-S. Similar experiments were conducted for PEO(2000)-2.0G-S. Although birefringence is seen at all temperatures upto 140°C, indicating some ordered structures, well formed crystals similar to the ones seen for PEO(2000)-3.0G-S were not observed even after annealing for over 16 hours at 80°C(figure 6.9).

The crystal habit seen in the PEO(2000)-3.0G-S film annealed at 80°C is very similar to the habits observed in low molecular weight PEO homopolymer films[17]. This similarity between the homopolymeric and copolymeric single crystals supports the picture of phase segregated PEO-dendrimer diblocks suggested by DSC and SAXS data.

Domain sizes estimated from the study of the bulk behavior of PEO-dendrimer diblocks was used to design the thickness of the spin coated films. As mentioned in the introduction to this chapter, the thickness of the spin coated films has to be in the order of the domain size to observe any surface induced ordering in the films.

6.3.3 Spin coated films of the linear-dendritic diblocks

Thin films of stearate terminated linear-dendritic diblock copolymers were made by spin-coating chloroform solutions of the copolymers onto gold or mica substrates. The concentration of the solution and speed of the spin-coater was adjusted to give two ranges of film thickness. Films with thickness in the lower range of 3-6nm corresponded to twice the measured size of the PEO(2000) diblocks in solution. The higher range of about 15nm corresponded to the domain sizes measured in SAXS. No ordered structures

were discernable on atomic force microscope(AFM) for the thinner films. However, an effect of the size of the PEO block on the wetting behavior was observed for these films. PEO(2000)-1.0G-S formed uniform continuous films. But the higher generation diblock films exhibited significant island formation.

Figures 6.10 and 6.11 show the AFM images of thicker films of PEO(2000)-1.0G-S and PEO(2000)-3.0G-S respectively. The substrate was mica in these experiments. To get an estimate of the film thickness, the same solutions of these copolymers were spin cast onto gold substrates. Ellipsometry gave a film thickness of 280Å for PEO(2000)-1.0G-S and 353Å for PEO(2000)-3.0G-S. These spin-cast films were annealed in a vacuum oven at 66°C for 16 hours prior to imaging the surface. Figure 6.10a shows the presence of some ordered structures on the film surface. A 2-D FFT of the micrograph for PEO(2000)-1.0G-S is also shown for PEO(2000)-1.0G-S(figure 6.10b). The ring in the 2-D FFT shows that the structures seen on the surface have a preference for a particular width of about 21nm. This is a little less than twice the domain size measured on SAXS for this diblock copolymer. Surface induced flattening of dendrimers on surfaces has been observed by other researchers[20] and could be the reason for the difference between the feature sizes measured on the AFM and SAXS. Ordered structures are also seen for PEO(2000)-3.0G-S films in the micrograph(figure 6.11). Depth analysis on this film gave a bimodal size distribution with one peak around 15nm and another around 5nm. For this diblock copolymer, the larger film thickness of 15nm is very close to the domain size measured on SAXS. Since SAXS suggests a lamellar ordering for the PEO(2000)-3.0G-S, it may be possible for the stearate terminated dendrimer block to be at the air interface and not be affected significantly by the presence of the mica substrate. Although all the data collected so far indicate the formation of ordered structures in bulk for stearate terminated PEO-PAMAM diblocks, TEM will be very useful in building a complete model to explain the interesting phenomena reported in this chapter.

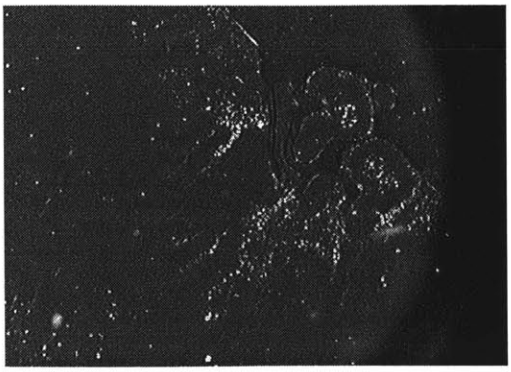

Film at 130°C (50x)

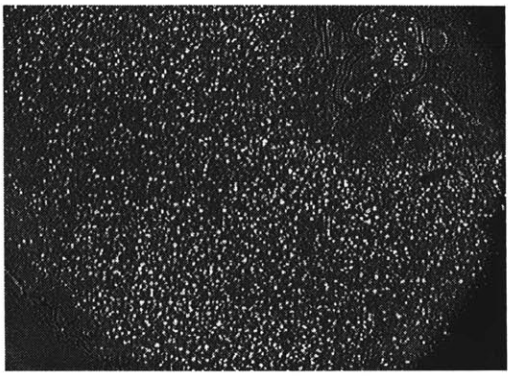

Film annealed at 45°C for 1 hour (50x)

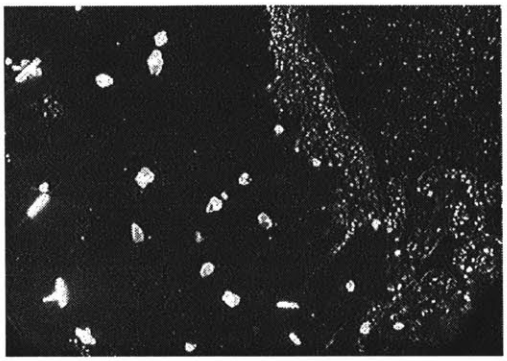

Film annealed at 80°C for 16 hours (50x)

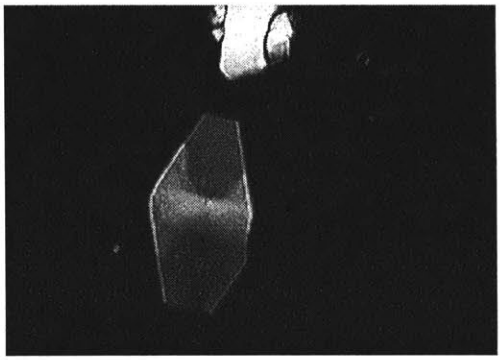

Detail of crystals seen after annealing at 80°C (400x)

Figure 6.8 Optical micrographs showing the birefringence of a PEO(2000)-3.0G-S film as function of temperature.

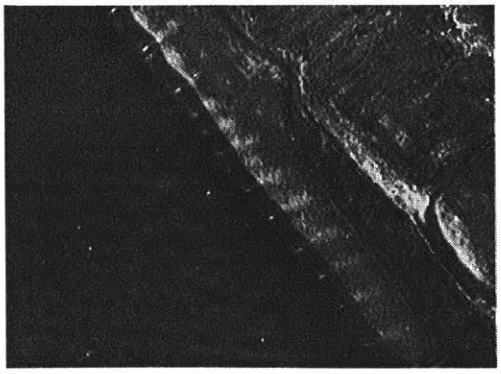

Film at 140°C (200x)

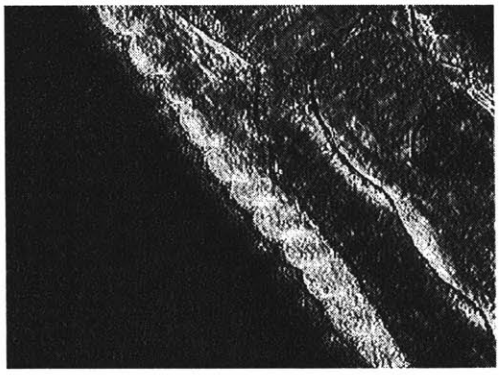

Film after annealing overnight at 80°C

Figure 6.9 Optical micrographs showing the birefringence of a PEO(2000)-2.0G-S film as a function of temperature.

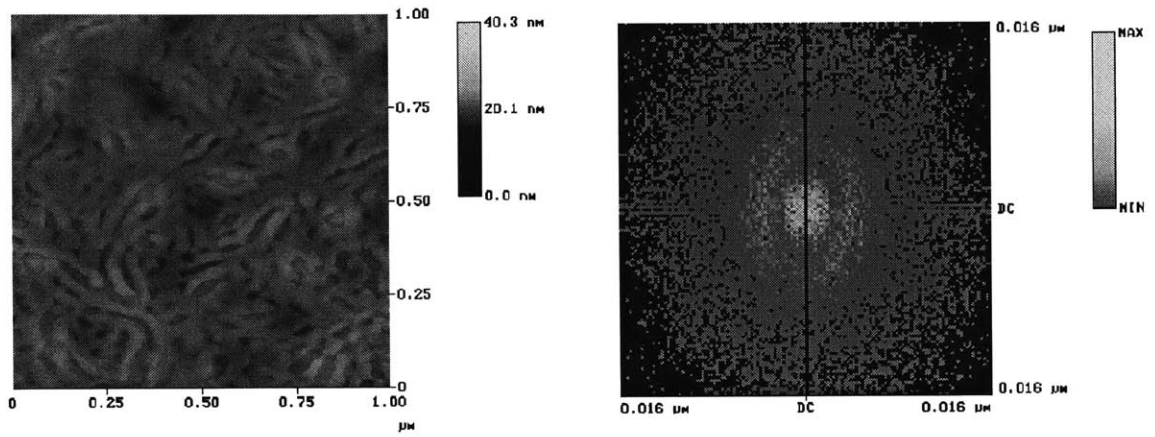

(a) (b)

Figure 6.10 Atomic force micrograph(a) of a PEO(2000)-1.0G-S film and the corresponding 2-D FFT(b).

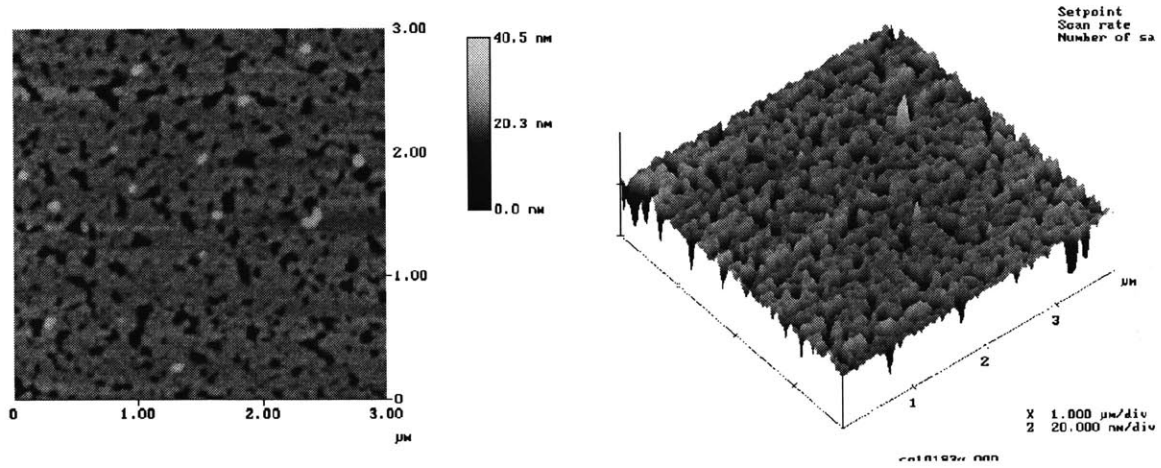

Figure 6.11 Atomic force micrograph of a PEO(2000)-3.0G-S film coated on a freshly cleaved mica substrate.

6.4 Chapter Summary

Thermal characterization suggests that PEO-PAMAM linear-dendritic diblock copolymers exhibit some degree of microphase segregation irrespective of the

composition of the diblock. Glass transition temperatures were observed for some of the diblocks . The dependence of glass transition on end group functionality of the dendrimer block was observed for the first time in such linear-dendrimeric hybrid copolymers. Stearate terminated linear-dendritic diblocks shows new endotherms in the DSC thermograms suggesting the formation of ordered phases in the modified diblock copolymers. SAXS studies on melt cast films of the modified diblocks indicate that the domain sizes in the bulk state were about 150Å. Spin-coated films with a thickness of roughly twice this domain size show ordered structures as seen by atomic force micrography.

6.5 References

1. (a) Xu, Z.; Moore, J.S., *Angew. Chem. Int. Ed. Engl.,* **1993**, 32, 9, 1354, (b) Scherrenberg, R.; Coussens, B.; van Vliet, P.; Edouard, G.; Brackman, J.; de Brabander, E., *Macromolecules*, **1998**, 31,456, (c) Mourey, T.H.; Turner, S.R.; Rubinstein, M.; Frechet, J.M.J.; Hawker, C.J.; Wooley, K.L., *Macromolecules*, **1992**, 25, 2401, (d) Prosa, T.J.; Baeur, B.J.; Amis, E.J.; Tomalia, D.A.; Scherrenberg, R., *J. Polym. Sci. Polym. Phys.*, **1997**, 35, 2913, (e) Gitsov, I.; Frechet, J.M.J., *Macromolecules*, **1993**, 26, 6536, (f) Gitsov, I.; Frechet, J.M.J., *Macromolecules*, **1994**, 27, 7309.
2. Padias, A.B.; Hall, H.K. Jr.; Tomalia, D.A.; McConnell, J.R., *J. Org. Chem.*, **1987**, 52, 5305.
3. (a) Tomalia, D.A.; Berry, V.; Hall, M.; Hedstrand, D.M., *Macromolecules*, **1987**, 20, 1167, (b) Tomalia, D.A.; Baker, H.; Dewald, J.; Hall, M.; Kallos, G.; Roeck, J.; Ryder, J.; Smith, P., *Macromolecules*, 1986, 19, 9, 2467.
4. Jackson, C.L.; Chanzy, H.D.; Booy, F.P.; Drake, B.J.; Tomalia, D.A.; Baeur, B.J.; Amis, E.J., *Macromolecules*, **1998**, 31, 6259.
5. Percec V.; Ahn, C. –H.; Ungar, G.; Yeardley, D.J.P.; Moller, M.;Shieko, S.S., *Nature*, **1998**, 391, 161-164.

6. van Hest, J.C.M., Delnoye, D.A.P.; Baars, W.P.L.; van Genderen, M.H.P., Meijer, E.W., *Science*, **1995**, 268, 1592.

7. Gitsov, I.; Frechet, J.M.J., *Macromolecules*, **1993**, 26, 6536.

8. (a) Kim, Y.H.; Beckerbauer, R., *Macromolecules*, **1994**, 27, 1968, (b) Wooley, K.L.; Hawker, C.J.; Pochan, J.M.; Frechet, J.M.J., *Macromolecules*, **1993**, 26, 1514, (c) de Brabander-van den Berg, E.M.M.; Meijer, E.W., *Angew. Chem. Int. Ed. Engl.*, **1993**, 32, 9, 1308.

9. Singh, N.; Kudrle, A.; Sikka, M.; Bates, F.S., *J. Phys. II France*, **1995**, 5, 377.

10. Gitsov,I.; Wooley, K.L.; Hawker, C.J., Ivanova, P.T.; Fréchet, J.M.J., *Macromolecules*, **1993**, 26, 5621-5627.

11. Wooley,K.L; Hawker,C.J.; Pochan,J.M.; Fréchet,J.M.J., *Macromolecules*, **1993**, 26, 1514 - 1519.

12. Tomalia, D.A.; Baker, H.; Dewald, J.; Hall, M.; Kallos, G.; Martin, S.; Roeck, J.; Ryder, J.; Smith, P., *Macromolecules, supplemetary material*, **1986**, 19, 9, 2466.

13. Zhao, M.; Liu, Y.; Crooks, R. M.; Bergbreiter, D.E., *MRS Abstracts(U8.19)*, December, **1998**, Boston, Massachusetts.

14. Ulman, A., *"An Introduction to Ultrathin Organic Films from Langmuir-Blodgett to Self-Assembly"*, **1991**, Academic Press Inc., New York.

15. Balijepalli, S.; Schultz, J.M.; Lin, J.S., *Macromolecules*, **1996**, 29, 20, 6601.

16. Bassett, D.C., *"Principles of Polymer Morphology"*, Cambridge University Press, **1981**, 154-157.

17. Kovacs, A.J.; Gonthier, A., *Kolloid-Z. u. Z. Polymere*, **1972**, 250, 530.

18. (a) Percec, V.; Johansson, G.; Ungar, G.; Zhou, J., *J. Am. Chem. Soc.*, **1996**, 118, 9855, (b) Percec, V.; Chu, P.; Ungar, G.; Zhou, J., *J. Am. Chem. Soc.*, **1995**, 117, 11441, (c) Balaguruswamy, V.S.K.; Ungar, G.; Percec, V.; Johansson, G., *J. Am. Chem. Soc.*, **1997**, 119, 1539, (d) Percec, V.; Cho, W. -D.; Mosier, P.E.; Ungar, G.; Yeardley, D.J.P., *J. Am. Chem. Soc.*, **1998**, 120, 11061.

19. (a) Coen, M.C.; Lorenz, K.; Kressler, J.; Frey, H.; Mulhaupt, R., *Macromolecules*, **1996**, 29, 8069, (b) Lorenz. K.; Holter, D.; Stuhn, B.; Mulhaupt, R.; Frey, H., *Adv. Mater.*, **1996**, 8, 50, 414, (c) Lorenz, K.; Frey, H.; Stuhn, B.; Mulhaupt, R., *Macromolecules*, **1997**, 30, 6860.

20. Tsukruk, V.V.; Rinderspacher, F.; Bliznyuk, V.N., *Langmuir*, **1997**, 13, 8, 2171.

Chapter 7. Summary and Conclusions

Two series of new linear-dendritic block copolymers have been synthesized in which the linear block is PEO and the dendritic block is PAMAM. The linear PEO tail had a molecular weight of 5000 in one series and 2000 in the other.. Monofunctionalized PEO having an amine end group was used as the starting point for the dendrimer block synthesis. Synthesis of the dendritic PAMAM block was a step-wise process and involved two reactions - a Michael addition followed by an ammonolysis. The Michael addition converted the primary amine end group to a methylester and introduced a branch point. The ammonolysis converted the methylester to an amide and regenerated the primary amine. These two steps were done iteratively to form the symmetrically branched dendrimer block. The dendrimer generations synthesized went up to 4.0 for the PEO(2000) tail, and up to 4.5 for the PEO(5000) tail. ^{1}H NMR, FTIR, and MALDI-TOF MS were used to verify the chemical structure of the diblocks synthesized.

The amine end groups of the full generation dendrimer block were functionalized with stearate or allyloxybenzene groups. The functionalization proceeded with 80-100% conversion and led to drastic changes in the solubility of the diblock copolymers. As the modification step involved the reaction between carboxylic anhydride and amine groups of the dendrimer block, this technique can be used to change the end groups of the dendrimer block to any "R" from an organic molecule of the form "RCOOH". The versatility of the modification reaction can hence be used to tailor the solubility and behavior of the linear-dendritic diblocks.

Intrinsic viscosity studies on unmodified PEO-PAMAM diblocks show that the solution behavior is greatly affected by the length of the PEO linear chain at low molecular weights, and the number and chemical nature of the dendrimer end group. PEO(2000)-dendrimer diblocks exhibit increasing [η] with increasing molecular weight as is observed for traditional linear polymers. For the PEO(5000)-dendrimer diblocks, [η] decreases with the introduction of the dendrimer block, suggesting a unimicellar like

structure formed by wrapping of the PEO chain around the dendrimer block. The variation of [η] with dendrimer generation in the PEO(5000) series is reminiscent of the relationship seen for pure dendrimers. The hydrodynamic radii calculated from intrinsic viscosity was between 1.4-1.8nm for the PEO(2000)-diblock series and between 2.2-3.0nm for the PEO(5000)-diblock series. Dynamic light scattering and gel permeation chromatography were also used to characterize the aqueous solution behavior and get an estimate of the size of the copolymers. The values for copolymer size obtained from these techniques fall in the same range as those calculated from intrinsic viscosity. However, intrinsic viscosity remained the most sensitive and reliable technique for determining the hydrodynamic size of these materials.

The interfacial behavior of the PEO-PAMAM linear-dendritic diblocks was studied using a Langmuir trough. Stearate terminated PEO(2000)-PAMAM linear-dendritic diblocks were found to be highly amphiphilic, and formed the most stable monolayers at the air-water interface of a LB trough. On compression of monolayers of stearate terminated diblocks, a condensed phase was observed for all dendrimer generations studied. Three interesting effects of increasing dendrimer generation on the amphiphilic behavior of linear-dendritic diblock copolymers, namely the exclusion of the linear PEO block from the interface for large dendron sizes, the effects of curvature of the dendron on the final surface area per molecule, and deformation of the dendron at high pressures have been reported here. The monolayers of diblocks with second, third, and fourth generation dendrimer blocks were very stable

Transfer of diblock copolymer monolayers onto functionalized substrates was found to be possible. Physisorbed uniform films of linear-dendritic diblock copolymers were made and are reported here for the first time. Transfer of monolayers at higher surface pressures gave uniform films with very few defects. Z-type multilayer films were formed by transfer of PEO(2000)-3.0G-S monolayers at a surface pressure of 54mN/m on to hydrophobically functionalized gold substrates. However, rearrangements of the physisorbed monolayers were found to take place in the multilayer films. For the other

diblocks, build up of multilayers was hindered by desorption on the downstroke of the monolayers adsorbed on the upstroke. To overcome these two problems, different subphase conditions were investigated. Water soluble polymers, such as PAA, BPEI, and PMAA, capable of hydrogen bonding with the PEO tail were used to modify the subphase. These polymers were expected to diffuse to the interface and hydrogen bond with the PEO block forming a composite diblock/polymer monolayer at the interface. The transfer of these composite monolayers was expected to increase adhesion between adsorbed monolayers and prevent their rearrangement in the film or desorption on the downstroke. Of the three polymers studied, PMAA in the water subphase at pH=2 resulted in very efficient multilayer build-up for the second generation copolymer. No monolayer deposition was possible under the same conditions in the absence of the complexing PMAA polymer. A multilayer film of PEO(2000)-2.0G-S having a thickness of around 170Å was built using this technique.

The thermal behavior of the diblock copolymers was studied using DSC. Thermal characterization suggests that PEO-PAMAM linear-dendritic diblock copolymers exhibit some degree of microphase segregation irrespective of the composition of the diblock. Glass transition temperatures were observed for some of the diblocks. Dependence of glass transition on end group functionality of the dendrimer block was observed for the first time in such linear-dendrimeric hybrid copolymers. Stearate terminated linear-dendritic diblocks show new endotherms in the DSC thermograms suggesting the formation of ordered phases in the modified diblock copolymers. SAXS was used to further investigate the bulk morphology of the modified diblock copolymers. Melt cast films of PEO(2000)-1.0G-S, PEO(2000)-2.0G-S, and PEO(2000)-3.0G-S showed that clear rings in the SAXS profiles. The measured d-spacings were 156Å for PEO(2000)-1.0G-S, 144Å for PEO(2000)-2.0G-S, and 150 Å for PEO(2000)-3.0G-S. A dependence of the d-spacing on the annealing temperature was seen for PEO(2000)-3.0G-S. When annealed at a lower temperature, the domain size measured for PEO(2000)-3.0G-S was 25 Å. Second order reflections were observed for PEO(2000)-3.0G-S alone at both the

annealing temperatures. Optical microscopy studies of thin films of the second and third generation diblock copolymers showed birefringence upto isotropization temperature.

Spin-coated films with a thickness of roughly twice this domain size measured on SAXS were imaged using an atomic force micrograph. The surface topography image showed the presence of uniformly sized features for first and third generation diblocks. The size of the features for PEO(2000)-1.0G-S was 21nm, which is higher than the domain size measured on SAXS. For PEO(2000)-3.0G-S, the feature size was very close to the domain size of 150Å measured on SAXS.

These exciting results suggest the formation of some ordered structures in the bulk for the stearate terminated PEO(2000)-dendrimer diblocks. However, other techniques such as TEM and WAXD are needed to obtain a more complete picture of the phenomenon observed.

A number of interesting questions still remain with regard to the behavior of these novel linear-dendritic amphiphiles. PEO(2000)-1.0G-S had a very large area in the condensed phase as seen in the LB experiments. Since this diblock copolymer is the only one soluble in water, micelles may be forming at the air-water interface. For the stearate terminated PEO-PAMAM diblocks, we have concentrated our efforts on the interfacial and bulk properties. The behavior of these molecules in solution will also make an interesting study.

Appendix A Synthesis of PEO-PAMAM Linear-Dendritic Diblock Copolymers

A.1 PEO(5000) Series

PEO(5000)-0.5G: 2.5g of pure CH_3O-PEO-NH_2(5000) was dissolved in 12.5ml of methanol and added drop-wise to 35ml of purified methyl acrylate at 35°C. After 48 hours, the methanol and unreacted methyl acrylate were removed under vacuum leaving in a sticky white residue. The residue was washed with at least 400ml of ethyl ether to remove any residual impurities and was filtered off to give the product, a white solid. The solid product, CH_3O-PEO-N<$(CH_2CH_2COOCH_3)_2$ {PEO(5000)-0.5G}, was dried under vacuum. (Yield = 2.34g, 93%)

^{1}H NMR in d_6-DMSO: $\delta_{PEO}(\mathbf{CH_2CH_2}O) = 3.515$(b); $\delta_{PEO}(\mathbf{CH_3}O\text{-}) = 3.246$(s); δ_{PAMAM}(-COOC$\mathbf{H_3}$) = 3.578(s); δ_{PAMAM}(-$\mathbf{CH_2}$COOCH$_3$) = 2.399(t); δ_{PAMAM}(protons next to tertiary amines) = 2.55-2.8 (m). FTIR peaks, ν cm^{-1}: 1113, 1735, 2882.

PEO(5000)-1.0G: 2.24g of PEO(5000)-0.5G was dissolved in 8ml of methanol and added drop-wise to 16.5ml of freshly distilled ethylene diamine containing 0.0044g of NaCN. After 48 hours at 50°C, methanol and ethylene diamine were removed under vacuum. The residue obtained was washed with 300-400ml of ethyl ether and filtered off to give the product. The white solid product, CH_3O-PEO-N$(CH_2CH_2CONHCH_2CH_2NH_2)_2$ {PEO(5000)-1.0G}, was dried under vacuum. (Yield = 2.14g, 95%)

^{1}H NMR in d_6-DMSO: $\delta_{PEO}(\mathbf{CH_2CH_2}O) = 3.513$(b); $\delta_{PEO}(\mathbf{CH_3}O\text{-}) = 3.244$(s); δ_{PAMAM}(-$\mathbf{CH_2}$CONH-) = 2.19(m); δ_{PAMAM}(-CONHC$\mathbf{H_2}$-) = 3.037(m); δ_{PAMAM}(protons next to primary and tertiary amines) = 2.5-2.8(m). FTIR peaks, ν cm^{-1}: 1106, 1541, 1662, 2875, 3270.

PEO(5000)-1.5G: 2.04g of PEO(5000)-1.0G was dissolved in 16.5ml of methanol and added drop-wise to 30ml of purified methyl acrylate kept at 35°C. After 42 hours, the

methanol and unreacted methyl acrylate were removed under vacuum. The white residue was washed with at least 400ml of ethyl ether and filtered off to give a solid white product, PEO(5000)-1.5G. The solid product was further dried under vacuum. (Yield = 1.906g, 93%)

^{1}H NMR in d_6-DMSO: $\delta_{PEO}(CH_2CH_2O)$ = 3.5(b); $\delta_{PEO}(CH_3O\text{-})$ = 3.23(s); $\delta_{PAMAM}(\text{-}COOCH_3)$ = 3.6(s); $\delta_{PAMAM}(\text{-}CH_2CONH\text{-})$ = 2.16(m); $\delta_{PAMAM}(\text{-}CONHCH_2\text{-})$ = 3.05(m); $\delta_{PAMAM}(\text{-}CH_2COOCH_3)$ = 2.4(m); δ_{PAMAM}(protons next to tertiary amines) = 2.5-2.7(b). FTIR peaks, ν cm^{-1}: 1115, 1540, 1661, 1734, 2880, 3237.

PEO(5000)-2.0G: 1.75g of PEO(5000)-1.5G was dissolved in 12ml of methanol and added drop-wise to 34ml of ethylene diamine containing 0.0067g of NaCN. After 48 hours at 50°C, methanol and ethylene diamine were removed under vacuum. The residue obtained was washed with 300-400ml of ethyl ether and filtered off to give the product. The product, PEO(5000)-2.0G, was a white solid and was dried over vacuum. (Yield = 1.74g, 99%)

^{1}H NMR in d^6-DMSO: $\delta_{PEO}(CH_2CH_2O)$ = 3.509(b); $\delta_{PEO}(CH_3O\text{-})$ = 3.24(s); $\delta_{PAMAM}(\text{-}CH_2CONH\text{-})$ = 2.191(m); $\delta_{PAMAM}(\text{-}CONHCH_2\text{-})$ = 3.072(m); δ_{PAMAM}(protons next to primary and tertiary amines) = 2.5-2.8(m). FTIR peaks, ν cm^{-1}: 1111, 1549, 1649, 2883, 3277.

PEO(5000)-2.5G: 1.6g of PEO(5000)-2.0G was dissolved in 25ml of methanol and added drop-wise to 22ml of methyl acrylate. After 24 hours, methanol and the unreacted methyl acrylate were removed under vacuum, and the white product washed with about 400ml of ethyl ether. PEO(5000)-2.5G was filtered off and dried under vacuum. (Yield = 1.43, 89%)

^{1}H NMR in d_6-DMSO: $\delta_{PEO}(CH_2CH_2O)$ = 3.51(b); $\delta_{PEO}(CH_3O\text{-})$ = 3.247(s); $\delta_{PAMAM}(\text{-}COOCH_3)$ = 3.583(s); $\delta_{PAMAM}(\text{-}CH_2CONH\text{-})$ = 2.16(m); $\delta_{PAMAM}(\text{-}CONHCH_2\text{-})$ = 3.06(m); $\delta_{PAMAM}(\text{-}CH_2COOCH_3)$ = 2.41(m); δ_{PAMAM}(protons next to tertiary amines) = 2.5-2.7.

FTIR peaks, ν cm^{-1}: 1113, 1539, 1662, 1733, 2880, 3258.

PEO(5000)-3.0G: 1.3g of PEO(5000)-2.5G was dissolved in 10ml of methanol and added drop-wise to 20ml of ethylene diamine. After 55 hours at 50°C, methanol and ethylene diamine were removed under vacuum. The residue was washed with about 400ml of ethylether and the precipitate filtered off to give the solid product, PEO(5000)-3.0G. PEO(5000)-3.0G was dried under vacuum. (Yield = 1.09g, 83%)

^1H NMR in D_2O: $\delta_{PEO}(CH_2CH_2O)$ = 3.7(b); $\delta_{PEO}(CH_3O\text{-})$ = 3.384(s); $\delta_{PAMAM}(\text{-}CH_2CONH\text{-})$ = 2.449(m); $\delta_{PAMAM}(\text{-}CONHCH_2\text{-})$ = 3.31(m); δ_{PAMAM}(protons next to primary and tertiary amines) = 2.6-2.9. FTIR peaks, ν cm^{-1}: 1111, 1548, 1646, 2878, 3272.

PEO(5000)-3.5G: 0.98g of PEO(5000)-3.0G was dissolved in 15ml of methanol and added slowly to 13ml of methyl acrylate. After 24 hours, the methanol and methyl acrylate were removed under vacuum. The product, PEO(5000)-3.5G, was washed with at least 200-300ml of ethyl ether and dried over vacuum. (Yield = 0.97g, 99%)

^1H NMR in d_6-DMSO: $\delta_{PEO}(CH_2CH_2O)$ = 3.507(b); $\delta_{PEO}(CH_3O\text{-})$ = 3.24(s); $\delta_{PAMAM}(\text{-}COOCH_3)$ = 3.573(s); $\delta_{PAMAM}(\text{-}CH_2CONH\text{-})$ = 2.175(m); $\delta_{PAMAM}(\text{-}CONHCH_2\text{-})$ = 3.05(m); $\delta_{PAMAM}(\text{-}CH_2COOCH_3)$ = 2.407(m); δ_{PAMAM}(protons next to tertiary amines) = 2.5-2.8. FTIR peaks, ν cm^{-1}: 1112, 1542, 1658, 1733, 2884, 3261.

PEO(5000)-4.0G: 0.809g of PEO(5000)-3.5G was dissolved in 9ml of methanol and added to 18ml of ethylene diamine slowly. After 54 hours at 50°C, the methanol and ethylene diamine were removed under vacuum. The residue is washed with 400ml of ethyl ether, filtered off, and dried over vacuum.

^1H NMR in D_2O: $\delta_{PEO}(CH_2CH_2O)$ = 3.7(b); $\delta_{PEO}(CH_3O\text{-})$ = 3.377(s); $\delta_{PAMAM}(\text{-}CH_2CONH\text{-})$ = 2.43(m); $\delta_{PAMAM}(\text{-}CONHCH_2\text{-})$ = 3.294(m); δ_{PAMAM}(protons next to primary and tertiary amines) = 2.5-2.85. FTIR peaks, ν cm^{-1}: 1113, 1549, 1645, 2880, 3273.

PEO(5000)-4.5G: 0.4g of PEO(5000)-4.0G was dissolved in 7.5ml of methanol and added slowly to 6.5ml of methyl acrylate. After 24 hours, methanol and unreacted methyl acrylate were removed under vacuum. The residue was washed with 400ml of ethyl ether, filtered off, and dried over vacuum to give the product, PEO(5000)-4.5G.

^{1}H NMR in $CDCl_3$: $\delta_{PEO}(CH_2CH_2O)$ = 3.654(b); $\delta_{PEO}(CH_3O\text{-})$ = 3.39(s); $\delta_{PAMAM}(\text{-}COOCH_3)$ = 3.677(s); $\delta_{PAMAM}(\text{-}CH_2CONH\text{-})$ = 2.373(m); $\delta_{PAMAM}(\text{-}CONHCH_2\text{-})$ = 3.28(m); $\delta_{PAMAM}(\text{-}CH_2COOCH_3)$ = 2.444(m); δ_{PAMAM}(protons next to tertiary amines) = 2.5-2.9. FTIR peaks, ν cm^{-1}: 1112, 1541, 1654, 1734, 2887, 3291.

A.2 PEO(2000) Series

PEO(2000)-0.5G

^{1}H NMR in d_6-DMSO: $\delta_{PEO}(CH_2CH_2O)$ = 3.511(b); $\delta_{PEO}(CH_3O\text{-})$ = 3.242(s); $\delta_{PAMAM}(\text{-}COOCH_3)$ = 3.574(s); $\delta_{PAMAM}(\text{-}CH_2COOCH_3)$ = 2.396(t); δ_{PAMAM}(protons next to tertiary amines) = 2.55-2.8. FTIR ν cm^{-1}: 1114, 1736, 2883.

PEO(2000)-1.0G

^{1}H NMR in D_2O: $\delta_{PEO}(CH_2CH_2O)$ = 3.612(b); $\delta_{PEO}(CH_3O\text{-})$ = 3.290(s); $\delta_{PAMAM}(\text{-}CH_2CONH\text{-})$ = 2.355(t); $\delta_{PAMAM}(\text{-}CONHCH_2\text{-})$ = 3.185(t); δ_{PAMAM}(protons next to primary and tertiary amines) = 2.6-2.8. FTIR ν cm^{-1}: 1115, 1547, 1657, 2880, 3243.

PEO(2000)-1.5G

^{1}H NMR in d_6-DMSO: $\delta_{PEO}(CH_2CH_2O)$ = 3.511(b); $\delta_{PEO}(CH_3O\text{-})$ = 3.243(s); $\delta_{PAMAM}(\text{-}COOCH_3)$ = 3.581(s); $\delta_{PAMAM}(\text{-}CH_2CONH\text{-})$ = 2.16(m); $\delta_{PAMAM}(\text{-}CONHCH_2\text{-})$ = 3.046(m); $\delta_{PAMAM}(\text{-}CH_2COOCH_3)$ = 2.398(t); δ_{PAMAM}(protons next to tertiary amines) = 2.5-2.8. FTIR ν cm^{-1}: 1112, 1539, 1661, 1734, 2875, 3248.

PEO(2000)-2.0G

^{1}H NMR in D_2O: $\delta_{PEO}(CH_2CH_2O)$ = 3.619(b); $\delta_{PEO}(CH_3O\text{-})$ = 3.296(s); $\delta_{PAMAM}(\text{-}CH_2CONH\text{-})$ = 2.353(m); $\delta_{PAMAM}(\text{-}CONHCH_2\text{-})$ = 3.19(m); δ_{PAMAM}(protons next to primary and tertiary amines) = 2.5-2.8. FTIR ν cm^{-1}: 1113, 1541, 1657, 2875, 3243.

PEO(2000)-2.5G

^{1}H NMR in d_6-DMSO: $\delta_{PEO}(CH_2CH_2O)$ = 3.511(b); $\delta_{PEO}(CH_3O\text{-})$ = 3.241(s); $\delta_{PAMAM}(\text{-}COOCH_3)$ = 3.577(s); $\delta_{PAMAM}(\text{-}CH_2CONH\text{-})$ = 2.178(m); $\delta_{PAMAM}(\text{-}CONHCH_2\text{-})$ = 3.06(m); $\delta_{PAMAM}(\text{-}CH_2COOCH_3)$ = 2.412(m); δ_{PAMAM}(protons next to tertiary amines) = 2.5-2.8. FTIR ν cm^{-1}: 1104, 1541, 1662, 1733, 2864, 3232.

PEO(2000)-3.0G

^{1}H NMR in D_2O: $\delta_{PEO}(CH_2CH_2O)$ = 3.60(b); $\delta_{PEO}(CH_3O\text{-})$ = 3.28(s); $\delta_{PAMAM}(\text{-}CH_2CONH\text{-})$ = 2.33(m); $\delta_{PAMAM}(\text{-}CONHCH_2\text{-})$ = 3.17(m); δ_{PAMAM}(protons next to primary and tertiary amines) = 2.5-2.8. FTIR ν cm^{-1}: 1107, 1546, 1658, 2870, 3254. M_w(theoretical) = 3576; M_w(MALDI-TOF) = 3450.

PEO(2000)-3.5G

^{1}H NMR in $CDCl_3$: $\delta_{PEO}(CH_2CH_2O)$ = 3.663(b); $\delta_{PEO}(CH_3O\text{-})$ = 3.4(s); $\delta_{PAMAM}(\text{-}COOCH_3)$ = 3.688(s); $\delta_{PAMAM}(\text{-}CH_2CONH\text{-})$ = 2.382(m); $\delta_{PAMAM}(\text{-}CONHCH_2\text{-})$ = 3.3(m); $\delta_{PAMAM}(\text{-}CH_2COOCH_3)$ = 2.453(m); δ_{PAMAM}(protons next to tertiary amines) = 2.5-2.9. FTIR ν cm^{-1}: 1110, 1539, 1662, 1734, 2864, 3243.

PEO(2000)-4.0G

^{1}H NMR in D_2O: $\delta_{PEO}(CH_2CH_2O)$ = 3.574(b); $\delta_{PEO}(CH_3O\text{-})$ = 3.252(s); $\delta_{PAMAM}(\text{-}CH_2CONH\text{-})$ = 2.299(m); $\delta_{PAMAM}(\text{-}CONHCH_2\text{-})$ = 3.151(m); δ_{PAMAM}(protons next to primary and tertiary amines) = 2.5-2.8. FTIR ν cm^{-1}: 1109, 1549, 1647, 2864, 2919, 3281.